Around planar dimer models: Schur processes and integrable statistical mechanics on isoradial graphs

Cédric Boutillier

Université Pierre et Marie Curie

École doctorale de sciences mathématiques de Paris centre

HABILITATION À DIRIGER DES RECHERCHES

Discipline : Mathématiques

présentée par

Cédric Boutillier

Around planar dimer models: Schur processes and integrable statistical mechanics on isoradial graphs

---

Soutenue le 1er décembre 2016 devant le jury composé de :

M. Vincent BEFFARA	CNRS & Université Grenoble Alpes
M. Philippe BIANE	CNRS & Université de Paris-Est
M. Dmitry CHELKAK	École Normale Supérieure, Paris
M. Philippe DI FRANCESCO	CEA, Saclay
M. Nathanaël ENRIQUEZ	Université de Paris-Ouest
M. Thierry LÉVY	Université Pierre et Marie Curie
M. Fabio TONINELLI	CNRS & Université de Lyon 1

après avis des rapporteurs :

M. Vincent BEFFARA	CNRS & Université Grenoble Alpes
M. Kurt JOHANSSON	KTH, Stockholm
M. Andrei OKOUNKOV	Columbia University, New-York

Université Pierre et Marie Curie

École doctorale de sciences mathématiques de Paris centre

Habilitation à diriger des recherches

Discipline : Mathématiques

présentée par

Cédric Boutillier

Around planar dimer models: Schur processes and integrable statistical mechanics on isoradial graphs

---

Soutenue le 1er décembre 2016 devant le jury composé de :

M. Vincent Beffara	CNRS & Université Grenoble Alpes
M. Philippe Biane	CNRS & Université de Paris-Est
M. Dmitry Chelkak	École Normale Supérieure, Paris
M. Philippe Di Francesco	CEA, Saclay
M. Nathanaël Enriquez	Université de Paris-Ouest
M. Thierry Lévy	Université Pierre et Marie Curie
M. Fabio Toninelli	CNRS & Université de Lyon 1

après avis des rapporteurs :

M. Vincent Beffara	CNRS & Université Grenoble Alpes
M. Kurt Johansson	KTH, Stockholm
M. Andrei Okounkov	Columbia University, New-York

Laboratoire de Probabilités
et Modèles Aléatoires
UMR 7599
Boîte courrier 188
4 place Jussieu
75252 Paris Cedex 05

Université Pierre et Marie Curie
École doctorale de sciences
mathématiques de Paris centre
Boîte courrier 290
4 place Jussieu
75252 Paris Cedex 05

Around planar dimer models: Schur processes and integrable statistical mechanics on isoradial graphs

Mémoire d'habilitation à diriger des recherches

Cédric Boutillier

یک چند به کودکی به استاد شدیم
یک چند به استادی خود شاد شدیم
پایان سخن شنو که ما را چه رسید
از خاک درآمدیم و بر باد شدیم

J'avais un maître alors que j'étais un enfant.
Puis je devins un maître et, par là, triomphant.
Mais écoute la fin : tout cela fut en somme
Un amas de poussière emporté par le vent.

(Omar Khayyam, 1048–1131)

Abstract

The dimer model is a probability measure on perfect matchings (or dimer configurations) on a graph. Dimer models on some subgraphs of the honeycomb and square lattices, which by duality, correspond to tilings with rhombi and dominos, are directly related to Schur processes, probability measures on sequences of interlacing partitions. Via bijections and other combinatorial correspondences, other integrable models of two-dimensional statistical mechanics can be mapped to planar dimer models: spanning trees, the Ising model...

This manuscript presents an overview of the results obtained by the author and his coauthors on questions around planar dimer models, with a strong emphasis, on one hand, on the relation with Schur processes, and on the other hand, on these models from statistical mechanics related to dimers, defined on isoradial graphs, a particular class of embedded planar graphs with interesting properties.

Résumé

Le modèle de dimères est une mesure de probabilité sur les couplages parfaits (ou configurations de dimères) d'un graphe. Les modèles de dimères sur certains sous-graphes du réseau hexagonal ou du réseau carré, qui par dualité, correspondent à des pavages par losanges ou par dominos, sont directement reliés aux processus de Schur, mesures de probabilités sur les suites de partitions entrelacées. Par le moyen de bijections et autres correspondances combinatoires, d'autres modèles intégrables de mécanique statistique en dimension deux peuvent être étudiés au moyen de modèles de dimères : les arbres couvrants, le modèle d'Ising...

Ce document présente un survol des résultats obtenus par l'auteur et ses collaborateurs sur des questions autour du modèle de dimères sur les graphes planaires, avec un accent d'une part sur la relation avec les processus de Schur, et d'autre part sur ces modèles de mécanique statistique liés aux dimères, définis sur les graphes isoradiaux, une classe particulière de graphes planaires plongés aux propriétés intéressantes.

Remerciements

Je tiens à remercier tout d'abord les trois rapporteurs de ce manuscript, Vincent Beffara, Kurt Johansson et Andrei Okounkov, d'avoir bien voulu consacrer de leur temps précieux pour lire et évaluer ce texte.

Vincent, Philippe, Dima, Philippe, Thierry, Nathanaël, Fabio, je suis très heureux et honoré que vous ayez accepté de faire partie de ce jury d'habilitation. Merci pour votre présence.

Je remercie Richard Kenyon, dont les idées et les travaux restent pour moi une source d'admiration et d'inspiration. Merci aussi à Kirone Mallick, qui a guidé mes premiers pas dans le monde de la recherche.

Je remercie aussi mes collaborateurs avec qui j'apprends beaucoup et ai un grand plaisir à travailler. J'ai partagé de formidables moments de recherche avec vous. Un merci particulier à Béatrice, ma grande sœur mathématique, qui a accepté de mener avec moi une partie importante des projets présentés ici. D'autres aventures scientifiques passionnantes nous attendent ! Un deuxième merci à Sylvie pour avoir été un élément moteur déterminant pour le lancement de rédaction de ce mémoire.

Je remercie le LPMA dans son ensemble. Tout d'abord l'institution et ses tutelles, pour les excellentes conditions de travail qui y sont offertes, mais surtout son personnel : en premier lieu les membres de son équipe d'administration et de gestion, en particulier Florence, Josette et Serena, pour leur efficacité et leur bonne humeur. Merci aussi aux collègues côtoyés au quotidien : Daphné, Nathalie, Damien, Thomas, Thierry, Omer, Vincent, Lorenzo, Gilles et tous les autres... Nos conversations mathématiques, et surtout non-mathématiques, sont autant de bonnes raisons pour venir au bureau.

Merci à mes parents. Une pensée aussi à ma mamy Anny qui vient de fêter ses 90 ans, et qui a déjà été exposée aux pavages et aux dimères lors de ma soutenance de thèse il y a maintenant un petit moment.

Merci à mes enfants Marie et Alexandre, et ma femme Olya, pour m'avoir supporté, soutenu et encouragé, chacun à votre manière, pendant la rédaction de ce mémoire.

Merci aussi à ces personnes qui ont partagé des moments de mon existence, pendant des années, quelques jours, ou juste quelques minutes, et qui ont marqué positivement et durablement ma vie.

Contents

Introduction

The *dimer model* is introduced in statistical mechanics to describe the chemical process of adsorption of diatomic molecules (*dimers*) on the surface of a crystal [FR37]. On planar graphs, it turns out that the model is completely solvable, meaning that one can, for example, compute exactly the number of configurations, or correlations between dimers, with algebraic tools. This property and the fact that this model is connected to several other combinatorial objects via bijections put this model at the intersection of several branches of mathematics (probability, combinatorics, real algebraic geometry), but also computer sciences and theoretical physics.

Dimer models have been the main topic of our research, presented in this manuscript, either directly, or as a tool to study related models. In this introduction, we first briefly present in Section 1 the dimer model and some of its properties. For a more complete treatment, we refer the reader to some lectures notes on this model [Ken04, Ken09, dT15, Cim14]. In Section 2, we discuss the link between the geometric constraints between dimers and the interlacing properties of partitions in Schur processes, which are the topic of the first part of this document. Then, in Section 3, we present the connection between dimer models and other models of statistical mechanics. On a special family of planar graphs, the *isoradial graphs*, these models have rich and interesting properties. They are discussed at length in the second part of the manuscript.

The documents ends with a third part, containing a summary of other works [10, 7], and some perspectives on ongoing or future research projects. The three parts are mostly independent from one another.

1. The dimer model

A *dimer configuration* of a graph $G = (V, E)$ is a subset of edges $M \subset E$ such that in the subgraph (V, M), all vertices have degree 1: all vertices of G are incident to exactly one edge of M. In graph theory, dimer configurations are also called *perfect matchings*: a dimer configuration pairs every vertex of the graph with one of its neighbors.

If G is a finite graph (which admits at least a dimer configuration) and positive weights $(\nu_e)_{e\in E}$ are assigned to edges, the *dimer model* on G is the Boltzmann probability measure on dimer configurations of G, where the probability of a configuration M is proportional to the product of the weights it contains. The proportionality factor

$$Z(G, \nu) = \sum_{\substack{M:\text{ dimer}\\ \text{configuration}}} \prod_{e\in M} \nu_e$$

is called the *dimer partition function*.

In the 1960's, it has been proven [TF61, Kas61] that the partition function of the dimer model on a finite planar graph can be expressed as the Pfaffian of a weighted oriented adjacency matrix of the graph, the *Kasteleyn matrix*. The orientation should satisfy the *clockwise odd condition*: around every face, the number of edges oriented clockwise is odd. When the graph is bipartite, the Kasteleyn matrix has a 2×2 block structure, reflecting the two classes of vertices, with zero blocks on the diagonal. The Pfaffian of the whole matrix can be reduced to the determinant of one of these blocks [Per69]. When the graph is not planar, but can be drawn on a surface with g handles, Kasteleyn's approach can be extended to compute the dimer partition function with 2^{2g} Pfaffians or determinants [GL99, Tes00, CR07, CR08].

Dimer configurations on planar graphs can be seen by duality as tilings of the plane, or regions of the plane. For example, on the square lattice, dimer configurations correspond to tilings with *dominos*, which are the union of two adjacent (dual) square faces. Similarly, dimer configurations on the hexagonal lattice correspond to tilings with rhombi, which are the union of two adjacent faces of the dual triangular lattice.

For a periodic infinite planar weighted graph G, the notion of Boltzmann measures is replaced by that of Gibbs measures, which are measures such that, when we condition on the configuration in some annular region:

- the configurations inside and outside of the annulus are independent
- the distribution on configurations in the finite region inside is the Boltzmann measure.

Gibbs measures are usually constructed as weak limits of Boltzmann measures on sequences of finite graphs approximating G, for example by taking quotients of G by lattices with a larger and larger mesh (toroidal graphs).

Correlations for the weak limit of uniform measures for domino tilings and rhombus tilings were obtained by Kenyon [Ken97]. The edges in a random dimer configuration for a determinantal point process, with a kernel given by the inverse of the infinite Kasteleyn matrix. This result has been extended to any two-dimensional bipartite lattices, and a full classification of ergodic Gibbs measures for dimer models on planar biperiodic graphs has been obtained in [KOS06], with very interesting connections to real algebraic geometry. See also [KO06].

2. Dimers, interlacing particles and Schur processes

A uniform tiling of a hexagon with rhombi, is represented on Figure 0.1, with different colors (yellow, red, blue) for tiles depending on their orientation. One sees that due to the geometric constraints, between two successive blue horizontal rhombi, there is exactly one blue rhombus on their left, and one on their right. They form what is called an *interlacing particle process*. This interlacing property has been used in [CLP98, Joh02] to study this model and obtain the asymptotic typical behaviour of these objects. This interlacing property is in fact true for any tiling with rhombi of simply connected regions of the plane, like the ones obtained as the projection of plane partitions (See Figure 4.3a, page 53 for an example).

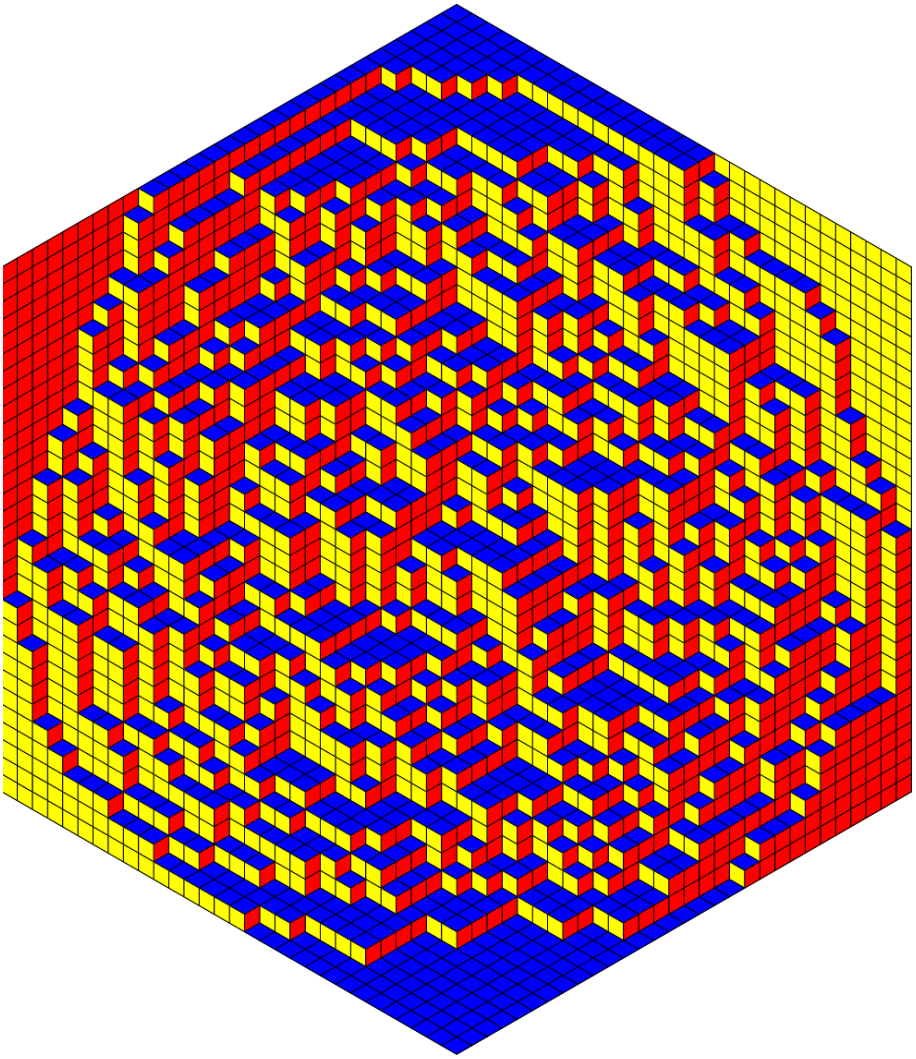

Figure 0.1.: A tiling with rhombi of a $30 \times 30 \times 30$ hexagon, chosen uniformly among the $\simeq 8.7 \times 10^{5442}$ possibilities

Such an interlacing structure can also be found in domino tilings of the Aztec diamond in [Joh02], see also [Nor10], where some types of dominos, interpreted as defects in patterns created by the other two types, have also this interlacing structure.

Another way to generate interlacing particle systems is through *Schur processes*. These are a special family of probability measures on interlacing particles configurations (or interlacing partitions) in the hierarchy of Macdonald processes [BC14]. It turns out that Schur processes can be studied via *vertex operators*, in connection with representation theory of infinite dimensional Lie algebra [Kac90]. They contain, via bijections, plane partitions [OR03] and tilings of the Aztec diamond [BCC14] as particular examples.

In Chapter 1, we define Schur processes and present the vertex operator formalism.

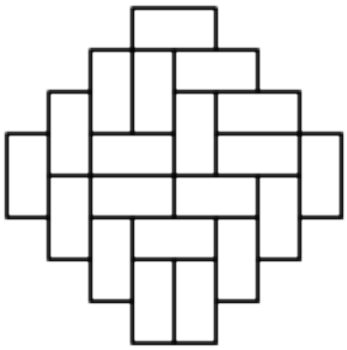

Figure 0.2.: A tiling with dominos of the Aztec diamond of size 4.

We explain how to use it in Chapter 2 to study the geometry of large plane and skew plane partitions. We briefly recall and compare the results about the typical behaviour of these combinatorial objects in two situations [OR07] and [11].

In Chapter 3 we present a general framework [15] to represent Schur processes as a dimer model on some family of planar graphs: the *rail yard graphs*, which places under the same roof plane partitions and the Aztec diamond. Our main result is a determinantal formula for dimer correlations (which are richer than just correlations for the Schur process), using the vertex operator formalism. We give some consequences on tilings and in particular for the Aztec diamond.

In Chapter 4, we provide an entropy minimal algorithm [13] to simulate Schur processes via bijective proofs of Cauchy and dual Cauchy identities for Schur function, and their operator counterparts. This algorithm can be used to produce efficiently perfect samples of plane partitions or steep domino tilings.

3. Dimers and other related models on Isoradial graphs

Dimer models are related to several other models from statistical mechanics. Spanning trees on a planar graph G are in bijection with dimer configurations on the double graph[1] of G via Temperley's bijection [Tem74, KPW00]. Edges of random spanning trees form a determinantal process [BP93], with a kernel given by the transfer impedance matrix, whose entries are linear combinations (discrete second derivatives) of the Green function. Through Temperley's bijection, there is an algebraic relation between the inverse Kasteleyn matrix on the double graph giving correlations for dimers and the Green function. This analytic correspondence can be used either to get information about spanning trees using dimers [Ken00a, Ken00b], or the other way around [BP93, BLR16].

Another example is the Ising model on a planar graph, which can be through the contours separating spin clusters [KW41a, KW41b] mapped to a dimer model, by Fisher's

[1] If G is finite, one needs to remove from the double graph two vertices, corresponding for example to the outer face of G and a vertex of G on its boundary.

bijection [Fis66]. See also [Kas67, DZM$^+$96]. Via dimer computations, many results on the Ising model can be derived. See *e.g.*, [MW73, Dub11b, CCK15]

In [Ken02], Kenyon introduces a Laplacian and a Kasteleyn operator on a family of planar graphs with a special embedding, called the isoradial graphs, where conductances and dimer weights are trigonometric functions. He gives an explicit formula for the associated Green function and the inverse Kasteleyn operator which have the locality property: their entries indexed by two vertices depends only on the geometry of the embedding of the graph along a path between these two vertices. The key tool is the existence of a family of harmonic functions, the *discrete exponential functions* [Mer04], computed at a vertex as the product of local terms on a path from a base point to that vertex.

In Chapter 5, we introduce the notion of isoradial graphs. We discuss the rhombic flip operation, in connection with the Yang-Baxter equation and the star-triangle transformation for the Ising model and electric networks, and the implication for the critical Laplacian [Ken02] and its Green function.

The study of critical Ising model on isoradial graphs [8, 9] is presented in Chapter 6. The main results are an explicit and local expression for the inverse Kasteleyn operator on the Fisher graph for an arbitrary infinite isoradial graph (without hypothesis of periodicity), which allows us to construct a Gibbs measure on spin configurations for the critical Ising model on isoradial graphs.

In Chapter 7, we summarize the results of [16], recently accepted for publication in *Invent. Math.* We construct a family of massive Laplacians, with masses and conductances expressed in terms of elliptic functions, which reduces to Kenyon's Laplacian when the mass goes to zero. We define a family of massive harmonic function with a product (zero curvature) structure which reduce to exponential. We give an explicit integral formula for the Green function, which has the locality property. As for the critical Ising model of Chapter 6, we explore the implications for an underlying model of statistical mechanics: the rooted spanning forests, which are the massive analogues of spanning trees. We also characterize completely the algebraic curves which can arise as spectral curves of these massive Laplacians on periodic isoradial curves, in the same spirit as what has been done for bipartite periodic planar dimer models [KOS06]: these are Harnack curve of genus 1, with an additional symmetry.

Using duality in the high/low temperature contour expansion of the Ising model, we exhibit in Chapter 8 a coupling between the double Ising model on a finite graph G drawn on a surface, and a bipartite dimer model on a decorated version G_Q of its medial graph, in such a way that the contours separating clusters where the spins of the two configurations agree and disagree (XOR contours) are the level line of the restriction of the height function of the dimer model on G_Q to a subset of vertices. When G is an infinite isoradial graph, so is G_Q, and the coupling extends to this situation for the Gibbs measures for the critical Ising model [9] and the bipartite dimer model on G_Q [dT07b]. This gives some insights on Wilson's conjecture about the scaling limit of the critical XOR contours [Wil11].

4. Notes on the manuscript

This document contains two bibliography indexes: the first one, on page 100, lists our publications, labeled with numbers like [16]. These publications can be downloaded from:

`http://www.lpma-paris.fr/pageperso/boutil/publications/`.

The other one, page 102, lists external references, and uses alphanumeric code from the name of the authors and year of publication, like [Bor11].

Part I.

Dimers and Schur processes

Abstract

After introducing Schur processes as a random process on sequences of integer partitions, and the formalism of vertex operators in Chapter 1, we explain how to compute various probabilistic quantities for Schur processes, and to derive the typical behaviour of large plane partitions [OR07][11] as an application in Chapter 2. In Chapter 3, we present a family of planar graphs, the rail yard graphs [15], on which a version of the dimer model is equivalent to Schur processes, with arbitrary parameters, extending the known correspondence for (skew) plane partitions [OR03] and steep domino tilings [BCC14]. Chapter 4 is dedicated to the description of an entropy optimal and efficient algorithm to perfectly simulate Schur processes and which thus can be used to produce efficiently samples of random tilings [13].

1. The Schur process

In this chapter, we give some notions and notation for *Schur processes*, which are probability measures on sequences of partitions. Although there are several ways to study them, we use here the formalism of *vertex operators*, following [OR03, OR07]. We refer the reader to these articles, as well as to [BR05] for more details about the Eynard-Mehta approach, and [Bor11].

Our study of Schur processes will be motivated by examples in connection with random tilings. So our definitions may not be the most general ones. However, they will be enough for us here, and the more complete ones can be obtained by taking suitable limits.

1.1. Partitions, Young and Maya diagrams, symmetric functions

1.1.1. Partitions and their Young diagrams

Definition 1. A *partition* of a non negative integer n is a non increasing sequence of non negative integers $\lambda = (\lambda_1, \lambda_2, \dots,)$ whose sum is equal to n. The integer $n = |\lambda| = \sum_{i=1}^{\infty} \lambda_i$ is called the *size* of the partition. The *Young diagram* of the partition λ is the left-justified array with $|\lambda|$ boxes, with λ_j boxes on the jth row.

We will generally write only the non zero parts of a partition. For practical purposes, it will be often convenient to draw the Young diagram in the so-called *Russian coordinates*, *i.e.*, rotated by 135 degrees, and reflected across the vertical axis. See Figure 1.2.

If λ and μ are two partitions, we say that $\mu \subset \lambda$ if for all i, $\mu_i \leq \lambda_i$. We will often identify a partition with its Young diagram. With this identification, the $\subset$ partial order on partitions coincides with the inclusion for Young diagrams. If $\mu \subset \lambda$, the shape obtained when we remove from the Young diagram of λ the boxes belonging to the Young diagram of μ, then we get a (corner-) connected shape, denoted λ/μ.

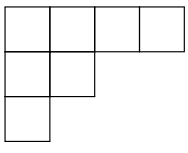

Figure 1.1.: Young diagram of the partition $\lambda = (4, 2, 1)$.

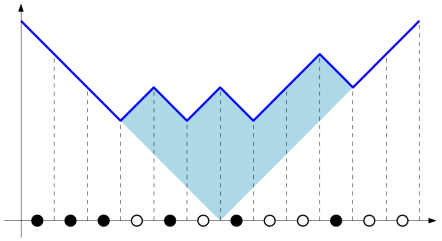

Figure 1.2.: The Maya diagram and the Young diagram of the partition $\lambda = (4, 2, 1)$ in Russian coordinates.

1.1.2. Maya diagrams

Definition 2. A *semi-infinite* sequence of half-integers I is a subset of $\mathbb{Z} + \frac{1}{2}$ such that $I \cap \mathbb{R}^+$ and $I^c \cap \mathbb{R}^-$ are finite subsets. A semi-infinite sequence I will be represented graphically by a *Maya diagram*, which is a collection of black marbles (or particles, $\bullet$) and white marbles (or holes, $\circ$) on $\mathbb{Z} + \frac{1}{2}$. There is a black (resp. white) marble at position k if and only if k belongs (resp. doesn't belong) to the semi-infinite sequence I. A Maya diagram has all sites filled with black marbles far enough on the left and white marbles far enough on the right. The *charge* of a semi-infinite sequence (or a Maya diagram) corresponding to a set of indices I is the quantity $C = |I \cap \mathbb{R}^+| - |I^c \cap \mathbb{R}^-|$.

We will often identify a semi-infinite sequence with the corresponding Maya diagram.

To a partition $\lambda = (\lambda_1, \lambda_2, \dots)$ is naturally associated a semi-infinite sequence of charge 0, $I_\lambda = \{\lambda_k - k + \frac{1}{2} \ ; \ k \in \mathbb{N}^*\}$. Translating this Maya diagram by a quantity $c \in \mathbb{Z}$ to the right gives a Maya diagram of charge c.

Reciprocally, given an infinite sequence of charge c, one can define in a unique way a partition λ, by the formula above, applied to the semi-infinite sequence $I - c$, where c is subtracted to all the elements of the infinite sequence I.

There is a nice graphical interpretation of this bijection: from the Maya diagram I, construct a continuous piecewise linear function f_I with slope ± 1 defined uniquely by these conditions:

- for all $j \in \mathbb{Z}$, f_I has slope -1 (resp. $+1$) on $(j, j+1)$ if and only if $j + \frac{1}{2}$ belongs (resp. does not belong) to I,
- the range of f_I is $\mathbb{R}^+$.

By the definition of Maya diagrams, f_I will have asymptotes with slope -1 (resp. $+1$) at $-\infty$ (resp. $+\infty$). These asymptotes will cross at an abscissa equal to the charge of I (the ordinate of this intersection can be chosen to be zero). The domain delimited by the graph of f_I and its asymptotes is the Young diagram of the partition λ associated to I by the bijection. See Figure 1.2.

1.1.3. Semi-standard Young tableaux and Schur functions

Partitions are basic blocks to construct more involved combinatorial objects, such as semi-standard Young tableaux, defined below:

Definition 3. Let λ be a partition. A *semi-standard Young tableau* (SSYT) of shape λ is a filling of the Young diagram of λ with positive integers which is
- weakly increasing along rows, from left to right,
- strictly increasing along columns, from top to bottom.

If T is a SSYT, and $\boldsymbol{x} = (x_1, x_2, \dots)$ a sequence of formal variables, we denote by $\boldsymbol{x}^T$ the monomial

$$\boldsymbol{x}^T = x_1^{\text{number of 1's in T}} x_2^{\text{number of 2's}} \cdots .$$

Definition 4. The *Schur function* s_λ associated to a partition λ is the function in an infinite number of variables $\boldsymbol{x} = (x_1, x_2, \dots)$ defined by

$$\mathrm{s}_\lambda(\boldsymbol{x}) = \sum_{\substack{T\text{: SSYT} \\ \text{of shape } \lambda}} \boldsymbol{x}^T.$$

Although it is not completely obvious from this combinatorial definition, s_λ is a symmetric function. In fact, the collection $(\mathrm{s}_\lambda)_\lambda$ indexed by all partitions is a basis for the algebra of symmetric variables, which is orthonormal for the standard scalar product $\langle \cdot, \cdot \rangle$ on the space of symmetric function, defined by requiring that monomial and complete symmetric functions are dual bases for this scalar product.

This combinatorial definition for Schur functions can be extended to skew shapes to define semi-standard skew Young tableaux, and obtain the so-called skew Schur functions:

Definition 5. Let $\lambda \supset \mu$ two partitions. A *skew semi-standard Young tableau* of shape λ/μ is a filling of the skew shape of λ/μ with positive integers which is
- weakly increasing along rows, from left to right,
- strictly increasing along columns, from top to bottom.

The *skew Schur function* $\mathrm{s}_{\lambda/\mu}$ is the symmetric function in an infinite number of variables $\boldsymbol{x} = (x_1, x_2, \dots)$ defined by

$$\mathrm{s}_{\lambda/\mu}(\boldsymbol{x}) = \sum_{\substack{T\text{: skew SSTY} \\ \text{of shape } \lambda/\mu}} \boldsymbol{x}^T.$$

When we write that a symmetric function depends only on a finite number of variables, it means that all the other formal variables have been set to 0.

Schur and skew Schur functions satisfy two algebraic relations which will play an crucial role in the properties of Schur processes:

Proposition 1 (Cauchy identity)**.**

$$\sum_\lambda \mathrm{s}_\lambda(\boldsymbol{x})\, \mathrm{s}_\lambda(\boldsymbol{y}) = \prod_{i,j} \frac{1}{1 - x_i y_j}. \tag{1.1}$$

Proposition 2 (branching rule)**.** *For any partitions λ and ν,*

$$\mathrm{s}_{\lambda/\nu}(\boldsymbol{x},\boldsymbol{y}) = \sum_{\mu} \mathrm{s}_{\lambda/\mu}(\boldsymbol{x})\,\mathrm{s}_{\mu/\nu}(\boldsymbol{y}). \tag{1.2}$$

For more details about the combinatorial definition of Schur functions, the connection with their classical definition in terms of ratio of Vandermonde like determinant, and relations with other classical families of symmetric functions, we refer the reader to [Sta99, Chapter 7] and [Mac15].

1.2. Interlacement, dual interlacement

Definition 6. Let λ and μ be two partitions. We write $\lambda \succeq \mu$ if for all $i \geq 1$, $\lambda_i \geq \mu_i \geq \lambda_{i+1}$. We say that that λ and μ *interlace*, or *or differ by a horizontal strip* if either $\lambda \succeq \mu$ or $\lambda \preceq \mu$.

If T is a SSYT of shape λ, define $(\lambda^{(i)})_i$ as the sequence of partitions included in λ, such that $\lambda^{(i)}$ is the union of boxes with a content in T less or equal to i. Then:

$$\lambda^{(0)} = \emptyset \preceq \lambda^{(1)} \preceq \cdots$$

The skew Schur function $\mathrm{s}_{\lambda/\mu}$ in one variable x has a very simple expression:

$$\mathrm{s}_{\lambda/\mu}(x) = x^{|\lambda|-|\mu|}\mathbf{1}_{\lambda\succeq\mu}. \tag{1.3}$$

There is a natural involution on the set of partitions, called *transposition*, and denoted by ω.

Definition 7. The *transposed* $\lambda' = \omega\cdot\lambda$ of a partition λ is a partition with parts $(\lambda'_1, \lambda'_2, \dots)$ defined by:

$$\forall i \in \mathbb{N}^*,\ \lambda'_i = \mathrm{Card}\{j \in \mathbb{N}^* \ :\ \lambda_j \geq i\}.$$

For example, if $\lambda = (4,2,2)$, then $\lambda' = (3,3,1,1)$ In terms of Young diagrams this involution corresponds to exchanging rows and columns. In terms of Maya diagram, it corresponds to a reflection with respect to 0 followed by an inversion of colors.

This naturally yields the relation of *dual interlacement*, denoted by $\succeq'$.

Definition 8. Two partitions λ and μ dually interlace if and only if λ' and μ' interlace:

$$\lambda \succeq' \mu \Leftrightarrow \lambda' \succeq \mu'.$$

We say then also that λ and μ *differ by a vertical strip.*

The branching rule (1.2) and Cauchy identity (1.1) are completed with the dual Cauchy identity:

Proposition 3 (dual Cauchy identity)**.**

$$\sum_{\lambda} \mathrm{s}_{\lambda}(\boldsymbol{x})\,\mathrm{s}_{\lambda'}(\boldsymbol{y}) = \prod_{i,j}(1+x_i y_j). \tag{1.4}$$

1.3. Schur processes

Definition 9. Let $\ell < r$ be two integers. A *Schur process* is a probability measure on sequences of partitions $(\lambda^{(\ell)}, \dots, \lambda^{(r+1)})$, characterised by three sequences:
- The LR sequence $\underline{a} = (a_\ell, \dots, a_r) \in \{L, R\}^{[\ell..r]}$,
- The sign sequence $\underline{b} = (b_\ell, \dots, b_r) \in \{+, -\}^{[\ell..r]}$,
- The parameter sequence $\underline{x} = (x_\ell, \dots, x_r) \in (\mathbb{R}_+^*)^{[\ell..r]}$,

such that the probability of a given sequence of partitions is proportional to:

$$\prod_{j=\ell}^{r} S_{a_j,b_j}(\lambda^{(j)}, \lambda^{(j+1)}; x_j) \tag{1.5}$$

where $\lambda^{(\ell)}$ and $\lambda^{(r+1)}$ are the empty partitions and

$$S_{a,b}(\lambda, \mu; x) = \begin{cases} \mathrm{s}_{\lambda/\mu}(x) & \text{if } a = L \text{ and } b = -, \\ \mathrm{s}_{\mu/\lambda}(x) & \text{if } a = L \text{ and } b = +, \\ \mathrm{s}_{\lambda'/\mu'}(x) & \text{if } a = R \text{ and } b = -, \\ \mathrm{s}_{\mu'/\lambda'}(x) & \text{if } a = R \text{ and } b = +. \end{cases}$$

Remark 1. A few comments about this definition:
- With probability one, for all j, $\lambda^{(j)}$ and $\lambda^{(j+1)}$ interlace (resp. dually interlace) if $a_j = L$ (resp. $a_j = R$), the direction of the inclusion being given by the sign of b_j.
- When λ and μ satisfy the correct interlacing relation, $S_{a,b}(\lambda, \mu; x)$ is just $x^{||\lambda|-|\mu||}$.
- Here, the transition between $\lambda^{(j)}$ and $\lambda^{(j+1)}$ is given by a specialisation of skew Schur functions in only one variable, taking a positive real value. More general specialisations can be used, if they give positive results. The characterisation of Schur-positive specialisations of symmetric functions is the content of Thoma's theorem [Tho64]. See also [VK81, Oko00, KOO98, BG15] for statement and proofs of this result. They can all be obtained from the definition here, by "forgetting" some of the intermediate partitions, and possibly taking suitable limits.

By Jacobi-Trudi identities expressing skew Schur function as determinants of complete symmetric functions, the weight (1.5) of a configuration can be written as a product of determinants. It follows from (an extended version of) Eynard-Metha's theorem [BR05] that the statistics of the particles form a determinantal process. However, we will see that in this context, the vertex operators together with the fermionic localisation operators can readily lead to determinantal formulas with an explicit kernel for the correlations.

1.4. Vertex operator formalism

There is an algebraic way to construct symmetric functions as the action of some operators on a vector space. These operators will act as *transfer matrices* to construct consecutive elements of the random sequence of partitions from the Schur process.

1.4.1. Bosonic operators

Definition 10. The *bosonic Fock space* is an infinite dimensional Hilbert space $\mathcal{B}$ with a countable orthonormal basis indexed by partitions $(|\lambda\rangle)_\lambda$.

On this space we define various vertex operators: the operator $\Gamma_+(x)$ acts on $\mathcal{B}$ as follows:

$$\Gamma_+(x)|\lambda\rangle = \sum_{\mu \preceq \lambda} x^{|\lambda \setminus \mu|} |\mu\rangle.$$

Its adjoint $\Gamma_-(x)$ acts on a basis vector as follows:

$$\Gamma_-(x)|\lambda\rangle = \sum_{\mu \succeq \lambda} x^{|\mu \setminus \lambda|} |\mu\rangle.$$

Note that even if the result is not a finite linear combination, all the coefficients are finite. They satisfy the following commutation relations: for all x and y,

$$\begin{aligned} \Gamma_+(x)\Gamma_+(y) &= \Gamma_+(y)\Gamma_+(x), \\ \Gamma_-(x)\Gamma_-(y) &= \Gamma_-(y)\Gamma_-(x), \\ \Gamma_+(x)\Gamma_-(y) &= \frac{1}{1-xy}\Gamma_-(y)\Gamma_+(x). \end{aligned} \tag{1.6}$$

One can construct the skew Schur functions specialised in n variables as a matrix element of a product of n operators $\Gamma_+(x_1),\ldots,\Gamma_+(x_n)$.

$$\langle \mu | \Gamma_+(x_1) \cdots \Gamma_+(x_n) | \lambda \rangle = \mathrm{s}_{\lambda/\mu}(x_1, \ldots, x_n).$$

The transposition on partitions and the notion of dual interlacement allow also one to define two new vertex operators $\Gamma'_+(x)$ and $\Gamma'_-(x)$, which are conjugates of the previous $\Gamma_+(x)$ and $\Gamma_-(y)$ by the involution ω:

$$\Gamma'_+(x) = \omega\Gamma_+(x)\omega = \Gamma_+(-x)^{-1}, \quad \Gamma'_-(y) = \omega\Gamma_-(y)\omega = \Gamma_-(-y)^{-1},$$

which corresponds in terms of action on partitions to:

$$\Gamma'_+(x)|\lambda\rangle = \sum_{\mu \preceq' \lambda} x^{|\lambda \setminus \mu|} |\mu\rangle, \qquad \Gamma'_-(x)|\lambda\rangle = \sum_{\mu \succeq' \lambda} x^{|\mu \setminus \lambda|} |\mu\rangle.$$

In the next chapters, instead of putting or not a prime to distinguish between interlacement and dual interlacement, we may use more symmetric notation, with symbols from the sequences $\underline{a}$ and $\underline{b}$.

$$\Gamma_{L\pm}(x) = \Gamma_\pm(x), \quad \Gamma_{R\pm}(x) = \Gamma'_\pm(x).$$

1.4.2. Fermionic operators

Let V a Hilbert space with an infinite countable basis $(e_k)_{k\in\mathbb{Z}+\frac{1}{2}}$.

Definition 11. The *fermionic Fock space* $\mathcal{F} = \bigwedge^{\frac{\infty}{2}} V$ is the linear space generated by the external product of vectors of the basis $(e_k)_{k\in\mathbb{Z}+\frac{1}{2}}$ indexed by a semi-infinite sequence $I = \{i_1 > i_2 > \ldots\}$. It is naturally $\mathbb{Z}$-graded by the charge. The basis vector corresponding to the semi-infinite sequence I is denoted

$$|I\rangle = e_{i_1} \wedge e_{i_2} \wedge \cdots$$

There are natural operators acting on $\bigwedge^{\frac{\infty}{2}} V$:

- *creation operators* ψ_k, $k \in \mathbb{Z} + \frac{1}{2}$ acting by external product:

$$\psi_k|I\rangle = e_k \wedge \big(e_{i_1} \wedge e_{i_2} \wedge \cdots\big) = \begin{cases} (-1)^{\#\{n:i_n>k\}}|I \cup \{k\}\rangle & \text{if } k \notin I, \\ 0 & \text{if } k \in I \end{cases}$$

- *annihilation operators* ψ_k^*, $k \in \mathbb{Z} + \frac{1}{2}$ acting by internal product:

$$\psi_k^*|I\rangle = \iota_{e_k}\big(e_{i_1} \wedge e_{i_2} \wedge \cdots\big) = \begin{cases} (-1)^{\#\{n:i_n>k\}}|I \setminus \{k\}\rangle & \text{if } k \in I, \\ 0 & \text{if } k \notin I \end{cases}$$

The action of these operators in term of Maya diagram is easy to describe: the operator ψ_k (resp. ψ_k^*) tries to add (resp. remove) a particle at site k to a Maya diagram, and gives 0 if a particle is present (resp. absent) at that site.

These operators satisfy the *canonical anticommutation relations*:

$$\forall\ k, l \in \mathbb{Z} + \frac{1}{2}, \quad \psi_k\psi_l^* + \psi_l^*\psi_k = \mathbf{1}_{k=l}.$$

Whereas ψ_k and ψ_k^* separately do not preserve the charge, their products do, and have in fact a very simple interpretation: $\psi_k\psi_k^*$ (resp. $\psi_k^*\psi_k$) is the projector on the subspace of $\mathcal{F}$ generated by Maya diagrams with a particle (resp. a hole) at position k.

The operators $\Gamma_+(x)$ and $\Gamma_-(y)$ can also act on $\mathcal{F}$. They preserve the charge, and satisfy commutation relations, that are nicely written if we introduced the generating functions for ψ_k's and ψ_k^*:

$$\psi(z) = \sum_{k\in\mathbb{Z}+\frac{1}{2}} z^k\psi_k, \qquad \psi^*(w) = \sum_{k\in\mathbb{Z}+\frac{1}{2}} w^{-k}\psi_k^*,$$

For example,

$$\Gamma_+(x)\psi(z) = \frac{1}{1-zx}\psi(z)\Gamma_+(x). \tag{1.7}$$

The complete list of commutation relations between $\Gamma_{ab}(x)$ and $\psi(z)$ or $\psi^*(w)$ can be found in [15, Proposition 11], and can be obtained from the relation above by taking duals, inverse and conjugates by ω. For a combinatorial proof, see [15, Appendix A]. For algebraic proofs, see for instance [Kac90, Chapter 14], [MJD00], [Oko01, Appendix A], [OR07], [Tin11] and [AZ13].

2. Plane partitions as Schur processes

Plane partitions are the two dimensional analogues of integer partitions, which can be seen as some tilings with rhombi with special steep boundary conditions. We explain in Section 2.1 how these objects, together with one of their generalizations, the *skew plane partitions*, can be encoded as sequences of interlacing partitions. Then we describe in Section 2.2 how to compute generating functions for these objects and correlations under the associated Boltzmann measure, following [ORV06, OR03, OR07], using the formalism of vertex operators. In Section 2.3 we describe briefly the implication on the shape of large skew plane partitions, comparing the results of [OR07] and [11] for different setups. The chapter ends with a description of *steep domino tilings* [BCC14], which are the domino counterpart of the steep rhombi tiling coming from skew plane partitions, and comprise as special examples the Aztec diamond and pyramid partitions.

2.1. Plane partitions and skew plane partitions

A plane partition is the two-dimensional analog of a partition:

Definition 12. A *plane partition* is a sequence $\pi = (\pi_{i,j})_{(i,j)\in\mathbb{N}^{*2}}$ of non negative integers which is weakly decreasing in i and j and has a finite number of nonzero coefficients. The *size* $|\pi|$ of the plane partition π is the sum of its coefficients: $|\pi| = \sum_{i,j} \pi_{i,j}$. When written like a matrix, the support of π (*i.e.*, the set of indices with positive coefficients) is a Young diagram, called the *shape* of π.

As for partitions, we usually just write down the non zero coefficients of a plane partition. Similarly, one can define *skew plane partitions*, where the sequence is now indexed by $\mathbb{N}^{*2}$ deprived from the Young diagram of a partition. Plane partitions can be represented graphically by *3D Young diagrams*, which are piles of cubes. Projected in the plane $x + y + z = 0$, orthogonal to the great diagonal of the cubes, these piles of cubes give tilings of some regions of the plane with rhombi, which are the projection of the visible faces of the cubes.

A plane partition π can be decomposed as a sequence of diagonal slices $(\lambda^{(i)})_{i\in\mathbb{Z}}$. These slices are partitions satisfying interlacing relations

$$\cdots \preceq \lambda^{(-2)} \preceq \lambda^{(-1)} \preceq \lambda^{(0)} \succeq \lambda^{(1)} \succeq \lambda^{(2)} \succeq \cdots$$

For example, the plane partition

$$\pi = \begin{array}{|c|c|c|c|}\hline 5 & 3 & 2 & 2 \\ \hline 4 & 2 & 2 & 1 \\ \hline 2 & 1 \\ \cline{1-2} 1 \\ \cline{1-1} \end{array}, \tag{2.1}$$

whose 3D Young diagram is represented on Figure 2.1, corresponds to the following sequence of interlacing partitions:

$$\cdots \preceq \emptyset \preceq (1) \preceq (2) \preceq (4,1) \preceq (5,2) \succeq (3,2) \succeq (2,1) \succeq (2) \succeq \emptyset \succeq \cdots$$

read along the diagonals of π (or vertical slices of its 3D Young diagram).

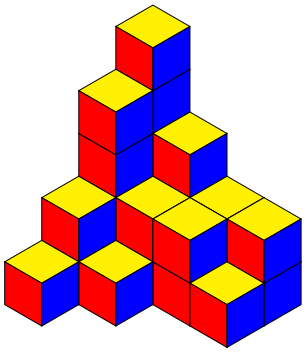

Figure 2.1.: 3D Young diagram corresponding to the plane partition π from (2.1), represented as a stack of cubes in the corner of a room. Projected in the plane, it becomes a tiling of a region of the plane with rhombi with $60/120^\circ$ angles. If the walls of the room are also represented, it gives a tiling of the whole plane with "steep" condition at infinity.

Let us fix two integers $\ell < 0 \leq r$. If we ask $\lambda^{(\ell)}$ and $\lambda^{(r+1)}$ to be the empty partitions, then sequences of partitions $(\lambda^{(j)})_j$ satisfying interlacing relations above are in bijection with plane partitions with support in a box $[1..|\ell|] \times [1..(r+1)]$. We can define a natural Boltzmann probability measure depending on a parameter $q \in (0,1)$ on this set of plane partitions, such that the probability of a plane partition π is:

$$\mathbb{P}_q(\pi) = \frac{1}{Z_{\ell,r}(q)} q^{|\pi|}$$

The quantity $-\log q$ is interpreted as a term of pressure, representing the cost to add a volume unit to the system. The size of a configuration can be decomposed as a sum of contributions, each term corresponding to what has been added/removed when moving from one slice to the next one:

$$|\pi| = \sum_j |\lambda^{(j)}| = \sum_{j=\ell}^{r} j \left(|\lambda^{(j+1)}| - |\lambda^{(j)}| \right)$$

Using the expression for skew Schur functions in one variable, (1.3) we write the weight of π as:

$$q^{|\pi|} = \prod_{\ell}^{r} q^{j(|\lambda^{(j+1)}|-|\lambda^{(j)}|)} = \prod_{j=\ell}^{-1} \mathrm{s}_{\lambda^{(j+1)}/\lambda^{(j)}}(q^{|j|}) \prod_{j=0}^{r} \mathrm{s}_{\lambda^{(j)}/\lambda^{(j+1)}}(q^j) =$$

$$\prod_{j=\ell}^{-1} \langle \lambda^{(j)} | \Gamma_+(q^{|j|}) | \lambda^{(j+1)} \rangle \prod_{j=0}^{r} \langle \lambda^{(j)} | \Gamma_-(q^j) | \lambda^{(j+1)} \rangle \quad (2.2)$$

This Boltzmann measure on bounded width plane partitions is thus a particular case of a Schur process, defined in Section 1.3, with the sequences

$$\underline{a} = (\underbrace{L, \dots, L}_{r-\ell+1}),\ \underline{b} = (\underbrace{+, \dots, +}_{-\ell}, \underbrace{-, \dots, -}_{r+1}) \text{ and } \underline{x} = (\underbrace{q^{|\ell|}, q^{|\ell+1|}, \dots, q}_{-\ell}, \underbrace{1, q, \dots, q^{r-1}, q^r}_{r+1}).$$

2.2. Partition function and particle statistics via vertex operators

The vertex operator formalism is very useful to study plane and skew plane partitions. Let us illustrate this with a very simple case: the computation with this formalism of the generating function (also called the partition function) $Z_{\ell,r}(q)$ of plane partitions with a shape fitting into a $|\ell| \times (r+1)$ rectangle, with a weight q to the number of cubes.

$$Z_{\ell,r}(q) = \sum_{\substack{\pi\text{: plane partition} \\ \text{shape}(\pi) \subset [1..|\ell|] \times [1..(r+1)]}} q^{|\pi|} = \langle \emptyset | \Gamma_+(q^{|\ell|}) \cdots \Gamma_+(q^1) \Gamma_-(q^0) \cdots \Gamma_-(q^r) | \emptyset \rangle,$$

just by summing (2.2) over the intermediate partitions $\lambda^{(\ell+1)}, \dots, \lambda^{(r)}$, using the fact that the boundary partitions $\lambda^{(\ell)}$ and $\lambda^{(r+1)}$ are empty, and that the vectors $|\lambda\rangle$ form an orthonormal basis. Applying several times the commutation relations (1.6), one gets:

$$Z_{\ell,r}(q) = \prod_{i=0}^{|\ell|-1} \prod_{j=0}^{r} \frac{1}{1-q^{i+j+1}},$$

from which in the limit when $|\ell|$ and r go to infinity, we recover the *MacMahon formula* for the generating function of plane partitions:

$$\sum_{\pi\text{: plane partition}} q^{|\pi|} = \prod_{k=1}^{\infty} \frac{1}{(1-q^k)^k}, \quad (2.3)$$

which is a two-dimensional analogue of the well-known Euler generating function for partitions[1]

$$\sum_{\lambda\text{: partition}} q^{|\lambda|} = \prod_{k=1}^{\infty} \frac{1}{1-q^k}. \quad (2.4)$$

[1] This partition generation function can also be derived in the vertex operator formalism, as the limit of $Z_{\ell,r}(q)$ when r goes to infinity and $|\ell|$ is kept equal to 1.

This construction is straightforwardly extended to skew plane partitions, giving a sequence of interlacing partitions, with arbitrary sequence of interlacement relation. One also can play with the parameters of the vertex operators $\Gamma_+(\cdot)$ and $\Gamma_-(\cdot)$ to have a probability measure on these objects giving different weights for cubes on every vertical slice.

Using also the fermionic operators allows one to compute correlations: to measure the presence of a particle in the Maya diagram at position ℓ in the jth partition of the Schur process, it suffices to insert the operator $\psi_\ell \psi_\ell^*$ after the jth operator $\Gamma_\pm(x)$. Suppose that the partition function for our skew plane partitions is

$$Z = \langle \emptyset | \prod_{m=\ell}^{r} \Gamma_\pm(x_m) | \emptyset \rangle.$$

If $(j_1, k_1), \dots (j_p, k_p)$ is such that $j_1 \leq \cdots \leq j_p$, the probability of seeing a particle in partition number j_i at position k_i for every $i \in [1..p]$.

$$\rho_{(j_1,k_1),\dots,(j_p,k_p)} = \frac{1}{Z} \langle \emptyset | \prod_{m_1 \leq j_1} \Gamma\pm(x_{m_1}) \psi_{k_1} \psi_{k_1}^* \prod_{j_1 < m_2 \leq j_2} \Gamma\pm(x_{m_2}) \dots \psi_{k_p} \psi_{k_p}^* \prod_{m_{p+1} > j_p} \Gamma\pm(x_{m_p}) | \emptyset \rangle \tag{2.5}$$

Applying again commutation relations (1.6) both in the numerator and the denominator, one can get rid of the denominator and obtain

$$\rho_{(j_1,k_1),\dots,(j_p,k_p)} = \langle \emptyset | \Psi_{k_1}(j_1) \Psi_{k_1}^*(j_1) \cdots \Psi_{k_p}(j_p) \Psi_{k_p}(j_p) | \emptyset \rangle \tag{2.6}$$

where $\Psi_k(j)$ (resp. $\Psi_k^*(j)$ is the operator ψ_k (resp. ψ_k^*) conjugated by a product of Γ_- and Γ_+^{-1}. Since, as one can see from (1.7), conjugating ψ_k (resp. ψ_k^*) by vertex operators gives a linear combination of ψs (resp. ψ^*s), one can use the following Wick's lemma[2] to compute (2.6):

Lemma 1 (Wick's lemma)**.** *Let $b_1, \dots, b_n$ (resp. $c_1, \dots, c_n$) be linear combinations of creation operators ψ_k (resp. annihilation operators ψ_k^*). Then*

$$\langle \emptyset | b_1 c_1 \cdots b_n c_n | \emptyset \rangle = \det_{1 \leq i,j \leq n} \big(A_{i,j} \big),$$

where

$$A_{i,j} = \begin{cases} \langle \emptyset | b_i c_j | \emptyset \rangle & \text{if } i \leq j, \\ -\langle \emptyset | c_j b_i | \emptyset \rangle & \text{if } i > j. \end{cases}$$

Since commuting operators $\Gamma_+(x)$, $\Gamma_-(y)$ and the generating functions for ψs and ψ^*s involve rational fractions, the quantities $\langle | \emptyset | \Psi_\ell(j) \Psi_{\ell'}^*(j') | \emptyset \rangle$ can be expressed as coefficients of a series expansion of a rational fraction in some domain, which in turn, for analytic purposes is conveniently rewritten as a double contour integral. See [OR03] for

[2]This Wick's lemma is the fermionic version of the usual Wick's lemma computing moments of Gaussian fields. The fact that creation and annihilation operators satisfy anticommutation relations in the fermionic case is at the origin of the signs in the determinant.

details. In particular, this shows that positions of the particles in the Maya diagram form a determinantal process, whose kernel has an integral form, suitable either for explicit evaluation via Cauchy residue theorem, or for asymptotic analysis.

These computations can be easily adapted for skew plane partitions. Particles statistics for Maya diagrams give statistics for the position of horizontal tiles in the random rhombus tilings obtained by the projection of the 3D Young diagrams of the random skew plane partitions, sampled according to such a Boltzmann measure.

2.3. Geometry of large plane partitions

The formalism of vertex operators is extremely useful to study the geometry of large random plane partitions or skew plane partitions. Large random (skew) plane partitions are obtained when the parameter q of the partition function $\sum_\pi q^{|\pi|}$ goes to 1 from below, so that the expected size diverges. In order to have a non degenerate limit, the boundaries ℓ and r also go to infinity in the following way: let $\varepsilon > 0$ be a small parameter which will eventually tend to zero.

- Set $q = q_\varepsilon = e^{-\varepsilon}$.
- Let ℓ_ε and r_ε such that $\varepsilon\ell_\varepsilon$ and $\varepsilon r_\varepsilon$ have a positive (possibly infinite) limit when ε goes to zero.
- Define partitions λ_ε such that the boundary of the Young diagram (in Russian coordinates), rescaled by a factor ε converges to some Lipschitz function f.

In a series of papers [OR03, OR06, OR07], Andrei Okounkov and Nikolai Reshetikhin, studied the case when the graph of the limiting function f is a polygonal line with slope ± 1. They proved:

- a limit shape phenomenon: the expected boundary of the 3D young diagram, rescaled by ε, seen as a graph above the plane $x + y + z = 0$, converges for the sup norm to a some Lipschitz function, which has an explicit description. Convergence in probability and a variational principle can be obtained by either manually controlling the exponential decay of some probabilities for statistics of particles using complex analysis, or adapting the variational principle for tilings derived by Cohn, Kenyon and Propp [CKP01] to this situation. See also [CK01] for a variational principle for (non restricted) large 3D Young diagrams.
- The liquid region is connected, and is tangent to the boundary. The upper boundary of the liquid region is almost everywhere at finite height. The number of points where the arctic curve goes to infinity is the number of *outer corners* of the polygonal line. The arctic curve has as many cusps as *inner corners*.
- The fluctuations are described by the extended incomplete Beta kernel in the bulk of the liquid region, by the GUE corner process close to the turning points, at the vertical boundaries, by the Airy process at a generic point of the arctic curve, and by the Pearcy process at non symmetric cusps.

These results are obtained by looking at the kernel of the determinantal process for the particles in its contour integral form, and performing steepest descent analysis.

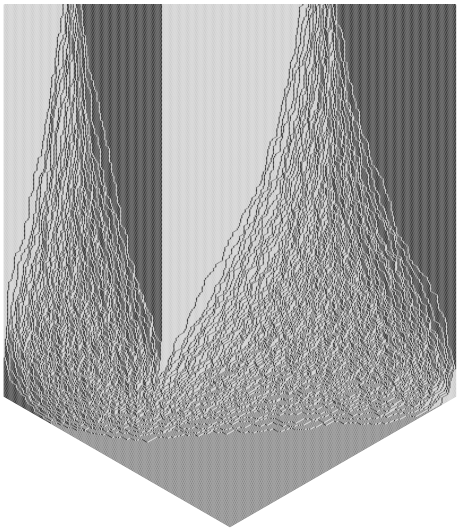

Figure 2.2.: Figure of a large skew plane partition in the setting studied by Okounkov and Reshetikhin, stolen from [OR07].

Random skew plane partitions with a piecewise periodic back wall

In a joint work [11] with Sevak Mkrchtyan, Nicolai Reshetikhin and Peter Tingley, we looked at another class of limiting situations: the sequence of renormalized profiles of the sequence (λ_ε) converges to a polygonal line f with slope always strictly between -1 and -1. Whereas several features were identical to the case studied by Okounkov and Reshetikhin (universality of the fluctuations in the bulk and close to the boundary), some others are drastically different:

Proposition 4 ([11], Proposition 3.1)**.** *The liquid region extends to infinity upwards above every point in the interior of the domain.*

The arctic curve has just a unique connected component, separating the liquid region above it, and frozen regions below, and projects injectively on f.

If we zoom in around a point of the liquid region, then the tiling seems to look like a tiling of the whole plane with rhombi. There is a two-parameter family of "conditionally uniform" ergodic Gibbs measures on tilings of the planes by rhombi [KOS06] (equivalently on dimers on the hexagonal lattice), the parameters corresponding to the average slope of the corresponding height function.

We proved the following:

Theorem 1 ([11], Theorem 4.1)**.** *Around a given point in the interior of the liquid region, the measure on tilings converges weakly to an ergodic Gibbs measure on tilings of the whole plane, with a slope expressed as a function of the critical points of the function appearing in the steepest descent analysis, which is also the slope of the limit shape at that point.*

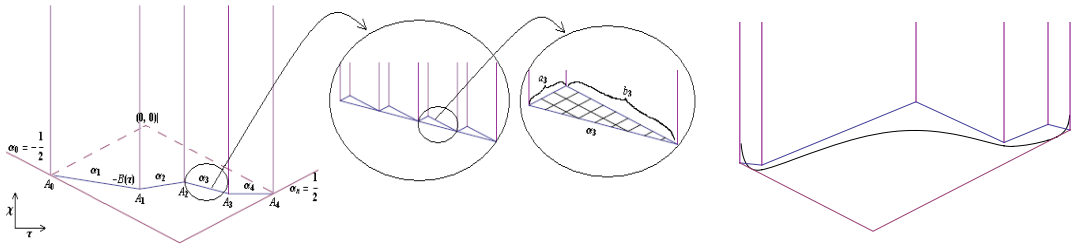

(a) (b)

Figure 2.3.: (a) Setup for large skew plane partitions with limiting f with slope strictly between -1 and 1 from [11]. (b) The limiting arctic curve in one example of this setup.

The fact that local correlations near a point in a large domain should behave like the ergodic measure with a slope given by the tangent plane to the limit shape is very natural statement for general dimer models of large domains, but is still a conjecture, except for specific cases where it has been proven (see for example [Ken08, Pet15]).

The idea of the proof is very simple in this case and consists in noticing that an ergodic Gibbs measure on dimers of the hexagonal lattice is, as the correlations for rhombi in the liquid region, like in [OR07], given by the extended incomplete Beta kernel, and relating the corresponding parameters to the slope of the height function.

When going up, the density of horizontal rhombi in a random configuration stays positive but decreases and converges to zero. A natural question is to study the statistics of the horizontal tiles, using a different scaling in both directions.

Theorem 2 ([11], Theorem 4.3)**.** *When going up, the distribution of horizontal rhombi, once the vertical direction is rescaled by a factor ε, converges to an ergodic Gibbs measure of the* bead process*.*

The bead process [6] is a determinantal point process on $\mathbb{Z}\times\mathbb{R}$, where configurations are interlacing point configuration: between two successive points on $\{n\}\times\mathbb{R}$, there is exactly one point on $\{n-1\}\times\mathbb{R}$ and $\{n+1\}\times\mathbb{R}$. It is a natural object to describe the limit of dimer models on the hexagonal lattice and more generally on any periodic bipartite graph, when the weight of one type of edge goes to zero. There is a two-parameter family of ergodic Gibbs measures for the bead process, whose corresponding kernels are *extended sine kernels*: the two parameters are the *density* (the average number of beads per unit interval) and the *tilt*, describing the tendency of a bead to prefer being closer to its north-east neighbor rather than to it south-east neighbour.

In the case of skew plane partitions, the expression for the density and the tilt is an explicit expression of the abscissa, and the limiting polygonal contour for the partitions (λ_ε), in terms of lengths of linear pieces and angles at corners.

These results have been generalised by Sevak Mkrtchyan [Mkr11] to the situation where the limiting function f for the boundary of the removed partition is piecewise linear with

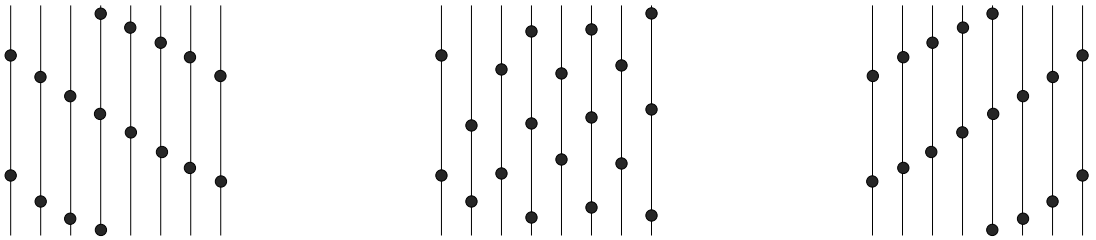

Figure 2.4.: Three pieces of configurations of the bead process for the same density, but different values of the tilt.

slopes in the closed interval $[-1, 1]$, where mixed behaviour between [OR07] and [11] can occur at corners (cusp-like on one side where the slope of f is ± 1, and liquid region up to the top where it is in $(-1, 1)$).

A slightly different situation where analogous results were obtained is for rhombus tilings corresponding to Gelfand-Tsetlin patterns, which can be described as a sequence of increasing interlacing partitions, starting from the empty one. A complete description when the rescaled Young diagram of the last partition converges to a polygonal broken line with slope ± 1 (corresponding to a density of particles in the Maya diagram converging to a union of indicator functions of intervals), was obtained by Leonid Petrov [Pet14, Pet15]. More general results when the particle density converges to some measure have been obtained in a series of papers by Erik Duse, Kurt Johansson and Anthony Metcalfe [DM15a, DM15b, DJM15].

2.4. Steep domino tilings

To describe plane partitions with a Schur process, we needed only the notion of interlacement $\preceq$. However, an implicit relation with the Schur processes was used to study the tilings of the Aztec diamond in [Joh02].

Recently, this connection with the Aztec diamond and a wider family of domino tilings, called *steep domino tilings*, was made explicit [BCC14]. The partition function of these models can be computed with the vertex operator formalism, following ideas from [You10]. They have a natural notion of volume, which, when used as a grading for enumeration, give a partition function with a product form with terms $(1 \pm q^{\text{some power}})^{\pm 1}$.

This includes the case of the Aztec diamond [EKLP92b] of size n

$$Z_{AD_n}(q) = \prod_{k=1}^{n} (1 + q^{2k-1})^{n+1-k},$$

and pyramid partitions

$$Z_{PP}(q) = \prod_{k \geq 1} \frac{(1 + q^{2k-1})^{2k-1}}{(1 - q^{2k})^{2k}}.$$

This formula was conjectured by Richard Kenyon [Ken05] and Balázs Szendrői [Sze08], and proved by Benjamin Young combinatorially [You09] and with vertex operators [You10].

They are obtained as Schur processes where now the $\underline{a}$ sequence is not constant equal to L, but alternates between L and R. The $\underline{b}$ sequence for the Aztec diamond is $(+-)^n$, whereas for pyramid partitions, it is $\cdots + + - - \cdots$. Combinatorial and enumerative facts about these steep tilings are given in [BCC14], in particular the way to compute the partition function as a result of the commutation relations between the vertex operators.

Sunil Chhita and Benjamin Young [CY14] gave an explicit expression for the inverse Kasteleyn matrix of the Aztec diamond, which is, up to minor details, the kernel of the determinantal process describing the position of the dominos. Their proof is using induction via the urban renewal transformation and explicit residue computation, but the formula has the same flavor as the one obtained by Okounkov and Reshetikhin with vertex operators. Can we derive the formula of Chhita and Young via vertex operators? What is the meaning of the presence of a domino in a steep tiling in terms of particles in the Maya diagram? Can this be extended to a general framework which would contain other Schur processes? In particular, it is remarkable that both skew plane partitions (giving rhombus tilings) and steep domino tilings were examples of dimer models. It is then natural to ask whether other Schur processes can be expressed as a dimer model. All those questions were answered in of [15], the main results of which are exposed in Chapter 3.

3. Dimers on Rail Yard Graphs

In a joint work [15] with Jérémie Bouttier, Guillaume Chapuy, Sylvie Corteel and Sanjay Ramassamy, we introduce a family of planar graphs, called *rail yard graphs*. They are periodic in the vertical direction, obtained by concatenating from left to right four kinds of elementary graphs. From dimer models on these rail yard graphs, with suitable boundary conditions, we can recover the Schur processes described in Chapter 1. The dimer statistics (and not only those corresponding to particles in the Schur process) can be computed using vertex operators, creating a bridge between this formalism and Kasteleyn approach.

3.1. Rail Yard Graphs

Rail yard graphs form a family of planar graphs, indexed by the following data $(\ell, r, \underline{a}, \underline{b})$, with two integers $\ell < r$, the *LR sequence* $\underline{a} = (a_\ell, \dots, a_r) = \{L, R\}^{[\ell..r]}$ and the *sign sequence* $\underline{b} = (b_\ell, \dots, b_r) = \{+, -\}^{[\ell..r]}$. Note that this is exactly the same data used to described Schur processes in Chapter 1, except the weight sequence $\underline{x}$, which will be introduced later when we talk about dimers.

Definition 13. The *rail yard graph* associated with the integers ℓ and r, the LR sequence $\underline{a}$ and the sign sequence $\underline{b}$, and denoted by $\mathrm{RYG}(\ell, r, \underline{a}, \underline{b})$, is the bipartite plane graph defined as follows. Its vertex set is $[2\ell - 1..2r + 1] \times (\mathbb{Z} + 1/2)$, and we say that a vertex is *even* (resp. *odd*) if its abscissa is an even (resp. odd) integer. Each even vertex $(2m, y)$, $m \in [\ell..r]$, is then incident to three edges: two *horizontal* edges connecting it to the odd vertices $(2m - 1, y)$ and $(2m + 1, y)$, and one *diagonal* edge connecting it to

- the odd vertex $(2m - 1, y + 1)$ if $a_m = L$ and $b_m = +$,
- the odd vertex $(2m - 1, y - 1)$ if $a_m = L$ and $b_m = -$,
- the odd vertex $(2m + 1, y + 1)$ if $a_m = R$ and $b_m = +$,
- the odd vertex $(2m + 1, y - 1)$ if $a_m = R$ and $b_m = -$.

A rail yard graph is infinite and 1-periodic in the vertical direction. When $\ell = r$, the LR and sign sequences both consist of a single element, and the corresponding rail yard graph, which is said *elementary*, is of one of four possible types, see Figure 3.1. Given two rail yard graphs $\mathrm{RYG}(\ell, r, \underline{a}, \underline{b})$ and $\mathrm{RYG}(\ell', r', \underline{a}', \underline{b}')$ such that $\ell' = r + 1$, we define their *concatenation* by taking the union of their vertex and edge sets. It is nothing but the rail yard graph $\mathrm{RYG}(\ell, r', \underline{aa}', \underline{bb}')$ where $\underline{aa}'$ and $\underline{bb}'$ denote the concatenations of the LR and sign sequences. Clearly, a general rail yard graph is obtained by concatenating elementary ones.

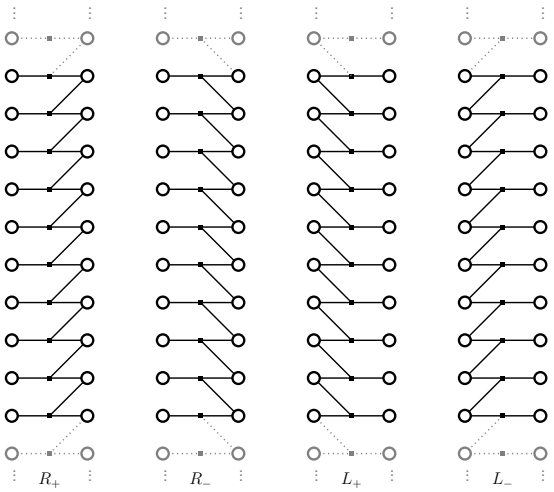

Figure 3.1.: The four elementary rail yard graphs $L+$, $L-$, $R+$, and $R-$ (up to horizontal translation)

The *left boundary* (resp. *right boundary*) of a rail yard graph consists of all odd vertices with abscissa $2\ell - 1$ (resp. $2r + 1$). Vertices which do not belong to the boundaries are said *inner*. When drawn in the plane, the graph delimits some faces, and the bounded ones are called *inner faces*. Note that inner faces may be incident to 4, 6 or 8 edges. Finally, observe that our definition works equally well if we take $\ell = -\infty$ and/or $r = +\infty$, thus considering infinite LR and sign sequences. In that case, the rail yard graph "fills" either the whole plane or a half-plane, boundaries being sent to infinity.

3.2. Dimer models on rail yard graphs

We will define a probability measure on dimer coverings of a rail yard graph. In contrast with the dimer coverings considered elsewhere in this text, here some of the vertices may stay unmatched, but only if they are boundary vertices, *i.e.*, in the leftmost or rightmost column.

Definition 14. Let $G = \mathrm{RYG}(\ell, r, \underline{a}, \underline{b})$. An *admissible dimer covering* of G is a partial matching of the graph such that:

- every inner vertex of G is matched,
- there exists $N \in \mathbb{N}$ such that any left boundary $(2\ell - 1, y)$ is covered for $y > N$ and uncovered if $y < -N$, and any right boundary $(2r + 1, y)$ is covered for $y < -N$ and uncovered if $y > N$,
- only a finite number of diagonal edges are used in the partial matching.

A *pure dimer covering* of G is an admissible dimer covering where the property above is true for $N = 0$.

Let $\underline{x} = (x_\ell, \ldots, x_r)$ a sequence of formal variables. Define for an admissible dimer

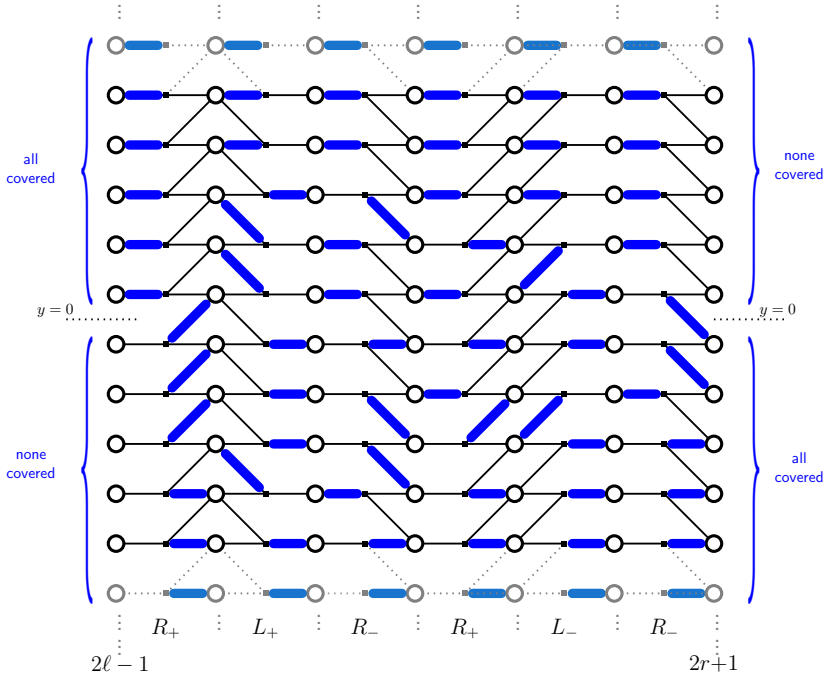

Figure 3.2.: A pure dimer covering of the rail yard graph RYG$(\ell, r, \underline{a}, \underline{b})$, with $\underline{a} = RLRRLR$ and $\underline{b} = ++-+--$.

covering C, its weight $w(C)$ as follows:

$$w(C) = \prod_{j=\ell}^{r} x_j^{d_j(C)},$$

where $d_j(C)$ is the number of diagonal edges in column i (*i.e.*, incident to an even vertex of abscissa $2i$).

The *partition function* $Z(G; \underline{x})$ of the dimer model on G is the sum of all the weights of all *pure* dimer coverings of G. The partition function has a very nice product formula:

Theorem 3 ([15], Theorem 1)**.**

$$Z(G; \underline{x}) = \prod_{\ell \le i < j \le r} z_{ij}, \qquad \textit{where} \qquad z_{ij} = \begin{cases} 1 + x_i x_j & \textit{if } a_i \neq a_j, \\ (1 - x_i x_j)^{-1} & \textit{if } a_i = a_j. \end{cases}$$

An interesting specialisation of the sequence of formal variables $\underline{x}$, called the q-RYG specialisation, is the following:

$$\forall\ j \in [\ell..r], \quad x_j = q^{-j b_j} = \begin{cases} q^j & \text{if } b_j = - \\ q^{-j} & \text{if } b_j = + \end{cases}$$

The exponent of q in the weight of C is equal to the minimal number of flips of dimers around a face to perform to get C from the *fundamental dimer covering*, where all the dimers are horizontal[1]. This is the one we used for plane partitions in the previous chapter, when the LR sequence $\underline{a}$ is constant equal to L: in that case, the rail yard graphs are strips of the honeycomb lattice, and their dimer coverings correspond by duality to rhombus tilings, which are projections of piles of a finite number of cubes.

3.3. Dimer correlations

We now suppose that the variables x_j are specialised in such a way that the weights of pure dimer configurations are positive and the partition function is finite, in order to have a probabilistic (or statistical physics) interpretation of the model. This means that $x_j > 0$ for all j, and $x_i x_j < 1$ if $b_i = +, b_j = -, a_i = a_j$ and $i < j$.

The probability $\mathbb{P}_{G;\underline{x}}(C)$ of a pure dimer configuration C is the ratio $w(C)/Z(G;\underline{x})$. Given a finite subset E of edges of the graph G, we denote also by $\mathbb{P}_{G;\underline{x}}(E)$ the probability that the edges of E are present in the random dimer covering of G.

We get a general formula for the probability of such a set of edges as a determinant of a matrix with explicit entries in terms of the geometry of the graphs and the edges in E.

Define for any integer k the following rational fraction:

$$F_k(z) = \frac{\displaystyle\prod_{\substack{i:(a_i,b_i)=(R,+)\\ 2i<k}} (1+x_i z) \prod_{\substack{j:(a_j,b_j)=(L,-)\\ 2j>k}} (1-\frac{x_j}{z})}{\displaystyle\prod_{\substack{i:(a_i,b_i)=(L,+)\\ 2i\leq k}} (1-x_i z) \prod_{\substack{j:(a_j,b_j)=(R,-)\\ 2j\geq k}} (1+\frac{x_j}{z})}$$

For $\alpha = (\alpha^{\mathrm{x}}, \alpha^{\mathrm{y}})$, $\beta = (\beta^{\mathrm{x}}, \beta^{\mathrm{y}})$ two vertices of G such that α^{x} is even and β^{x} is odd, define

$$\mathcal{C}_{\alpha,\beta} = \oint_{C_z} \oint_{C_w} \frac{F_{\alpha^{\mathrm{x}}}(z)}{F_{\beta^{\mathrm{x}}}(w)} \frac{w^{\beta^{\mathrm{y}}}}{z^{\alpha^{\mathrm{y}}}} \frac{\sqrt{zw}}{z-w} \frac{\mathrm{d}z}{2i\pi z} \frac{\mathrm{d}w}{2i\pi w}. \tag{3.1}$$

where the simple positively oriented contours C_z and C_w should satisfy the following conditions:

- C_z should encircle 0 and all negative poles of $F_{\alpha^{\mathrm{x}}}(z)$, but not the positive ones
- C_w should encircle 0 and the positive zeros of $F_{\beta^{\mathrm{x}}}(w)$, but not the negative ones
- C_z and C_w should not intersect and C_z should surround C_w if and only is $\alpha^{\mathrm{x}} < \beta^{\mathrm{x}}$

It corresponds to the extraction of the coefficient of $z^{\alpha^{\mathrm{y}}}\ w^{-\beta^{\mathrm{y}}}$ in a series expansion in z and w of the rational fraction $\frac{F_{\alpha^{\mathrm{x}}}(z)\sqrt{zw}}{F_{\beta^{\mathrm{x}}}(w)(z-w)}$ in a particular domain of convergence.

Theorem 4 ([15], Theorem 5)**.** *Let $E = \{e_1, \ldots, e_s\}$ be a finite set of edges of $G = \mathrm{RYG}(\ell, r, \underline{a}, \underline{b})$, with $e_i = (\alpha_i, \beta_i)$. Then:*

$$\mathbb{P}_{G;\underline{x}}(E) = (-1)^{H(E)} \underline{x}^{\underline{n}} \det_{1\leq i,j\leq s} (\mathcal{C}_{\alpha_i,\beta_j}),$$

[1] It is easy to check that such a pure dimer covering with only horizontal dimers exists for any rail yard graph and is unique.

with $H(E)$ the number of horizontal edges in E whose right endpoint is at an even abscissa, $\underline{x}^{\underline{n}} = x_\ell^{n_\ell} \cdots x_r^{n_r}$, with n_k the number of diagonal edges in column k.

The fact that this probability is a determinant is not surprising: since the graph G is planar and bipartite, the Kasteleyn theory of dimer models tells us that this probability can be computed via a minor of the inverse of a Kasteleyn matrix associated to the graph[2] G. We prove [15, Theorem17] that indeed, the matrix $\mathcal{C}$ whose entries are defined by Equation (3.1) is indeed the inverse of such a Kasteley matrix.

From a pure dimer covering C of a rail yard graph G, one can construct a sequence of Maya diagrams, which describe the state of edges at the juncture of two successive elementary graph which compose G.

For $j \in [\ell..r+1]$, the jth Maya diagram $\mathbf{m}_k(C) \in \{\circ, \bullet\}^{\mathbb{Z}+\frac{1}{2}}$ is constructed as follows:

$$\mathbf{m}_j(C)_k = \begin{cases} \circ & \text{if } (2j-1,k) \text{ is not connected to a dimer on its left in } C, \\ \bullet & \text{if } (2j-1,k) \text{ is not connected to a dimer on its right in } C. \end{cases}$$

This construction gives in particular the following:

Lemma 2. *Under the measure $\mathbb{P}_{G;\underline{x}}$, the sequence of Maya diagrams follows a Schur process with parameters given by the sequences $\underline{a}$, $\underline{b}$ and $\underline{x}$.*

On some of the edges in G, those in simple columns[3], the presence or absence is directly related to the presence of a white or a black marble in the closest Maya diagram to these edges. See Figure 3.3 (A). The statistics for those edges can be computed directly from statistics for Schur processes, either by the vertex operator formalism as presented in the previous chapter, or by Eynard-Mehta theorem (see *e.g.*,[BR05]). In particular, if the sequence $\underline{a}$ is constant equal to L and the edges in E are all horizontal edges in simple columns, Theorem 4 reduces to correlations for plane partitions of [OR03].

For edges in double columns, there is no direct direct correspondence between dimers and marbles in Maya diagrams. However, there is a bijection between configurations with given dimers on double columns and dimer coverings with defects. The partition function of the configurations with defects can be written down in terms of vertex operators and creation/annihilation operators appearing in more complicated combination than just projectors, see Figure 3.3 (B) and (C). Although these quantities do not have directly a direct probabilist interpretation on Maya diagrams, they allow one to compute correlations of dimers, with the kind of formula as (2.6).

One of the interesting features of Theorem 4 is that we have an explicit formula for the kernel of the determinantal process, with a double contour integral which can be evaluated explicitly if needed. As in the case of Okounkov and Reshethin, this integral form is particularly suitable for asymptotic analysis via the steepest descent analysis, and allows to get results for large rail yard graphs.

[2] once we have removed the unmatched vertices on the boundary.

[3] The simple column of elementary graph of type L (resp. R) is the rightmost (resp. leftmost), which contains only horizontal edges.

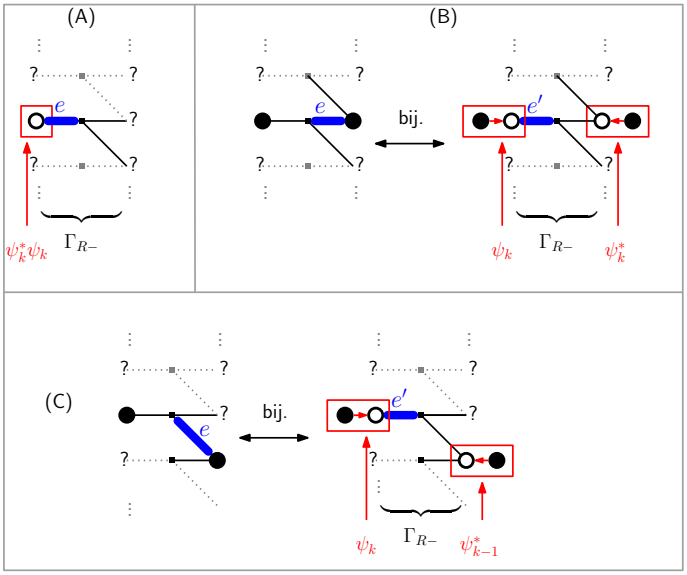

Figure 3.3.: Localization of dimers in the case of the elementary graph or type $R-$ (the case of $R+$ is similar). Marbles (resp. edges) whose status is not fixed by the discussion are represented with question marks (resp. dotted lines). (A) There is a horizontal dimer in the left column if and only if the left odd vertex is occupied by a white marble. This marble is localized by applying the operator $\psi_k^*\psi_k$. (B) Configurations with a horizontal dimer in the right column are such that both marbles on this level are black (although this condition is not sufficient). They are in bijection with configurations with a dimer in the left column such that both marbles on this level are white. The operator ψ_k^* (resp. ψ_k) inserted on the right (resp. left) has the double effect of switching the color of marbles on the k-th level and of forcing the colors of these marbles. (C) The case of a diagonal dimer.

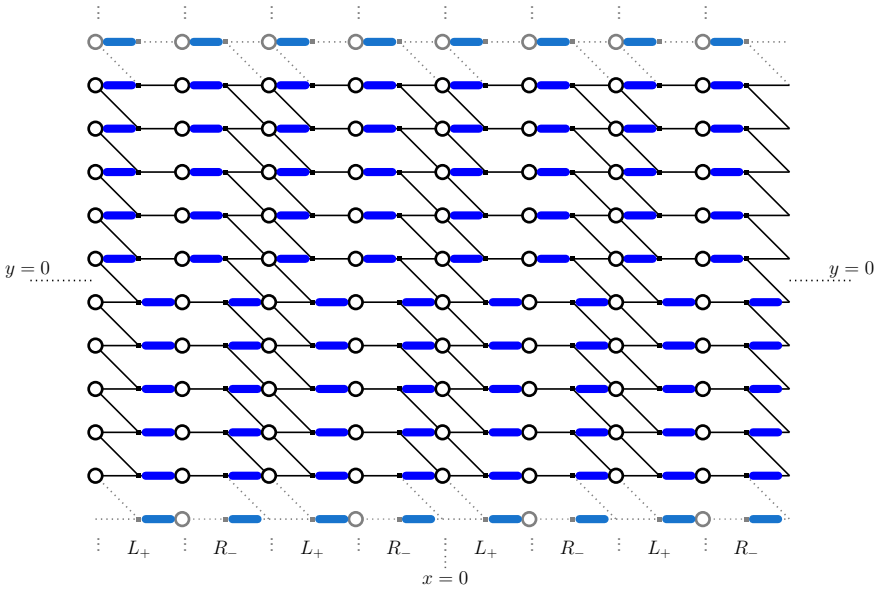

Figure 3.4.: A rail yard graph with LR sequence $\underline{a} = (LR)^n$ and sign sequence $\underline{b} = (+-)^n$ for $n = 4$, equipped with its fundamental dimer covering.

These results thus generalize those obtained for skew plane partitions, and their corresponding rhombus tilings, when the LR sequence is constant to L. Instead of taking the $\underline{a}$ sequence constant equal to L, which gives rail yard graphs with degree 6 internal faces, one can alternate L and R. By doing so, one gets graphs with internal faces of degree 4 or 8, but degree 8 faces have two degree 2 vertices, which can reduced (by contracting the two incident edges and merging their two neighbors) to get a graph on which the dimer model is equivalent, and where all faces are degree 4: it is even a slice of the square lattice. Pure dimer coverings are in fact in bijective correspondence with steep tilings.

A particular example is the Aztec diamond discussed briefly earlier. In the following section, we list some classic or recent results, published or unpublished, about this tiling model, obtained with various specific approaches, but which can now be rederived with this formalism, as consequences of Theorem 4.

For more details, and connection to other tiling models, we refer the reader to the original article [15].

3.4. Applications to the case of the Aztec diamond

When $\ell = 0$, $r = 2n-1$, $\underline{a} = (LR)^n$ and $\underline{b} = (+-)^n$, the dimer model on the corresponding rail yard graph is reducible to tilings of the Aztec diamond of size n by dominos. See Figures 3.4 and 3.5.

There are several probability measures on tilings of the Aztec diamond, which correspond to specialisations of the weights x_i:

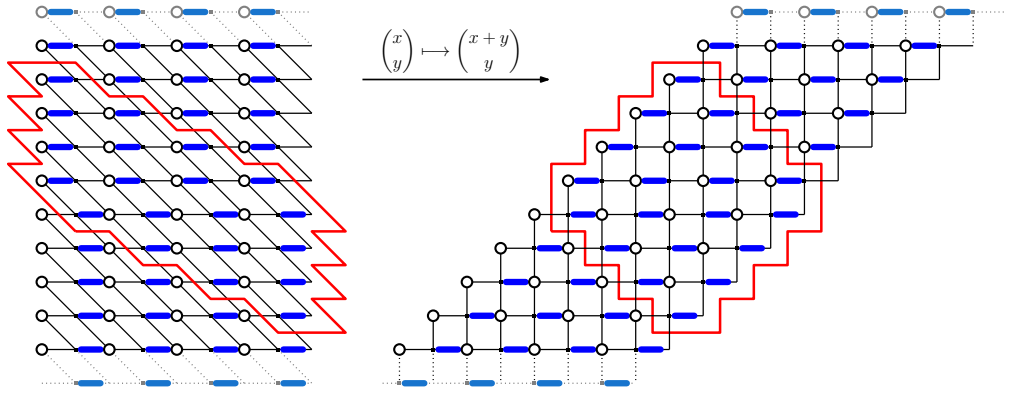

Figure 3.5.: Left: The graph obtained by contracting all the vertices of degree 2 in the RYG of Figure 3.4, that is, all the vertices of abscissa congruent to 2 mod 4. Right: the image of the graph on the left by the linear transformation $\binom{x}{y} \mapsto \binom{x+y}{y}$. The graph is a portion of a square lattice of mesh 1. On both sides, the region of the graph where a covering may differ from the fundamental one is represented in red. One recognizes the shape of the Aztec diamond of size $n = 4$. Note that the coordinate transformation on uncontracted vertices to go directly from the graph of Figure 3.4 to the graph on the right is given by $\binom{x}{y} \mapsto \binom{\phi(x)+y}{y}$ where $\phi(x) = x - 2\lfloor \frac{x+2}{4} \rfloor$ if $x \geq 0$ and $\phi(-x) = -\phi(x)$.

- the uniform distribution, obtained by taking $x_i = 1$ for all i,
- the *biased* distribution, obtained by taking $x_i = 1$ for i even and $x_i = \lambda > 0$ for i odd (or equivalently $x_i = \sqrt{\lambda}$ for all i): this corresponds to attaching a weight λ to each pair of diagonal dimers (which become vertical dominos in the Aztec diamond picture),
- the so-called q^{vol} distribution, obtained by taking $x_i = q^i$ for i odd and $x_i = q^{-i}$ for i even (which is the q-RYG specialization), and more generally the biased q^{vol} distribution, obtained by taking $x_i = \lambda q^i$ for i odd and $x_i = q^{-i}$ for i even.

3.4.1. Creation rate and edge probability generating function

A quantity of interest is, under the biased distribution, the probability $\mathbb{P}_\lambda(x, y; n)$ that $(x - 1/2, y)$ is the center of a *west going domino*[4] in the Aztec diamond of size n. From Figure 3.4, one sees that a west going domino corresponds to a diagonal edge in a $L+$ column of the corresponding rail yard graph.

The probability $\mathbb{P}_\lambda(x, y; n)$ can be computed readily from Theorem 4. Related quantities

[4]The terminology comes from the *domino shuffling* algorithm: a west going domino corresponds to vertical dimer in the square lattice with a top white vertex. In a step of the domino shuffling algorithm, these dimers move to the left.

of interest are the so-called *biased creation rate*

$$\mathrm{Cr}_\lambda(x,y;n) = \frac{\lambda+1}{\lambda}\big(\mathbb{P}_\lambda(x,y;n) - \mathbb{P}_\lambda(x+1,y;n-1)\big),$$

and the *edge probability generating function*

$$\Pi_\lambda(u,v,t) = \sum_{x,y,n} \mathbb{P}_\lambda(x,y;n) u^x v^y t^n.$$

Proposition 5 ([15], Proposition 21)**.** *The biased creation rate equals*

$$\mathrm{Cr}_\lambda(x,y;n) = \left(\frac{\lambda}{\lambda+1}\right)^{n-1} c_\lambda(A,B,n-1)c_\lambda(B,A,n-1)$$

where $A = n-m-y = (x-1-x-y)/2$, $B = m-1 = (n-1+x-y)/2$, *and* $c_\lambda(A,B,n)$ *is the coefficient of* z^A *in* $(1-z)^B(1+\lambda^{-1}z)^{n-B}$.

Remark 2. The quantities $c_\lambda(A,B,n)$ are Krawtchouk polynomials, which play a great rôle in the analysis of the Aztec diamond, see [Joh02].

The idea of the proof is that taking the difference of two $\mathbb{P}_\lambda$ makes appear in the numerator of the rational fraction a factor $(z-w)$, which cancels the same factor in the denominator. After this cancellation, the rational fraction decouples, and the result can be rewritten as a product of two single contour integrals, which can both be transformed into integral representations of the Krawtchouk polynomials.

Proposition 6 ([15], Proposition 21)**.** *The biased edge probability generating function equals*

$$\Pi_\lambda(u,v,t) = \frac{\lambda t}{(1-t/u)((1+\lambda)(1+t^2) - t(u+u^{-1}) - \lambda t(v+v^{-1}))}. \tag{3.2}$$

To prove this formula, one plugs the integral formula of $\mathbb{P}_\lambda(x,y;n)$ in the definition of $\Pi(u,v,t)$. The sums over x and n can be performed explicitly as geometric series. The sum over y acts as a Dirac distribution, and allows one to remove one of the contour integrals. Computing explicitly the remaining integral by Cauchy theorem yields the result.

These results were used for example in [CEP96] as a way to prove the arctic circle theorem, and its generalization for arbitrary λ. However, the formula appeared without proofs, supposed to appear in an article by Gessel, Ionescu and Propp, that has not been published so far. Formula (3.2) for $\lambda = 1$ appears in [Hel00] and [Du11], and used in [BP11] as yet another route to the arctic circle. See [15], Section 6.1, for more details about these quantities.

3.4.2. The inverse Kasteleyn matrix

In [CY14], Sunil Chhita and Ben Young give an explicit expression for the inverse of the Kasteleyn matrix for the biased q^{vol} distribution. They write down an expression by extrapolating the expression of the kernel of the determinantal process for a particle system encoded in the Aztec diamond [Hel00] in the uniform case. To prove that the expression they give is indeed the inverse Kasteleyn matrix, they do an *ad-hoc* computation, based on induction, which is long and tedious.

We prove [15, Section 6.2] that up to a simple change of variables that the entries of their inverse Kasteleyn matrix are equal (up to multiplicative factors cancelling in the determinant) to the coefficients $\mathcal{C}_{\alpha,\beta}$. The interpretation in terms of rail yard graphs gives thus a constructive proof of that formula, and an explanation of the double contour integral representation.

The formula for the inverse Kasteleyn matrix from [CJY15] for the biased distribution on Aztec diamond can be also obtained from the formula for $\mathcal{C}_{\alpha,\beta}$.

The technique used by Chhita and Young in [CY14] also applies to more general weights on the Aztec diamond, like the *double weighting*, which yields in that case to a quadruple integral representation for the entries of the inverse Kasteleyn matrix, and two of them can be performed explicitly [CJ16]. To our knowledge, this weighting does not fit in the rail yard graph framework.

3.4.3. The arctic circle theorem

Yet another proof of the arctic circle [JPS98] can be given, by following the ideas of Okounkov and Reshetikhin in the case of skew plane partitions. To prove convergence in expectation of the limit shape, it is enough to look at the probability that at a given point even vertex $\alpha = (2m, y - \frac{1}{2})$ is connected to a diagonal dimer. When n is large, $m = \tau n$ and $y = \chi n$, this probability can be written as

$$p_\alpha = \oint_{C_z} \oint_{C_w} e^{n(S(\chi,\tau;z) - S(\chi,\tau;w) + o(1))} \frac{1}{z-w} \frac{\mathrm{d}z \mathrm{d}w}{(2i\pi)^2},$$

where

$$S(\tau, \chi; z) = -\tau \log(1-z) - (1-\tau)\log(1+\frac{1}{z}) - \chi \log z.$$

We now proceed as in [OR03] to obtain the asymptotics of this probability. For fixed (τ, χ), the function $z \mapsto S(\tau, \chi; z)$ has two critical points.

- If the two critical points are real, the integral goes to 0 or 1 exponentially fast with n by the saddle point method. The point (τ, χ) is in the frozen region.
- If the two critical points are complex conjugate, one can move the contours so that they cross transversally at the complex critical points to apply again the saddle point method. By doing so, we pick the contribution of the residue at $z = w$, which gives the main contribution of the integral, giving a result strictly between 0 and 1.

The transition between those two regimes correspond to the value of (τ, χ) for which the two critical points merge. This happens when the discriminant of the numerator of

$\partial S(\tau, \chi; z)/\partial z$ is equal to zero. This gives

$$(2\tau - 1)^2 - 4(\tau + \chi)(1 - \chi - \tau) = 0, \tag{3.3}$$

which under the change of variables

$$\begin{cases} u = 2\tau + \chi \\ v = \chi \end{cases} \tag{3.4}$$

corresponds to the circle $2(u-1)^2 + 2v^2 = 1$ inscribed in the limiting square of the Aztec diamond, given by $|u - 1| + |v| \leq 1$.

4. Perfect simulations of Schur processes

In a joint work [13] with Dan Betea, Jérémie Bouttier, Guillaume Chapuy, Sylvie Corteel, and Mirjana Vuletić, we describe a simple sampling algorithm for Schur processes This algorithm is a sequence of atomic steps, which are based on bijective proofs of the Cauchy identities (1.1) and (1.4). Since some Schur processes correspond bijectively to rhombus or domino tilings, this algorithm can be used to efficiently generate random tilings.

Exact sampling algorithms for classes of tilings have been proposed before, including the case of plane and skew plane partitions [Bor11] and the Aztec diamond [EKLP92b]. See also [BF14] for a general approach, and [BF15] for an application of this approach to a restricted class of graphs including, but not limited to the Aztec diamond. Our algorithm described below, different from but somewhat similar to that of [Bor11] allows one to sample general Schur processes, which under appropriate specialisation, give plane and skew plane partitions, tilings of the Aztec diamond by dominos, pyramid partitions and more generally steep tilings.

Moreover, the algorithm we propose is entropy optimal (if we suppose that we can generate Bernoulli and geometric random variables optimally), in the sense that the random input of the algorithm can be reconstructed completely from the output. See [13], Proposition 3.8.

Following the notation of the previous chapters, our Schur processes will be defined by the sequences $\underline{a} = (a_\ell, \dots, a_r)$ and $\underline{b} = (b_\ell, \dots, b_r)$, and parameters $\underline{x} = (x_\ell, \dots, x_r)$, and will generate random sequences of interlacing/dually interlacing partitions $\Lambda = (\lambda^{(\ell)}, \dots, \lambda^{(r+1)})$, such that $\lambda^{(\ell)} = \lambda^{(r+1)} = \emptyset$. The measure on sequences of partitions is such that, according to (1.5),

$$\mathbb{P}(\Lambda) \propto \prod_{j=\ell}^{r} x_j^{\left||\lambda^{(j+1)}|-|\lambda^{(j)}|\right|}.$$

For notation convenience, we will suppose here that $\ell = 0$ and $r = n-1$, so that the non trivial partitions are labelled from 1 to $n-1$, and the sequences $\underline{a}$, $\underline{b}$ and $\underline{x}$ have length n.

The *encoded shape* of the Schur process is the Young diagram whose boundary is the lattice path of length $n+1$ constructed by the sequence $\underline{b}$ as follows: $+$ corresponds to a horizontal step to the right, and $-$ corresponds to a vertical up step[1]. See Figure 4.1.

The edges of the path encoded by $\underline{b}$ are decorated with the elements of the sequences $\underline{a}$ and $\underline{x}$. The different partitions of the realisation of the Schur process Λ are attached to vertices visited by this path.

[1] In [13], the encoded shape is represented as a Young diagram in *French coordinates*, so the notion of vertical *up* and *down* steps are exchanged.

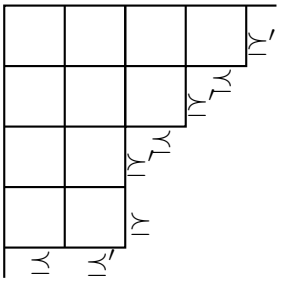

Figure 4.1.: The sequence of interlacing relations $(\preceq, \preceq', \succeq, \succeq', \preceq, \succeq', \preceq, \succeq')$, whose $\underline{b}$ sequence is $(--++-+-+)$, has an encoded shape given by the partition $\pi = (4, 3, 2, 2)$.

If the encoded shape is empty (*i.e.*, the $\underline{b}$ sign sequence is of the form $-\cdots-+\cdots+$), then there is a unique admissible sequence of partitions Λ for the corresponding Schur process, whatever the values of the $\underline{a}$ and $\underline{x}$ sequences, namely the one where all partitions $\lambda^{(j)}$ are empty. This one is thus particularly easy to simulate.

The idea of the algorithm to simulate a generic Schur process with arbitrary sequences $\underline{a}$, $\underline{b}$ and $\underline{x}$ is to start from the empty encoded shape with the same number of horizontal/vertical steps as would give the sequence $\underline{b}$, decorated with the empty partitions on vertices, and the elements of the sequences $\underline{a}$ and $\underline{x}$ reordered in a particular way. Then we grow the encoded shape, by adding a square at a time, so that at each step, the shape is still a Young diagram (with the same starting and ending points). When a square is added, say at position k along the path, then the successive vertical and horizontal edges forming the corner (together with their attached elements of the $\underline{a}$ sequence) are exchanged, and partition $\lambda^{(k)}$ is updated using the information in $\lambda^{(k-1)}$, $\lambda^{(k+1)}$ and the external input of a discrete random variable (Bernoulli or geometric), which we will write down inside the corresponding square. The operation corresponding to adding a square and updating the various data attached to the boundary of the encoded shape is called an *atomic step*. We explain in more details below the update of the partitions involved in the atomic steps.

4.1. Bijective atomic steps

We have four kinds of atomic steps, depending on the values of the $\underline{a}$ sequence on the edges of the path involved in the atomic step. They are based on bijective proofs of the Cauchy identities (1.1) and (1.4), or equivalently, on commutation relations for operators $\Gamma_{a,b}(x)$. Bijective proofs of Cauchy identities and versions of the bijections we describe here appeared earlier in the literature. See, *e.g.*, the work of Gessel [Ges93] for the Cauchy case, and those of Pak–Postnikov [PP96] and Krattenthaller [Kra06] for the dual case. In [BP13], Alexei Borodin and Leonid Petrov discuss a more general framework of nearest neighbor dynamics for Macdonald processes. In Section 7, they discuss the

special case of Schur processes with bijections for the Cauchy case.

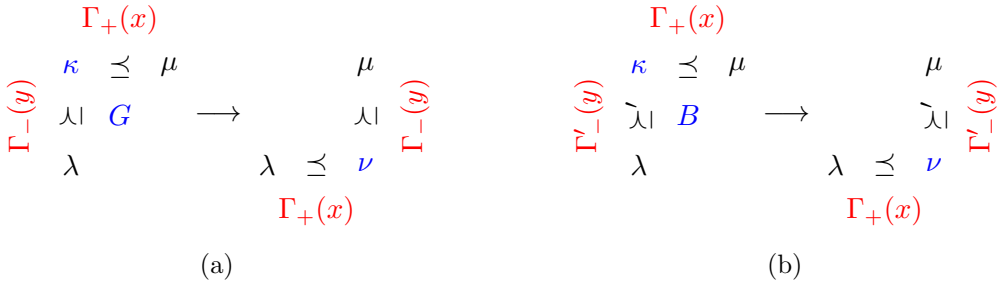

Figure 4.2.: A diagrammatic representation of the two bijections. In the Cauchy case (a) we map a pair (κ, G) such that $\lambda \succeq \kappa \preceq \mu$ and $G \in \mathbb{N}$ to ν such that $\lambda \preceq \nu \succeq \mu$. In the dual Cauchy case (b) we map a pair (κ, B) such that $\lambda \succeq' \kappa \preceq \mu$ and $B \in \{0, 1\}$ to ν such that $\lambda \preceq \nu \succeq' \mu$.

4.1.1. The Cauchy case

We start with the case when the a labels on the edges involved in the atomic step are both L (corresponding to usual interlacing relation between partitions). In this atomic step, the extra data contained in the box that will be added to the encoded shape is a non negative integer G. The atomic step is diagrammatically depicted on Figure 4.2a.

Before the atomic step is performed (left), we have three partitions along the path: $\lambda \succeq \kappa \preceq \mu$. Given a non negative integer G, we want to construct a partition ν such that:

$$\lambda \preceq \nu \succeq \mu, \quad \text{and} \quad |\lambda| + |\mu| + G = |\kappa| + |\nu|.$$

A convenient choice for ν is

$$\nu_i = \begin{cases} \max(\lambda_1, \mu_1) + G & \text{if } i = 1, \\ \max(\lambda_i, \mu_i) + \min(\lambda_{i-1}, \mu_{i-1}) - \kappa_{i-1} & \text{if } i > 1. \end{cases}$$

It is easily checked that the partition constructed this way satisfies the conditions above, and that the construction realizes a bijection between the set of pairs (κ, G) and the set of partitions ν, where κ and ν satisfy the interlacing constraint.

From this bijection, we see that:

$$\sum_{\nu:\lambda\preceq\nu\succeq\mu} x^{|\nu\setminus\lambda|} y^{|\nu\setminus\mu|} = \sum_{G=0}^{\infty} \sum_{\kappa:\lambda\succeq\kappa\preceq\mu} y^{|\lambda\setminus\kappa|+G} x^{|\mu\setminus\kappa|+G} = \frac{1}{1-xy} \cdot \sum_{\kappa:\lambda\succeq\kappa\preceq\mu} y^{|\lambda\setminus\kappa|} x^{|\mu\setminus\kappa|}$$

which amounts to the commutation relation between $\Gamma_+(x)$ and $\Gamma_-(y)$ (evaluated between vectors $\langle\lambda|$ and $|\mu\rangle$), or equivalently, the Cauchy identity (1.1) for Schur functions, when the set of variables are reduced to a unique variable.

In terms of distribution for Schur processes, this identity also tells us that if $\lambda \succeq \kappa \preceq \mu$ are such that, given λ and μ, the probability of κ is proportional to $s_{\lambda/\kappa}(x) s_{\mu/\kappa}(y) =$

$x^{|\lambda\setminus\kappa|}y^{|\mu\setminus\kappa|}$, and if G is distributed as a geometric random variable with parameter xy, then the conditional probability of the partition ν constructed above is proportional to $s_{\nu/\lambda}(x)s_{\nu/\mu}(y)$. In particular, if $\lambda \succeq \kappa \preceq \mu$ is a piece of a sample of a Schur process with sequences

$$\underline{a} = \cdots LL \cdots , \quad \underline{b} = \cdots - + \cdots , \quad \underline{x} = \cdots xy \cdots ,$$

(the indicated terms of the sequences correspond to transitions $\lambda \to \kappa \to \mu$), then the same sequence of partitions, where κ is replaced by ν is sampled according to a Schur process with new sequences:

$$\underline{a} = \cdots LL \cdots , \quad \underline{b} = \cdots + - \cdots , \quad \underline{x} = \cdots yx \cdots ,$$

where all the parameters for the two transitions are exchanged.

The construction above can also be used to perform atomic steps when all the partitions *dually interlace*. First, transpose λ, κ, and μ; then perform the previous atomic step to produce ν' from λ', κ', μ' and a geometric random variable G, then transpose again, to get a new partition ν, such that $\lambda \preceq' \nu \succeq' \mu$, distributed according to the correct marginal. This operation is equivalent to the commutation relation satisfied by the operators $\Gamma'_+(x)$ and $\Gamma'_-(y)$.

4.1.2. Dual Cauchy case

In order to recover the commutation relation between $\Gamma_+(x)$ and $\Gamma'_-(y)$, a different construction is needed: by looking at the commutation relation, we see that the factor $\frac{1}{1-xy}$, which was interpreted before as the generating function of a geometric random variable is replaced by $(1 + xy)$ which the generating function for a variable B taking values 0 or 1. This will be the extra data contained in the box to be added to the encoded shape. See the diagram on Figure 4.2b.

Let λ, κ, μ such that $\lambda \succeq' \kappa \prec \mu$. Given a integer $B \in \{0, 1\}$, we now want to construct a partition ν such that

$$\lambda \preceq \nu \succeq' \mu \quad \text{and} |\lambda| + |\mu| + B = |\kappa| + |\nu|.$$

The bijection is concisely presented in the following pseudo-code, which provides the random update from κ to ν, from λ and μ, by generating the Bernoulli variable B with parameter $\xi = xy$:

def `sampleHV`$(\lambda, \mu, \kappa, \xi)$
  sample $B \sim Bernoulli(\frac{\xi}{1+\xi})$
  for $i = 1 \dots \max(\ell(\lambda), \ell(\mu)) + 1$
    if $\lambda_i \leq \mu_i < \lambda_{i-1}$ **then** $\nu_i = \max(\lambda_i, \mu_i) + B$
    else $\nu_i = \max(\lambda_i, \mu_i)$
    if $\mu_{i+1} < \lambda_i \leq \mu_i$ **then** $B = \min(\lambda_i, \mu_i) - \kappa_i$
  return ν

This bijection implies that

$$\sum_{\nu:\lambda\preceq\nu\succeq'\mu} x^{|\nu\setminus\lambda|}y^{|\nu\setminus\mu|} = \sum_{B=0}^{1}\sum_{\kappa:\lambda\succeq'\kappa\preceq\mu} y^{|\lambda\setminus\kappa|+B}x^{|\mu\setminus\kappa|+B} = (1+xy)\cdot\sum_{\kappa:\lambda\succeq'\kappa\preceq\mu} y^{|\lambda\setminus\kappa|}x^{|\mu\setminus\kappa|},$$

which is equivalent to the commutation relation between $\Gamma_+(x)$ and $\Gamma'_-(y)$.

As in the Cauchy case, the structure of Schur process is preserved: given λ and μ, if κ (subject to the previous interlacing conditions) is sampled with a probability proportional to

$$x^{|\lambda\setminus\kappa|}y^{|\mu\setminus\kappa|} = s_{\lambda'/\kappa'}(x)s_{\mu/\kappa}(y),$$

and B is a Bernoulli random variable with parameter $\frac{xy}{1+xy}$, then ν has the marginal distribution of a Schur process, where the parameters of the three sequences $\underline{a}$, $\underline{b}$, and $\underline{x}$ corresponding to the transitions involved are exchanged.

The fourth case (corresponding to the commutation between $\Gamma'_+(x)$ and $\Gamma_-(y)$ is readily obtained from the bijection above by transposing partitions before and after the bijective construction, as above.

4.2. Sampling algorithm

The sampling algorithm to simulate a Schur process of length n encoded by the sequences $\underline{a}$, $\underline{b}$ and weight $\underline{x}$ is now being explained: first compute the encoded shape π of the Schur process. For each $i \in [0..n-1]$, the $(i+1)$th edge of the lattice path describing the boundary of π is labeled by (a_i, b_i, x_i). If this edge e is vertical (resp. horizontal), this label is propagated on all vertical (resp. horizontal) edges on the left (resp. above) e until the coordinate axis. This gives a consistent labelling of the edges in the smallest rectangle[2] of size $p \times q$ containing the encoded shape π, such that all monotone paths from the top left corner to the bottom right corner collect the same labels, but in a different order.

This gives a partition of the sequence of weights $\underline{x}$ into two subsequences $X = (X_1, X_2, \ldots, X_p)$ and $Y = (Y_1, Y_2, \ldots, Y_q)$ attached respectively to the horizontal and vertical edges. Similarly, the $\underline{a}$ sequence can be split into two subsequences $A = (A_1, \ldots, A_p)$ and $\tilde{A} = (\tilde{A}_1, \ldots, \tilde{A}_q)$.

Fill every box (i, j) of the Young diagram of π with a geometric variable of parameter X_iY_j (resp. a Bernoulli variable of parameter $\frac{X_iY_j}{1+X_iY_j}$) if the values A_i and A_j are the same (resp. different).

If $N = |\pi|$ is the size of π, choose an increasing sequence $(\pi^{(0)} = \emptyset, \ldots, \pi^{(N)} = \pi)$ of partitions starting from the empty partition and ending at π, where at each step, a unique box is added in the Young diagram[3]. This gives an order to add the boxes to construct the encoded shape π. All the choices yield the same the result.

[2]The quantities p and q are respectively the number of $+$ and $-$ in the sequence $\underline{b}$ and satisfy $p+q=n$.
[3]Such a sequence is given by a standard Young tableau of shape π.

For the Schur process with encoded shape $\pi^{(0)} = \emptyset$, with the sequence of a parameters and weights read along the path, there is a unique sequence of partitions with non zero probability, because of the order of the interlacing conditions along the path, given by $(\emptyset, \dots, \emptyset)$.

For every k between 1 and N, the transition from $\pi^{(k-1)}$ to $\pi^{(k)}$ is done by adding a box (i_k, j_k) at an inner corner of $\pi^{(k-1)}$, at a position ℓ_k, along the path forming the boundary of the encoded shape.

At the vertices of the box (i_k, j_k), three partitions are known. When adding the box to the encoded shape, generate the fourth one (north-east corner) by using one of the four corresponding atomic step, depending on the value of A_{i_k} and $\tilde{A}_{j_k}$, and using the input of the three other partitions, and the random variable in the box.

Once all the boxes have been added to the encoded shape π, the sequence of partitions read along the boundary of π is a sample of the Schur process with sequences $(\underline{a}, \underline{b})$ and weights $\underline{x}$.

4.3. Markov chains intertwiners

In fact, the sequence of partitions read along any monotone path from $(0, q)$ to $(p, 0)$ is a sample of a Schur process with some $\underline{a}$, $\underline{b}$ sequences and weights obtained from the original sequences by a common permutation. This is an example of intertwined Markov process, see [BF15] and references therein for more details. The same mechanism of intertwined Markov chains is used in [BG09] to generate tilings of hexagons with rhombi.

4.4. Application to random tilings and extensions

We present below some pictures of random plane partitions, and tilings of the Aztec diamond with dominos, generated by the algorithm described above. For more examples, we refer the reader to [13].

4.4.1. Connection with Robinson-Schensted-Knuth correspondence and the domino shuffling

For plane partitions inside a $p \times q$ rectangle, our algorithm is equivalent Fomin's description of Robinson-Schensted-Knuth correspondence, between integer values matrices and sequences of integers [Sta99, Chapter 7, Appendix].

Another tiling example fitting this framework is, as explained in Section 2.4, tilings by dominos of the Aztec diamond, corresponding to sequences $\underline{a} = (LR)^n$ and $\underline{b} = (+-)^n$. The so called *domino shuffling algorithm* [EKLP92a] is a random algorithm which allows to grow a random tiling from an Aztec diamond of size n to one of size $n + 1$. This algorithm has three steps: two deterministic ones (suppression of "bad" 2×2 blocks, migration of dominos) and random one (filling of the empty spaces left by dominos after migration by good blocks). Following carefully the shuffling algorithm in terms of Maya

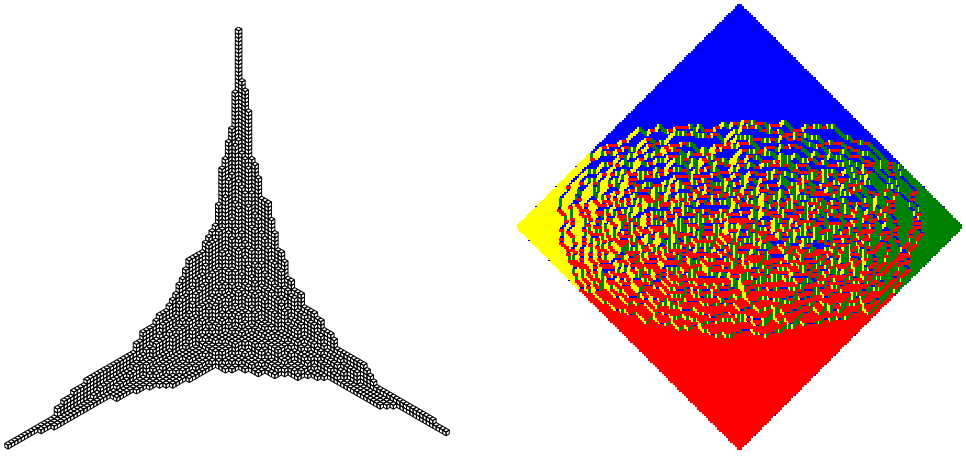

(a) (b)

Figure 4.3.: A random large plane partition with base contained in a 100×100 box and $q = 0.93$ (a) and a random 100×100 Aztec diamond with $q = 0.99$ (b). Both exhibit deterministic limit shapes.

diagrams shows that the extra randomness needed is $n + 1$ binary bits (associated to "diagonals" of the Aztec diamond).

The encoded shape corresponding to the Aztec diamond of size n is a staircase partition $\pi = (n, n-1, \ldots, 1)$. The $n+1$ bits from the domino shuffling algorithm correspond to the extra data contained in the $n+1$ boxes that will be added to the staircase partition to produce an Aztec diamond of size $n+1$. Building an Aztec diamond of size n requires then $\frac{n(n+1)}{2}$ independent binary bits. Taken for granted the bijective atomic step for the dual Cauchy case, this construction gives another direct bijective proof that the number of Aztec diamonds of size n is $2^{\frac{n(n+1)}{2}}$.

4.4.2. Extension to the symmetric case

Using the same techniques, one can also deal with *right free* Schur processes, where the rightmost partition is not necessarily empty, but can be any partition, and the probability of a sequence $\Lambda = (\lambda^{(0)} = \emptyset, \ldots, \lambda^{(n)})$ is

$$\mathbb{P}(\Lambda) \propto \prod_{i=0}^{n-1} x_i^{\left||\lambda^{(i+1)}|-|\lambda^{(i)}|\right|} t^{|\lambda^{(n)}|}.$$

The parameter t can be reabsorbed in the x_i's, so one can always assume that $t = 1$. These right free Schur processes are also called *symmetric* Schur processes, because they correspond to a Schur process of size $2n+1$, starting and ending at the empty partition, conditional on $\lambda^{(2n+1-i)} = \lambda^{(i)}$ for all $i \in [0..n-1]$, the partition $\lambda^(n)$ acting as a mirror.

In the vertex operator formalism, the right boundary state is not the empty partition,

but a sum over all partitions, possibly weighted by their size:

$$|\underline{t}\rangle = \sum_{\nu} t^{|\nu|} |\nu\rangle.$$

The additional ingredient is the Littlewood identity [Mac15, p. 93]

$$\sum_{\nu} \mathrm{s}_{\nu/\mu}(\mathbf{x}) = \prod_{i} \frac{1}{1-x_i} \prod_{i<j} \frac{1}{1-x_i x_j} \sum_{\kappa} \mathrm{s}_{\mu/\kappa}(\mathbf{x}),$$

or equivalently, the reflection identity for vertex operators:

$$\Gamma_+(x)|\underline{t}\rangle = \frac{1}{1-xt} \Gamma_-(xt^2)|\underline{t}\rangle.$$

which corresponds to a new atomic step for the generation of the rightmost partition. See [13, Section 4] for more details.

There is also modified versions of the Littlewood identity where the sums over ν and κ are restricted to partitions with only even (resp. odd) parts. This corresponds to restricting the sum in the definition of the right boundary state $|\underline{t}\rangle$ to partitions with only even (resp. odd) parts.

4.4.3. Schur processes with infinitely many parameters

The definition of a Schur process we used involves only a finite number of partitions. But in some situations (*e.g.* for plane partitions or pyramid partitions), one wants to consider *unbounded* Schur processes where the sequence of partition is (bi)infinite.

The condition on the weights x_i for the weight of a configuration to be normalizable into a probability is exactly the condition that among the infinite number of geometric and Bernoulli random variables one would need to use to generate the process using the previous atomic steps, only a finite number of them are non zero. One can even write down explicitly the distribution[4] of the index of the first non-zero such variable.

After having simulated the index of the last non-zero random input, and value of that random input according to a biased distribution, one is then back to a finite situation, where the non-zero partitions are generated from a (random) finite number of external random variables. See [13, Section 5] for the details of the implementation.

[4] As it is given as an infinite product, it is delicate to use it in practice for simulations, because of numerical instabilities.

Part II.

Statistical mechanics on isoradial graphs

Abstract

We define isoradial graphs in Chapter 5, as well as some of their properties, in connection with integrability of electric networks and the Ising model. We then summarize results obtained on integrable models of statistical mechanics on planar isoradial graphs. These include the critical Ising model [8, 9] (Chapter 6), the XOR Ising model [14] (Chapter 8), and spanning rooted forests [16] (Chapter 7). They are all intimately related to dimer models, either via bijections or combinatorial correspondences, or more indirectly through their spectral curve.

5. Isoradial graphs

After some generalities and definitions, on graphs drawn on surfaces in Section 5.1, we introduce a special class of embedded planar graphs, the so-called *isoradial graphs* [Duf68, Mer01, Ken02]. We discuss their properties in Section 5.2, and motivate why they form a natural support for statistical mechanics in dimension 2, in connection with the Yang-Baxter equation for integrable models (Section 5.3). Two examples are thus discussed which will serve as reference and motivation for the following chapters: the Laplacian on isoradial graphs (Section 5.4) and the Ising model (Section 5.5). This chapter ends with some considerations about spectral curves of operators on periodic graphs and the formulation of the Ising model as a measure on contours.

5.1. Planar graphs, surface graphs and associated notions

We first give some terminology associated to graphs drawn on surfaces and particularly planar graphs. Let G be a connected graph drawn on a boundaryless connected oriented surface Σ, in such a way that no two edges cross each other in their interior, and that cutting Σ along the edges of G, one gets only pieces that are homeomorphic to disks. These pieces are the *faces* of G. In other words, G is the 1-skeleton of a cellular decomposition of Σ. Then one can define the dual graph G^*, where vertices of G^* are the faces of G and two dual vertices are connected by a dual edge if the corresponding faces share an edge in G.

From G and G^*, one can construct the *diamond graph*, $G_\diamond$. The vertices of $G_\diamond$ are vertices and faces of G. A vertex v and face f of G are connected by an edge in $G_\diamond$ if and only if v is on the boundary of f. The graphs G and G^* have the same diamond graph, and the faces of $G_\diamond$ are quadrilaterals. The dual $(G_\diamond)^*$ of $G_\diamond$ is a regular degree-4 graph, called the medial graph, and denoted G_M. An edge path on G_M which goes straight at every intersection is called a *train-track*.

These definitions extend to the case when the surface Σ has a boundary, by taking special care of what happens at the boundary. Several choices are possible. However, we will mainly be interested in the boundaryless case.

5.2. Isoradial graphs

We consider a family of planar graphs, with an embedding on the plane, *i.e.*, a special placement of the vertices and the edges in the plane.

Definition 15. A planar embedded graph G is said to be *isoradial* if all the bounded faces are inscribed in a circle of radius 1.

The value 1 of the radius we chose is not crucial. It can be anything as long as it is the same for all the faces. If we impose further that the centers of all the circles of G are in the interior of the corresponding faces, then the embedding of G^* where dual vertices are represented by these centers of circles, is also isoradial. This is what we will do implicitly in the rest of this manuscript.

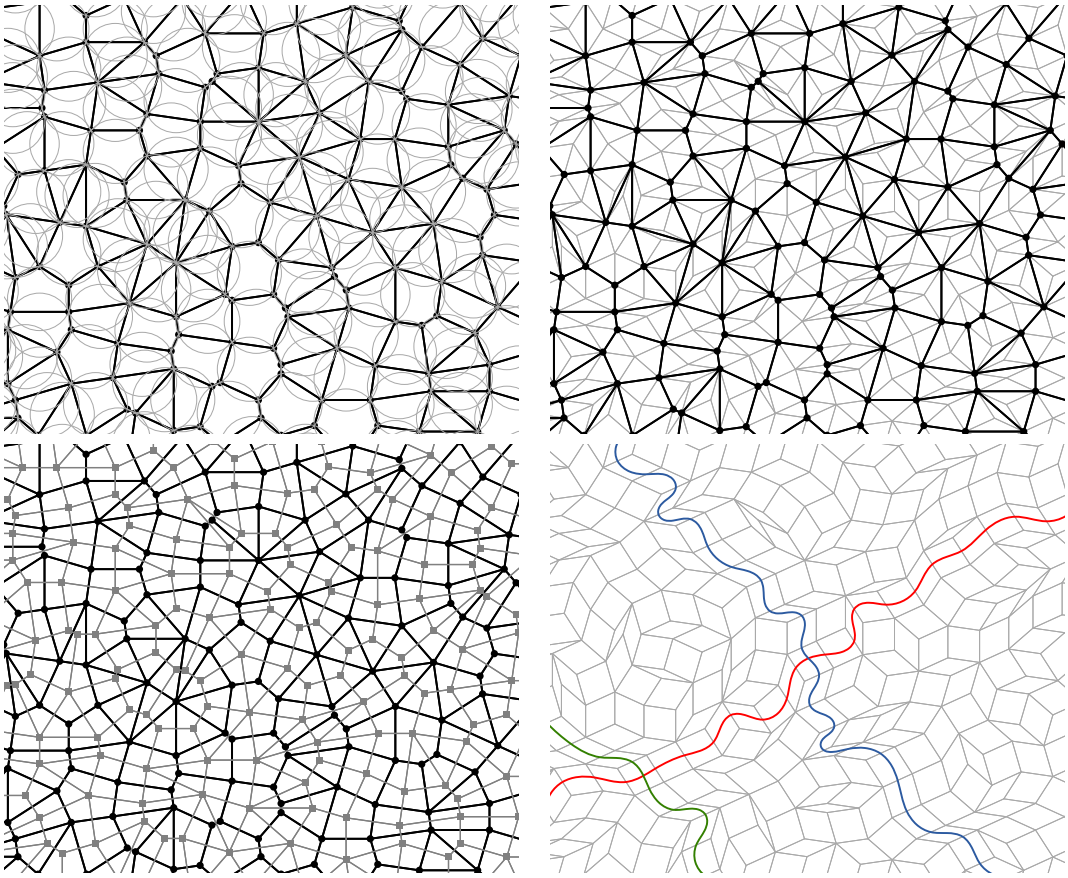

Figure 5.1.: Top left: piece of an infinite isoradial graph G (in black) with the circumcircles of the faces. Top right: the same piece of infinite graph G with its diamond graph $G_\diamond$. Bottom left: the isoradial graph superimposed with its dual graph, whose vertices are the centers of the circumcircles. Bottom right: the diamond graph with a few train-tracks pictured as paths of the dual graph of $G_\diamond$.

Because the segment between a vertex and the center of the circumscribing circle of a face it sits on is a radius of a circumcircle, it has unit length: all the edges of the diamond graph have the same length, thus its faces are rhombi. Edges crossed by train-tracks have the same direction. A given isoradial graph has many isoradial embeddings: if we change simultaneously the direction of all the edges crossed by a train-track by a small

amount, we get a new isoradial embedding. This operation is called *train-track tilting*.

To construct an isoradial graph, one can start from the tiling of a region, or the whole plane, with rhombi of unit edge length. The constructed graph is bipartite. Color the vertices of $G_\diamond$ in white and black alternatively. Take the black ones to be the vertices of G, its edges being the diagonals of rhombi connecting those black vertices. The white vertices are the dual vertices, and the other diagonals, the dual edges. Such rhombic tilings can be seen as the projection of monotone surface in $\mathbb{Z}^d$ if the number of possible directions for the unit edges is finite (quasicrystalline hypothesis).

The same construction can be used to construct isoradial graphs on *translation surfaces* (the torus, or other surfaces with flat metric with conic singularities of angle multiple of 2π). On these surfaces, an angle in $[0, 2\pi)$ with respect to a fixed direction based at a vertex can be transported in a consistent way through the whole graph. If rhombi are glued together in such a surface, and if closed (non-trivial) paths on this rhombic graph have even length, then the graph $G_\diamond$ obtained this way is again bipartite and can be split into an isoradial graph G and its dual G^*, drawn on that translation surface.

Richard Kenyon and Jean-Marc Schlenker give a characterisation of the graphs possessing an isoradial embedding in terms of the topology of the train-tracks:

Theorem 5 ([KS05])**.** *A graph G drawn on a surface has an isoradial embedding if and only if*

- *no train-track intersects itself,*
- *no train-track intersects another train-track back and forth.*

For planar graphs, it means that pairs of train-tracks cannot intersect more than once.

Train-tracks are also known as *de Bruijn lines* in the field of non-periodic tilings [dB81a, dB81b], or *rapidity lines* in integrable systems [Bax86].

Rhombic tilings were introduced by Duffin [Duf68] to develop a discrete theory of complex analysis, as rhombi are well adapted to write discrete versions of the Cauchy-Riemann equation. Rhombic tilings were then used by Mercat [Mer01] to study the critical Ising model in connection with discrete complex analysis. Kenyon coined the name isoradial graphs, and studied the Laplacian and Dirac operators, as well as properties of their inverses [Ken02]. Conformal invariance of the scaling limit of the critical Ising model on isoradial graphs has been proven by Chelkak and Smirnov [CS12] by developing and taking advantage the discrete complex analysis and potential theory on these graphs [CS11].

5.3. Rombic flips and integrable statistical mechanics on isoradial graphs

In this section, we relate an operation on isoradial graphs (or the underlying rhombic tiling), called *flips*, and the Yang-Baxter (or more generally star-triangle relations) satisfied by the weights of integrable models.

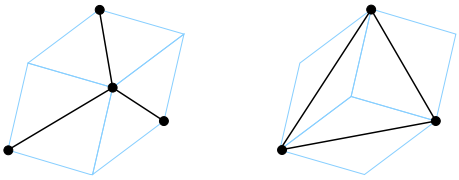

Figure 5.2.: A rhombic flip on $G_\diamond$, and its effect on the isoradial graph G: a star-triangle transformation.

5.3.1. Rhombic flips

In addition to the train-track tilting operation, another set of transformations, the *rhombic flips*, plays a fundamental role. Whereas the topology of the graph was preserved under train-track tilting, it is not the case with flips.

Let us describe them on $G_\diamond$: every time one sees three rhombic faces of $G_\diamond$ forming a small hexagon, then one can move them around to create another tiling. In terms of the isoradial graph G, it corresponds to transforming a triangular face to a star, by adding a vertex of degree 3, or *vice-versa*.

The following theorem by Richard Kenyon, reformulated to fit the particular context of rhombus tilings, says that these operations are locally transitive on the set of isoradial graphs in the following sense:

Theorem 6 ([Ken93])**.** *Let B be a bounded, simply connected domain tiled by rhombi of unit side lengths. Then any other tiling of B with rhombi can be obtained for the initial one by a sequence of tilts.*

In other words, if two isoradial graphs coincide except in a bounded simply connected region, then one can transform one into the other by applying a sequence of star-triangle transformations.

5.3.2. The Yang–Baxter equation and Z-invariant models

In statistical mechanics, the probability of a configuration is directly related to the energy of the configuration via Boltzmann's formalism. This energy depends on interaction constants of the model, often attached to edges of the graph. Those interaction constants are an input of the model.

On regular lattices, with homogeneous or inhomogeneous coupling constants, to be able to compute in details various quantities, one can assume that the transfer matrices, giving the transitions from the configuration on one row of the model to the next one, commute. This commutation between transfer matrices is guaranteed when a simpler, more local, relation is satisfied. This relation, called *Yang-Baxter equation* or *star-triangle equation*[1], can be presented as follows: if G and G' are two planar graphs differing by a single star-triangle transformation, with some vertices x_1, x_2, x_3. Then there should

[1] In fact, the Yang-Baxter equation can have several forms, depending on the class of the model: vertex model, edge model...

exist a positive constant C such that for every configuration outside the locus of the star-triangle transformation connecting G and G', the sum of all statistical weights for configurations inside this locus compatible with the outside configuration on G and G' are proportional with the constant C.

When solving these relations, we find that the weights associated to edges connected to x_1, x_2 and x_3 satisfy some algebraic relation. Sometimes, the weights satisfying this relation can be parameterized by a parameter u describing a curve, in such a way that the algebraic relation satisfied by the curve corresponds to a simple relation on the parameters u (like an addition formula).

Taking advantage of the fact that every edge e on an isoradial graph has also a natural parameter, the half-angle θ_e of the rhombus containing it, we can identify the unit circle with a component of the real locus of this curve, and assign to edges the weights given by the particular parameter corresponding to its half-angle. This way, we have a natural way to define integrable statistical models on isoradial graphs. When a model has such weights, it is said to be Z-invariant [Bax86].

We will see examples of this in the next two sections, for conductances of electric networks, and coupling constants for the Ising model.

5.4. Laplacian on isoradial graphs

5.4.1. Conductances and their star-triangle relation

In [Ken02], Kenyon introduces conductances on edges of an isoradial graph as function of their half-angle: if an edge e is a diagonal of a rhombus with half-angle θ, then its conductance $\rho(e) = \rho(\theta)$ is equal to $\tan(\theta)$. A Laplacian Δ is then defined on functions on vertices of the isoradial graph by:

$$\forall\ f \in \mathbb{C}^G,\ \forall\ v \in G, \quad \Delta f(v) = \sum_{w \sim v} \rho(e)\big(f(v) - f(w)\big).$$

These conductances have the property that the associated random walk is a martingale with steps which have a scalar covariance matrix [CS11, Bef08].

It has also the property that when doing a rhombic flip in the underlying diamond graph, the new conductances give an equivalent electric network. Indeed, the star-triangle relation which should be satisfied by conductances for equivalent electric networks [Ken99] yields the following equation for the three conductances a, b, c adjacent to a trivalent vertex:

$$a + b + c = abc$$

which is parameterized by the tan function through the triple tangent identity:

$$\tan(\theta) + \tan(\phi) + \tan(\psi) = \tan(\theta)\tan(\phi)\tan(\psi) \tag{5.1}$$

under the condition that $\theta+\phi+\psi = \pi$, which is exactly the relation satisfied by half-angles around a trivalent vertex.

5.4.2. Discrete exponential functions and harmonicity

A 1-parameter family of functions on pairs of vertices of $G_\diamond$, found in the work of Christian Mercat [Mer04], indexed by $\lambda \in \hat{\mathbb{C}} = \mathbb{C} \cup \{\infty\}$ are defined as follows: to any oriented edge ϵ of $G_\diamond$ identified with the unit vector $e^{i\alpha(\epsilon)} = e^{i\alpha}$, we attach a rational factor:

$$\mathrm{Exp}_\epsilon(\lambda) = \frac{\lambda - e^{i\alpha}}{\lambda + e^{i\alpha}}.$$

Note that, if $\bar{\epsilon}$ represents the same edge but with the reverse orientation, then

$$\mathrm{Exp}_{\bar{\epsilon}}(\lambda) = \frac{\lambda - e^{i(\alpha+\pi)}}{\lambda + e^{i(\alpha+\pi)}} = \mathrm{Exp}_\epsilon(\lambda)^{-1}. \tag{5.2}$$

Given two vertices v and w in $G_\diamond$, and a path of edges $\epsilon_1 = e^{i\alpha_1}, \ldots, \epsilon_n = e^{i\alpha_n}$ from v to w, the *discrete exponential function* from v to w is defined as

$$\mathrm{Exp}_{v,w}(\lambda) = \prod_{j=1}^{n} \mathrm{Exp}_{\epsilon_j}(\lambda) = \prod_{j=1}^{n} \left(\frac{\lambda - e^{i\alpha_j}}{\lambda + e^{i\alpha_j}} \right) \tag{5.3}$$

These functions are called *discrete exponential functions*. Because of (5.2), $\mathrm{Exp}_{v,w}(\lambda)$ does not depend on the edge path connecting v and w, $\mathrm{Exp}_{v,v}(\lambda) = 1$ and $\mathrm{Exp}_{w,v}(\lambda) = \mathrm{Exp}_{v,w}(\lambda)^{-1}$. When λ is of the form e^{iu}, then $\mathrm{Exp}_\epsilon(\lambda) = i\tan(\frac{u-\alpha}{2})$. One can therefore write for two neighboring vertices v and w on the diagonal of a rhombus such that $w - v = e^{i\alpha} + e^{i\beta}$, and $\lambda = e^{iu}$:

$$\begin{aligned}
&\tan\left(\frac{\beta-\alpha}{2}\right)\left(\mathrm{Exp}_{v,w}(\lambda) - \mathrm{Exp}_{v,v}(\lambda)\right) = \\
&\quad -\tan\left(\frac{\beta-\alpha}{2}\right)\left[\tan\left(\frac{u-\alpha}{2}\right)\tan\left(\frac{u-\beta}{2}\right) + 1\right] = \tan\left(\frac{u-\beta}{2}\right) - \tan\left(\frac{u-\alpha}{2}\right)
\end{aligned}$$

which is a telescopic quantity when summing over all the neighboring vertices w of v. This proves that restriction of these discrete exponential functions to vertices of G are harmonic[2]. Because of their product structure, they form what is called a *zero curvature representation*[3] of the solution of the discrete Laplace equation $\Delta f = 0$, and their existence is related the integrability of the discrete Laplace equation. See [BS08, Chapter 6]. Harmonicity of exponential functions and integrability of the Laplace equation is thus a consequence of (5.1) when the angles can take complex values (by taking $\theta = \frac{\beta-\alpha}{2}$, $\phi = \frac{u-\beta}{2}$ and $-\psi = \frac{u-\alpha}{2}$).

Richard Kenyon used these exponential functions to build an exact expression for the Green function on any isoradial graph, as an integral of the discrete exponential function against a singular measure in the λ-space:

[2] More, the restriction to G^* is also harmonic for the Laplacian on the isoradial graph G^*, and is the natural dual harmonic of the restriction on G.

[3] In this language, the (exponential of the) curvature of a domain is the product along the boundary of the domain of the connection defined on edges by the local factors.

Theorem 7 ([Ken02])**.** *Let G be an isoradial graph. The Green function $\mathcal{G}$ between two vertices v and w of the graph G is given by the following formula:*

$$\mathcal{G}_{v,w} = -\frac{1}{8\pi^2} \oint \mathrm{Exp}_{v,w}(\lambda) \log \lambda \mathrm{d}\lambda \tag{5.4}$$

where the integration is performed in the complex plane along a simple positively oriented contour which encloses all the poles of the integrand, but excludes zero and does not cross the branch cut of the logarithm.

5.5. The Ising Model and its star-triangle relation

The *Ising model* [Len20] is a probability measure on *spin configurations* on the graph G, *i.e.*, on functions on vertices of $G = (V, E)$ with values in $\{-1, +1\}$. See *e.g.*, [Bax89, McC10, MW73, Wer09] for references on this model. If the graph G is finite and positive constants $J = (J_e)_{e \in E}$ are assigned to edges, then the Boltzmann probability measure of a configuration $\sigma \in V^{\{-1,+1\}}$ is

$$\mathbb{P}(\sigma) = \frac{1}{Z_{\mathrm{Ising}}(G, J)} \exp\Big(\sum_{e:v\sim w} J_e \sigma_v \sigma_w\Big)$$

where

$$Z_{\mathrm{Ising}}(G, J) = \sum_{\sigma} \exp\Big(\sum_{e:v\sim w} J_e \sigma_v \sigma_w\Big) \tag{5.5}$$

is the Ising partition function. Suppose that G and G' are planar and differ by a star-triangle transformation: in G, a degree 3 vertex x_0 is incident with vertices x_1, x_2, x_3, which are connected in a triangle in G'.

Denote for $i \in \{1, 2, 3\}$, denote e_i (resp. e'_i) the edge in G connecting x_0 to x_i (resp. the edge in G' connecting x_j to x_k, with $\{i, j, k\} = \{1, 2, 3\}$). Following [Bax89][Section 6.4], write $J_i = J_{e_i}$, $K_i = J_{e'_i}$.

If we want the Ising Boltzmann measures on G and G' to give the same probability to local events not involving spins at x_i, with $i \in [0..3]$, then it is enough to require that given the spins at x_i, $i \in [1..3]$, the (partial) weights of the local configurations inside the star/triangle locus are proportional. If we fix these spins in G', then everything is fixed, but in G, we should sum over the two possible values of the spin in x_0. Table 5.1 lists the relative weights from spin interactions along the edges in the star/triangle, as a function of the values of the spins on the boundary.

The two columns of Table 5.1 should be proportional, by a factor, say R. Multiplying the first two rows of the table and dividing by the last two, and playing with hyperbolic trigonometric formulas, one gets:

$$\sinh(2K_1)\sinh(2J_1) = \frac{2\sinh(2J_1)\sinh(2J_2)\sinh(2J_3)}{2\sqrt{\cosh(J_1+J_2+J_3)\cosh(-J_1+J_2+J_3)\cosh(J_1-J_2+J_3)\cosh(J_1+J_2-J_3)}}$$

spins $x_1x_2x_3$	G	G'
$+++\ /\ ---$	$2\cosh(J_1+J_2+L3)$	$\exp(K_1+K_2+K_3)$
$+--\ /\ -++$	$2\cosh(-J_1+J_2+J_3)$	$\exp(K_1-K_2-K_3)$
$-+-\ /\ +-+$	$2\cosh(J_1-J_2+J_3)$	$\exp(-K_1+K_2-K_3)$
$--+\ /\ ++-$	$2\cosh(J_1+J_2-J_3)$	$\exp(-K_1-K_2+K_3)$

Table 5.1.: Relative weights of the local configurations in a star (G on the left) or a triangle (G' on the right), depending on the boundary spins x_1, x_2 and x_3.

Note that the right hand side is completely symmetric under permutation of the indices. Call it $1/k'$. The factor R, obtained by considering the product of the four rows of the can be expressed now as follows

$$R^2 = 2k' \sinh 2J_1 \sinh 2J_2 \sinh 2J_3 = 2/(k'^2 \sinh 2K_1 \sinh 2K_2 \sinh 2K_3)$$

Eliminating the constant R and the J_j's from the equations, we get the following relation:

$$k' = \frac{(1-v_1^2)(1-v_2^2)(1-v_3^2)}{4(1+v_1v_2v_3)(v_1+v_2v_3)(v_2+v_1v_3)(v_3+v_1v_2)}$$

where $\frac{1-v_i^2}{2k'v_i} = \sinh 2J_i$.

This algebraic relation can be parameterized by $J_i = f(\theta_i)$, with $\theta_1+\theta_2+\theta_3 = \pi$, by taking

$$J = f(\theta) = \frac{1}{2}\ln\left(\frac{1+\mathrm{sn}(\underline{\theta}|k)}{\mathrm{cn}(\underline{\theta}|k)}\right), \quad \text{or equivalently,} \quad \sinh(2J) = \mathrm{sc}(\underline{\theta}|k). \tag{5.6}$$

where sn and sc are Jacobi elliptic functions, with parameter $k = \sqrt{1-k'^2}$, and $\underline{\theta} = \frac{2K}{\pi}\theta$, where K is the complete elliptic integral of first kind. See Section 7.3 or [16, Section 2.2] for a short introduction. See also for example [Bax89, Section 15.10] for a general approach to parameterize symmetric biquadratic relations with elliptic functions.

When $k' = 1$ (or equivalently when $k = 0$), the elliptic functions sn and sc degenerate to circular trigonometric functions sin and tan. In particular, in that case, $\sinh(2J)$ has the same expression as the conductance for the Laplacian.

For works in the physics literature about the Z-invariant Ising model, see for example [AYP87, AP04, AP07, RM97, RM98, CS06] and the references within. We just mention that similar parameterizations exist for other integrable models, such that the 6-vertex and 8-vertex models, although maybe not readily expressed in terms of angles, but more with the language of rapidities. See [Bax89, Chapters 8 and 10], and [Bax86].

5.6. Periodic isoradial graphs and spectral curves

When the isoradial graph G is periodic, the Laplacian is a periodic operator. One can then look at its Fourier transform $\Delta(z,w)$, for $(z,w) \in (\mathbb{C}^*)^2$. It is a finite-size matrix

with rows and columns indexed by vertices in a fundamental domain of the graph. It is the matrix of the action of Δ on (z,w)-quasiperiodic functions on G, satisfying:

$$\forall v \in V, \quad f(v+(m,n)) = z^{-m}w^{-n}f(v).$$

The *characteristic polynomial* $P(z,w)$ is the determinant of $\Delta^m(z,w)$ and the *spectral curve* C is the set of roots of the characteristic polynomials.

A parameterization of the spectral curve is obtained by $(z(\lambda), w(\lambda))_{\lambda\in\hat{\mathbb{C}}}$, where $z(\lambda)$ (resp. $w(\lambda)$) is the exponential function from a vertex v and its copy by a horizontal (resp. vertical) translation:

$$z(\lambda) = \mathrm{Exp}_{v,v+(1,0)}(\lambda), \quad w(\lambda) = \mathrm{Exp}_{v,v+(0,1)}(\lambda).$$

We know several properties of the spectral curve of the Laplacian on isoradial graphs:
- it has genus 0, because it is parameterized with rational/trigonometric functions;
- it has symmetry $(z,w) \leftrightarrow (z^{-1}, w^{-1})$ because the Laplacian is symmetric;
- it is a Harnack curve, because, by generalized Temperley's bijection [Tem74], it is also equal to the spectral curve of a bipartite planar dimer model [KOS06].

The construction of the Fourier transform, the characteristic polynomial and the spectral curve is not specific to the Laplacian or isoradial graph, and can be carried through for any periodic operator on any biperiodic graph. We will give results about the spectral curve of other operators (massive Laplacians, Kasteleyn operators...) in the next chapters. Since these operators and their inverses have a probabilistic interpretation for models of statistical mechanics (*e.g.*, correlations for dimers), algebraic features of the spectral curves have consequences on the statistical properties of these models, in particular universality behaviour.

5.A. Graphical methods for the Ising model on surface graphs

We recall briefly here some basic facts about the low and high temperature expansion of the Ising model on graphs drawn on surfaces as a reference for the following chapters. For a complete treatment, see [14, Section 2], and the references mentioned there.

For the moment, let us suppose that G is a planar graph, with coupling constants $(J_e)_e$ on edges. We can rewrite the partition function of the Ising model $\mathcal{Z}_{\mathrm{Ising}}$ as a statistical sum over polygonal contours, either on G or on G^*, based on two ways to rewrite $e^{J_e\sigma_v\sigma_w}$.

These two developments were introduced by Kramers and Wannier [KW41a, KW41b] to show criticality of the Ising model on the square lattice.

5.A.1. Low temperature expansion

The quantity $e^{J_e\sigma_v\sigma_w}$ can be rewritten as

$$e^{J_e\sigma_v\sigma_w} = e^{J_e}(\mathbf{1}_{\sigma_v=\sigma_w} + e^{-2J_e}\mathbf{1}_{\sigma_v\neq\sigma_w}).$$

The quantity $\mathbf{1}_{\sigma_v\neq\sigma_w}$ can be graphically interpreted as the edge e^*. Expanding all the terms above present in the partition function, and using this graphical interpretation,

the partition function can be reinterpreted as a sum over contours on G^* separating spins with different signs. A contour configuration can come from two different spin configurations, which yields:

$$\mathcal{Z}_{\text{Ising}} = 2\left(\prod_{e\in E} e^{J_e}\right) \sum_{\substack{\Gamma^* \text{ dual} \\ \text{polyg. contour}}} \prod_{e^*\in\Gamma^*} e^{-2J_e} = 2\left(\prod_{e\in E} e^{J_e}\right) Z_{LT}(G,J).$$

This is the so-called *low-temperature expansion* of the Ising partition function, as it can be viewed as a perturbation series close to the zero temperature where all the spins are equal: the weight per edge e^{-2J_e} is small when J_e is large, which corresponds to a low temperature.

5.A.2. High temperature expansion

Another way to rewrite the quantity $e^{J_e\sigma_v\sigma_w}$ is the following:

$$e^{J_e\sigma_v\sigma_w} = \cosh(J_e) + \sigma_v\sigma_w \sinh(J_e) = \cosh(J_e)\left(1 + \sigma_v\sigma_w \tanh(J_e)\right).$$

Injecting this expression into the definition of $\mathcal{Z}_{\text{Ising}}$, and expanding every factor, we get a polynomial in the σ_v's. If in a monomial, the degree of one of the σ_v's is odd, then, when re-summing over σ, the contribution of this monomial vanishes. When all the σ_v's have even degree, then the summation over σ gives an additional factor $2^{|V|}$, where $|V|$ is the number of vertices of G. The terms corresponding to situations where all σ_v have even degree can be identified with subgraphs of G with even degrees, *i.e.*, primal polygonal contours. One gets:

$$\mathcal{Z}_{\text{Ising}} = 2^{|V|}\left(\prod_{e\in E} \cosh J_e\right) \sum_{\substack{\Gamma \text{ primal} \\ \text{polyg. contour}}} \left(\prod_{e\in\Gamma} \tanh J_e\right) = 2^{|V|}\left(\prod_{e\in E} \cosh J_e\right) Z_{HT}(G,J)$$

This is the high temperature expansion of the partition function, as the weight associated to a piece of contour is small when J is small (or the temperature is high).

5.A.3. Duality

An Ising model on G and G^* will both give rise to a model of random polygonal contours on G, if we apply the high (resp. low) temperature expansion to them. The induced measures on contours will be the same provided that

$$\tanh(J_e) = e^{-2J_{e^*}} \tag{5.7}$$

If this relation is satisfied for all edges, we say that the Ising models on G and G^* are dual one of another.

The square lattice is isomorphic to its dual. If all the coupling constants are chosen to be the same and equal to β (which is in physics is interpreted as the inverse temperature) on G, and to β^* on G^*, then relation (5.7) becomes

$$\tanh(\beta) = e^{-2\beta^*}$$

which is equivalent to $\sinh(2\beta)\sinh(2\beta^*) = 1$. Taking $\beta = \beta^*$, this equation has a unique solution

$$\beta_c = \log\left(\sqrt{2+\sqrt{2}}\right).$$

which turns out to be the critical temperature for the square lattice.

On an isoradial graph, the half-angles θ and θ^* associated to an edge e and its dual e^* sum to $\frac{\pi}{2}$. The duality described above translates to the following identity on the weights for the Z-invariant Ising model (5.6)

$$J(\theta|k) = \frac{1}{2}\ln\left(\frac{1+\mathrm{sn}(\underline{\theta}|k)}{\mathrm{cn}(\underline{\theta}|k)}\right) = \frac{1}{2}\ln\left(\frac{1+\mathrm{sn}(\underline{\theta^*}|k^*)}{\mathrm{cn}(\underline{\theta^*}|k^*)}\right) = J(\theta^*|k^*)$$

with $(1-(k^*)^2)(1-k^2) = 1$. If we impose that the model is self-dual to have $J(\theta|k) = J(\theta|k^*)$ for all θ, we find that $k = 0$ and obtain the following expression

$$J(\theta|k) = \frac{1}{2}\ln\left(\frac{1+\sin(\theta)}{\cos(\theta)}\right) \tag{5.8}$$

for the Z-invariant self-dual Ising model which is indeed critical [Li10, Li12, CDC13].

5.A.4. Higher genus and boundary

If G is not planar, but instead drawn on a surface Σ with a boundary, then the duality described above is not valid anymore: for example, when going around a handle, we come back to our starting point, and thus observe the same spin. As a consequence, the number of low temperature contours we cross is even. On the contrary, there is no parity constraint for the high temperature expansion.

A possible way is to introduce variants of the Ising model with defect lines, which correspond to possible relative homology classes in $H^1(\Sigma, \partial\Sigma; \mathbb{Z}/2\mathbb{Z})$. The duality relation then extends. See [14, Equation (5)].

6. The critical Ising model on isoradial graphs via dimers

We present the main results obtained in collaboration with Béatrice de Tilière in two articles [8] and [9], about the critical Z-invariant Ising model on isoradial graphs. See also [5] for an early report. We construct a Gibbs measure for the Z-invariant critical Ising model on any infinite isoradial graph, provide an explicit formula to compute correlations for contours separating spin clusters of different signs, and make a connection with the Laplacian on isoradial graphs from Section 5.4, through their spectral curve. The tool we use is Fisher's correspondence [Fis66] described in Section 6.1 and Kasteleyn's technology to study the corresponding dimer model. The formula for the correlation is expressed through the inverse Kasteleyn matrix for the corresponding dimer model, which has an explicit integral expression in terms of discrete exponential functions. As such, this matrix has a locality property, like the Green function: the entry indexed by two vertices depends only on the geometry of the isoradial graph along a path between these two vertices.

We consider here the thermodynamic limit, where the graph which supports the Ising model becomes infinite, while staying at a microscopic level (spins stay at finite distance from one another). Another point of view, when the mesh size is going to zero and the rescaled graph is approaching some bounding domain in the plane), is studied by Dmitry Chelkak and Stanislav Smirnov [CS12], where they prove conformal invariance of some observables of the Ising model to conformally covariant quantities under this scaling limit, using a toolbox of discrete harmonic analysis on isoradial graphs [CS11].

6.1. Fisher's correspondence

In [Fis66], Fisher gives a correspondence between the Ising model on a planar graph G (or its dual) and dimer configurations on a decorated version, denoted by G_D, which is still planar.

In the construction of G_D we used, every vertex $\boldsymbol{x}$ of G of degree d is replaced with a decoration made of $3d$ vertices: $v_1(\boldsymbol{x}), w_1(\boldsymbol{x}), z_1(\boldsymbol{x}), \dots, v_d(\boldsymbol{x}), w_d(\boldsymbol{x}), z_d(\boldsymbol{x})$. These $3d$ vertices are arranged into d triangles, labeled from 1 to d. The triangle with label k has three vertices $v_k(\boldsymbol{x}), w_k(\boldsymbol{x}), z_k(\boldsymbol{x})$ counterclockwise, and is attached by the vertex $v_k(\boldsymbol{x})$ to one of the original edges connected to $\boldsymbol{x}$ in G. Then for every k, $w_{k-1}(\boldsymbol{x})$ and $z_k(\boldsymbol{x})$ are connected by an edge. See Figure 6.1. Some other decorations are possible, like the simpler one described in [Dub11b, CDC13]. See also [DZM$^+$96] for a similar construction.

Figure 6.1.: The neighborhood of a vertex $\boldsymbol{x}$ in G and the corresponding decoration in G_D by Fisher's correspondence.

The corresponding mapping between Ising configurations on G and dimer configurations on G_D goes through a contour expansion of the partition function. It might be easier to think of the low-temperature expansion of the Ising model on G^*, meaning that the spins are on the faces of G. See Appendix 5.A. From an Ising configuration on G^*, draw the contours on G separating the connected components of vertices with the same spins (the + and − clusters). Now for every edge *not belonging* (resp. belonging) to a contour of G, declare that the corresponding long edge on G_D *will be* (resp. will not be) a dimer. This determines the dimer configuration on long edges. The remaining inside parts of each decoration can be covered with dimers in exactly two manners. For a finite graph with n vertices, this correspondence assigns to every contour configuration on G (which comes from 2 spins configurations) 2^n dimer configurations. See Figure 6.2.

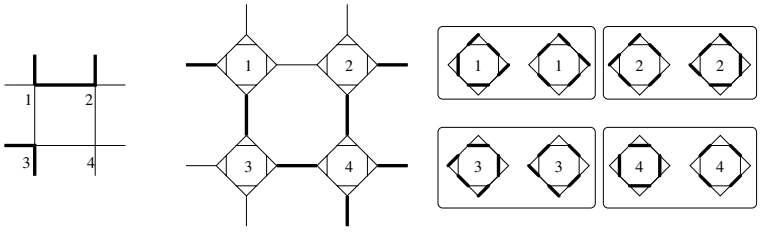

Figure 6.2.: Polygonal contour of $\mathbb{Z}^2$, and corresponding dimer configurations of the associated Fisher graph.

If we want this correspondence to be weight preserving, then one should assign to a dimer e the weight:

$$w_e = \frac{1}{\tanh(2J_e)} \tag{6.1}$$

to (long) edges e coming from the original graph G, and 1 to the (short) internal edges to the decorations. In the case of isoradial graphs with critical Z-invariant coupling constants, replacing J_e by its expression (5.8), we get:

$$w(\theta) = \cot(\theta/2). \tag{6.2}$$

Since the graph G_D is planar, one can use Kasteleyn theory to compute the correlation between dimers: they are given by Pfaffians of submatrices of the inverse of the Kasteleyn matrix, which is the weighted adjacency matrix of the graph G_D with a *clockwise odd*

orientation. However, since the graph G_D is not bipartite, the results from [KOS06] cannot be used in this context.

6.2. Spectral curve and Kasteleyn inverse matrix

We suppose in this section that the isoradial graph G is periodic. Since the Kasteleyn operator K on G_D is now a periodic operator, one can define according to Section 5.6 its characteristic polynomial $P_K(z,w)$ and the corresponding spectral curve $\mathcal{C}_K$.

We proved the following result about the spectral curve:

Theorem 8 ([8], Theorem 8)**.** *The spectral curve of the dimer model corresponding to the critical isoradial Ising model on G is the same as the spectral curve of the Laplacian on G. In other words, the characteristic polynomials are equal, up to a multiplicative constant.*

The spectral curve $\mathcal{C}_K$ has the properties described for the spectral curve of the Laplacian (See Section 5.6).

Proof. Our proof is indirect. We first show that the characteristic polynomial of the Laplacian is a divisor of $P_K(z,w)$: for every (z,w) on the spectral curve of the Laplacian on G, parameterized by discrete exponential functions, we construct a (z,w)-quasiperiodic function on G_D in the kernel of the Kasteleyn matrix, also using the discrete exponential functions. Therefore, the spectral curve of the Laplacian is included in $\mathcal{C}_K$. Then, interpreting combinatorially the monomials of both polynomials, and comparing the terms corresponding to extremal monomials, we prove that the degree of P_K is not larger than that of P_Δ. □

Béatrice de Tilière proved [dT16] a combinatorial correspondence between configurations counted by $P_\Delta(z,w)$ (rooted spanning forests) and the configurations counted by $P_K(z,w)$, providing an alternative, more constructive, proof of this identity.

Knowing the singularities the inverse of the Fourier transform of the Kasteleyn matrix K on the unit torus allowed us to prove existence of a unique inverse A for the operator K, with entries $A_{x,y}$ going to zero when the distance between x and y tends to infinity. It is possible to compute its entries using Fourier transform, as the extraction of a certain coefficient of a certain rational fraction whose denominator is P_K.

Knowing also in generality the possible singularities of P_K on the unit torus, we proved that the sequence of Boltzmann measures on dimer configurations of larger and larger quotients of G_D converge to a Pfaffian process, with a kernel given by this inverse A of the Kasteleyn matrix.

6.3. The inverse Kasteleyn matrix for non periodic G_D

Even when G is not periodic, it is possible to give an explicit expression for the inverse A. The formula is built on the same model as the Green function: let x and y be two

vertices of G_D belonging to decorations decorations, coming from vertices $\boldsymbol{x}$ and $\boldsymbol{y}$ of the isoradial graph G, respectively. Construct a function $g_{x,y}(\lambda)$ as

$$g_{x,y}(\lambda) = f_x(\lambda)\,\mathrm{Exp}_{\boldsymbol{xy}}(\lambda) f_y(-\lambda),$$

where Exp is the discrete exponential function on G introduced in Section 5.4.2, and f_x depends only on the type (v, w, z) of x:

$$f_x(\lambda) = \begin{cases} \frac{e^{i\alpha_x/2}}{e^{i\alpha_x}-\lambda} & \text{if } x = w_k(\boldsymbol{x}), \\ -\frac{e^{i\alpha_x/2}}{e^{i\alpha_x}-\lambda} & \text{if } x = z_k(\boldsymbol{x}), \\ f_{w_k(\boldsymbol{x})}(\lambda) + f_{z_k(\boldsymbol{x})}(\lambda) & \text{if } x = v_k(\boldsymbol{x}), \end{cases}$$

where α_x is an angle modulo 4π associated to x, corresponding to the direction of the unit length edge in $G_\diamond$ the closest to x. See [8, Section 4.2.2] for details.

Theorem 9 ([9], Theorem 5)**.** *The entry of the inverse Kasteleyn matrix for two vertices x and y is equal to:*

$$A_{x,y} = \oint_{\mathcal{C}_{x,y}} g_{x,y}(\lambda) \log \lambda \frac{\mathrm{d}\lambda}{(2\pi)^2} + c_{x,y} \tag{6.3}$$

where $\mathcal{C}_{x,y}$ is a simple closed curve oriented counterclockwise, which contains in its interior the poles of $g_{x,y}$, but avoids a cone with vertex at the origin, and containing a certain ray $d_{x,y}$.

When x and y are not too close to each other, the ray $d_{x,y}$ is the geometric ray from $\hat{\boldsymbol{x}}$ to $\hat{\boldsymbol{y}}$, which are vertices of $G_\diamond$ at distance at most 2 from $\boldsymbol{x}$ and $\boldsymbol{y}$ respectively. The constant $c_{x,y}$ is equal to $\pm\frac{1}{4}$ if x and y are interior vertices of the same decoration, of type w or z (the sign depends on the clockwise odd orientation in the decoration), and is zero otherwise.

Remark 3. The explicit expression for $A_{x,y}$ given in (6.3) has the very interesting feature of being *local*, just like the Green function from Section 5.4, *i.e.*, it only depends on the geometry of the embedding of the isoradial graph G on a path between $\hat{\boldsymbol{x}}$ and $\hat{\boldsymbol{y}}$.

A nice consequence of this property is the following. For $i = 1, 2$, let G_i be an isoradial graph with corresponding Fisher graph $(G_i)_D$. Let K_i be the Kasteleyn matrix of the graph $(G_i)_D$, whose edges are assigned the dimer critical weight function. Let A_i be the inverse of K_i given by Theorem 9. If G_1 and G_2 coincide on a ball B, and if the Kasteleyn orientations on $(G_1)_D$ and $(G_2)_D$ are chosen to be the same in that ball, then for every couple of vertices (x, y) in B at distance at least 2 from the boundary, we have

$$(A_1)_{x,y} = (A_2)_{x,y}.$$

6.4. Construction of a Gibbs measure for the critical Ising model on non periodic isoradial graphs

The locality property described above allows one to define a Gibbs measure on the set of dimer configurations of G_D, by mimicking the expression given by the Boltzmann measure on finite planar graphs, and using the inverse A defined in Theorem 9.

Theorem 10 ([9], Theorem 9)**.** *There is a unique probability measure $\mathcal{P}$ on dimer configurations of G_D, such that for every finite collection of edges $\mathcal{E} = \{e_1 = x_1y_1, \cdots, e_k = x_ky_k\} \subset E(G_D)$, the probability that these edges covered by dimers is*

$$\mathcal{P}(\textit{edges of } \mathcal{E} \textit{ are covered}) = \left(\prod_{i=1}^{k} K_{x_i,y_i}\right) \mathrm{Pfaff}\big((A_{\{x_1,y_1,\cdots,x_k,y_k\}})^T\big), \qquad (6.4)$$

where A is given by Theorem 9, and $A_{\{x_1,y_1,\cdots,x_k,y_k\}}$ is the submatrix of A whose rows and columns are indexed by vertices $\{x_1, y_1, \cdots, x_k, y_k\}$.

Moreover, $\mathcal{P}$ is a Gibbs measure. When G_D is $\mathbb{Z}^2$-periodic, $\mathcal{P}$ is the Gibbs measure obtained as weak limit of the Boltzmann measures $\mathcal{P}_n$ on the toroidal exhaustion $\{G_D/(n\mathbb{Z}^2)\}_{n\geq 1}$ of G_D.

Proof. The proof of this theorem is done in several steps:

First, we prove that if G_D is periodic, then the Boltzmann measure on dimers configurations on $G_D/n\mathbb{Z}^2$ converges as n to infinity to a measure of the form (6.4), where A is the unique inverse of the Kasteleyn matrix with entries decaying to zero, given by the Fourier transform. This is done by writing explicitly the finite dimensional distributions of the Boltzmann measure, as a linear combination of 4 Pfaffians, and taking explicitly the limit, taking advantage of the symmetries of the graph to block diagonalize the Kasteleyn matrices, and the fact that we know explicitly the singularity of the rational fraction in the inverse Fourier transform.

When G is not periodic, it is not clear from the definition of A that (6.4) is a real quantity, between 0 and 1. But if B is a ball of the graph G containing in its interior all the vertices corresponding to the decorations hosting these vertices, then there exists a periodic isoradial graph $\tilde{G}$ with a fundamental domain containing G [dT07a]. Since the expression of A is *local*, the entries of the matrix in (6.4) depend only on the geometry of the isoradial graph in the ball B. Therefore, this formula is the same for G and $\tilde{G}$. But because of the uniqueness result for the inverse Kasteleyn matrix in the periodic case, we know that the local formula coincides with the inverse Fourier formula, and thus (6.4) on $\tilde{G}$ is the limit of Boltzmann measure on periodic graphs.

This ensures that this expression defines on G a family of compatible finite-dimensional probability distributions. By Kolmogorov's extension theorem, there is a unique probability measures on the set of edge configurations for which those distributions are the finite-dimensional marginals. □

This probability measure on dimer configurations can now be lifted via Fisher's correspondence to a Gibbs measure on contours separating spin clusters. Then choose the sign of a given spin at random with a fair coin, independently from the contours. The values of all the other spins are completely determined.

Corrolary 11. *Let G be an isoradial graph. Then there exists a Gibbs measure for the Ising model on G^* for which the law of contours separating clusters of same spins is a Pfaffian process*[1] *with a kernel given by the inverse Kasteleyn matrix* (6.3)*.*

[1] In fact, this is not entirely exact: in our version of Fisher's correspondence, what corresponds to

In the low temperature expansion picture, the computation of correlations between spins amounts to computing the parity of the number of pieces of contour one sees along a path connecting these spins. Since statistics of pieces of low-temperature contours are directly related to dimer statistics on G_D which in turn depend only on the local geometry of the graph, because of the local property of the inverse Kasteleyn matrix, the spin correlations are themselves local, *i.e.*, they depend only on the geometry of the graph trough a neighborhood of a path connecting those two spins.

6.5. From criticality to non-criticality

An open question after this work was whether a similar study could be carried over for the Z-invariant non-critical Ising model, where now the elliptic parameter k could be nonzero. Although we knew explicitly the weights to put on the dimers by (5.6) and (6.1), the first step already could not be performed directly, because no analogue of the Laplacian and discrete exponential functions for noncriticality were known.

Since correlations should decay exponentially fast out of criticality, we have been looking for a massive Laplacian, for which the Green function would decay exponentially fast. Connections between noncritical Ising models and massive Laplacians or killed random walks were known [Mes06, BDC12], but these were specific to the square lattice.

This led Béatrice de Tilière, Kilian Raschel and myself to search and define a family of Z-invariant massive Laplacian on isoradial graphs, described in Chapter 7, which turned out to be very rich and interesting objects by themselves, which postponed a little bit the initial goal about the non critical Z-invariant Ising model.

the presence of a dimer on a long edge is the absence of that edge in the contours. This can be solved by either considering the complement of the contour configuration, changing the kernel to its "complement", or by changing slightly the version of the Fisher correspondence to a simpler version where dimers correspond directly to contours.

7. Massive Laplacian on isoradial graphs

In [16], in collaboration with Béatrice de Tilière, and Kilian Raschel, we define a one parameter family of integrable massive Laplace operators on isoradial graphs. We introduce a family of zero-curvature massive harmonic functions, the so called *massive exponential functions*, depending on a parameter u living on a torus, and give an explicit representation representation of the associated Green function as an integral along a contour in the u-space of massive exponential functions. We discuss implications on a model from statistical mechanics, the *rooted spanning forests*, where configurations are "counted" by the determinant of this massive Laplacian. In the periodic case, we also characterize the set of algebraic curves which can arise as spectral curve of these massive Laplacians.

7.1. Definitions

Let $G = (V, E)$ be a graph. Every edge e (resp. every vertex v) is associated a positive (resp. nonnegative) number ρ_e (resp. m_v). ρ_e is called the *conductance* of the edge e and m_v the *(squared) mass* at the vertex v.

The *massive Laplacian* Δ^m on G (for these conductances and masses) is defined by its action on functions on vertices of G: for every function f on vertices of G, and any vertex v,

$$(\Delta^m f)(v) = \sum_{e:v\sim w} \rho_e(f(v) - f(w)) + m_v f(v).$$

See for example [LJ11, Chapter 1], for some more definitions and properties of this operator.

7.2. Statistical mechanics

The massive Laplacian is naturally connected to various systems from statistical mechanics. The first example is the killed random walk: the massive Laplacian can be interpreted as the generator of a Markov process in continuous time describing the evolution of a particle which, at a vertex v, either jumps to one of the neighbouring vertices after an exponential random time, or gets absorbed at that vertex forever.

The second example is the random rooted spanning forest model. A *rooted tree* is a cycle-free connected subgraph with a distinguished vertex, called the *root* of the tree. A *rooted spanning forest* is a spanning subgraph whose all connected components are

rooted trees. The *weight* of a spanning forest F with tree T_j rooted at v_j for all j, is

$$\mathsf{weight}(F) = \prod_j m_{v_j} \prod_{e \in T_j} \rho_e.$$

If the graph is finite, then there is a finite number of rooted spanning forests, and we can define a Boltzmann probability measure:

$$\mathbb{P}(F) = \frac{1}{Z_{\text{forest}}} \mathsf{weight}(F)$$

The *partition function* for the rooted spanning forests Z_{forest} is equal to the determinant of the massive Laplacian, by Kirchhoff's matrix-tree theorem. See [16, Section 6 and Appendix D] for more details.

Local statistics can be computed explicitly: edges (and roots) present in the random rooted spanning forest form a determinantal point process by [BP93] (See [16, Section 6] for details) whose kernel is the *transfer impedance matrix* H, defined from the massive Green function $\mathcal{G}^m$ as follows: if $e = (e_-, e+)$ and $e' = (e'_-, e'_+)$ are oriented edges of G, the transfer impedance between e and e' is

$$\mathsf{H}(e, e') = \rho(e')(\mathcal{G}^m(e_-, e'_-) - \mathcal{G}^m(e_+, e'_-) - \mathcal{G}^m(e_-, e'_+) + \mathcal{G}^m(e_+, e'_+)). \tag{7.1}$$

Other expressions for the transfer impedance between edges and roots can be found in [16, Theorem 33]. As for usual spanning trees, random rooted spanning forests can be sampled easily from Wilson's algorithm [Wil96], using loop erased trajectories of (now killed) random walks.

7.3. Massive Laplacians on isoradial graphs

On isoradial graphs, it is natural, as in the massless case, to take advantage of the rhombic embedding make the conductances depend on the local geometry: the conductance ρ_e of e will be a function of θ_e, the half-angle of the rhombus containing e, and m_v will be a function of the half-angles of the edges incident to v.

Our choice for conductances is expressed in terms of elliptic functions, more precisely using the Jacobi elliptic trigonometric functions.

For any $k \in [0, 1]$, we define $k' = \sqrt{1 - k^2}$,

$$K = K(k) := \int_0^{\pi/2} \frac{1}{\sqrt{1 - k^2 \sin^2(\phi)}} \mathrm{d}\phi, \quad \text{and} \quad K' = K'(k) := K(k').$$

$K(k)$ is the complete elliptic integral of 1st kind. $K(k)$ and $K'(k)$ are both finite when $k \in (0, 1)$. Let us define also the complete elliptic integral of 2nd kind,

$$E = E(k) := \int_0^{\pi/2} \sqrt{1 - k^2 \sin^2(\phi)} \mathrm{d}\phi.$$

All the quantities we will consider will depend implicitly on the parameter k, which is fixed once and for all.

The 12 Jacobi elliptic functions are represented by a two-letter symbol pq where $\mathrm{p}, \mathrm{q} \in \{\mathrm{s}, \mathrm{n}, \mathrm{d}, \mathrm{c}\}$. They are defined as meromorphic functions on the torus $\mathbb{C}/(4K\mathbb{Z} + 4iK'\mathbb{Z})$ with some prescribed poles and zeros Their notation has convenient properties, such as the fact that $\mathrm{pr} = \mathrm{pq} \,/\, \mathrm{rq}$, with the convention that $\mathrm{pp} = 1$. The most important functions for us will be sn, cn and $\mathrm{sc} = \mathrm{sn} \,/\, \mathrm{cn}$.

In the extremal case when $k = 0$, the torus becomes a cylinder, and the functions sn and cn become sin and cos respectively and dn degenerates to the constant function equal to 1. The function sc can thus be seen as an elliptic generalisation of the usual trigonometric tan function, which was used to define conductances in the massless case.

We define the following conductances and masses, indexed by the elliptic parameter k, to construct our massive Laplacians on isoradial graphs.

Definition 16 (conductances)**.** The conductance of an edge e with half-angle θ is

$$\rho_e = \rho(\theta) = \mathrm{sc}(\underline{\theta}),$$

where[1] the parameter $\underline{\theta} = \frac{2K}{\pi}\theta \in [0, K]$.

Definition 17 (masses)**.** The (squared) mass at a vertex v of degree d, and half-angles $\theta_1, \dots \theta_d$ is

$$m_v = \sum_{j=1}^{d} (A(\underline{\theta_j}) - \rho(\theta_j))$$

where

$$A(u) = \frac{1}{k'} \left(\int_0^u \mathrm{dc}^2(t)\mathrm{d}t + \frac{E-K}{K} u \right)$$

is connected to Jacobi's Epsilon function via Jacobi's imaginary transformation.

7.4. Massive exponential functions

We define a family of *massive discrete exponential* functions $\mathrm{Exp}(\cdot|k)$ on pairs of vertices (x, y) of G, depending on an extra *spectral parameter* $u \in T(k) = \mathbb{C}/(4K\mathbb{Z} + 4iK'\mathbb{Z})$. As in the massless case, a factor is attach to each oriented edge ϵ of $G_\diamond$, identified with the unit vector $e^{i\alpha(\epsilon)} = e^{i\alpha}$:

$$\mathrm{Exp}_\epsilon(u|k) = i\sqrt{k'}\,\mathrm{sc}\big(\frac{u - \underline{\alpha}}{2}\big|k\big).$$

Given two vertices x and y and a path of edges $\epsilon_1 = e^{i\alpha_1}, \dots \epsilon_n = e^{i\alpha_n}$ from x to y, the massive discrete exponential function from x to y is defined as

$$\mathrm{Exp}_{x,y}(u|k) = \prod_{j=1}^{n} \mathrm{Exp}_{\epsilon_j}(u|k) = \prod_{j=1}^{n} \left(i\sqrt{k'}\,\mathrm{sc}\big(\frac{u - \underline{\alpha}_j}{2}\big|k\big) \right).$$

[1] We use here a different convention than in [16], by keeping θ, α,... for the geometric angles. In [16], the parameters without bar were living on $\mathbb{R}/4K\mathbb{Z}$ and the geometric angles denoted by $\bar{\theta}$, $\bar{\alpha}$,....

One can easily check that the function is well defined, doesn't depend on the path and is a meromorphic function of $u \in T(k)$. $T(k)$ is a priori is smaller than the fundamental domain for a single factor $\mathrm{Exp}_\epsilon(\cdot|k)$, but because x and y are vertices of G, n is even, which adds an extra symmetry to the function. Moreover,

$$\mathrm{Exp}_{x,y}(u+2K|k) = \big(\mathrm{Exp}_{x,y}(u|k)\big)^{-1} = \mathrm{Exp}_{y,x}(u|k).$$

Lemma 3. *For every $u \in T(k)$ and y vertex of G, $x \mapsto \mathrm{Exp}_{x,y}(u)$ is a massive harmonic function for the massive Laplacian defined by the conductances and the masses above.*

Proof. This is very similar to the proof of harmonicity of (critical) exponential function, using the elliptic version of the triple tangent identity (5.1), which turns into a pseudo sum formula for the function A,

$$-k'\,\mathrm{sc}(u|k)\,\mathrm{sc}(v|k)\,\mathrm{sc}(v-u|k) - A(v-u|k) = A(v|k) - A(u|k). \tag{7.2}$$

□

The massive discrete exponential functions give also, as in the massless case, a zero-curvature representation of solutions of the equation $\Delta^m f = 0$ on G. In the limit when k goes to 0, we recover the discrete exponential function from Kenyon and Mercat, with the relation $\lambda = e^{iu}$:

$$\mathrm{Exp}_\epsilon(u|0) = i\tan\big(\frac{u-\alpha}{2}\big) = \mathrm{Exp}_\epsilon(e^{iu}).$$

7.5. The massive Green function

The *massive Green function* on an isoradial graph, as in the massless case, has a local expression: the entry $\mathcal{G}^k_{x,y}$ between two vertices x and y of G depends only on the geometry of a(ny) path between x and y in $G_\diamond$. The argument used in [9, Lemma 17] shows that there exists a real interval I_{xy} on $T(u)$ of length less than $2K$ containing all the poles of $u \mapsto \mathrm{Exp}_{x,y}(u|k)$.

Theorem 12 ([16], Theorem 12)**.** *For any vertices x and y, $\mathcal{G}^k_{x,y}$ is given by the following integral formula:*

$$\mathcal{G}^k_{x,y} = \frac{k'}{4i\pi}\oint_{C_{x,y}} \mathrm{Exp}^k_{x,y}(u)\mathrm{d}u, \tag{7.3}$$

where $C_{x,y}$ is a closed contour on $T(k)$ winding once vertically and crossing the real axis outside of $I^k_{x,y}$.

In order to compute explicitly values of the massive Green function one may find convenient to use another equivalent integral representation: if $H(\cdot|k)$ is a function which is meromorphic and satisfies

$$\forall\ u \in \mathbb{C} \quad H(u+4K|k) = H(u|k) + 1, \quad H(u+i4K'|k) = H(u|k),$$

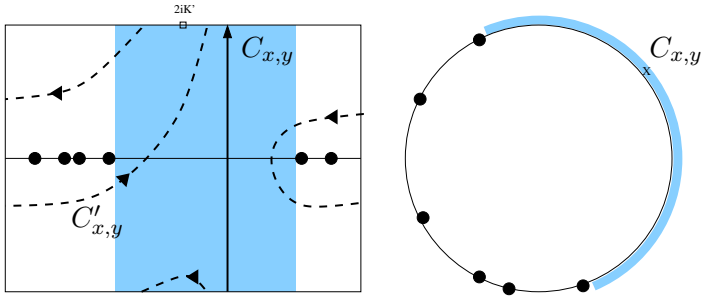

Figure 7.1.: Left: the torus $T(k)$ with the poles of $\mathrm{Exp}_{x,y}(u|k)$ (black dots), the contours $C_{x,y}$ (plain line, which can in fact move inside the blue region) and $C'_{x,y}$ (dashed line). Right: the real axis on the torus $T(k)$ seen from above. The cross marks the intersection with $C_{x,y}$.

for example the following, expressed in terms of the function A:

$$H(u|k) = \frac{-ik'K'}{\pi} A(\frac{iu}{2}|k').$$

Then (7.3) can be rewritten as

$$\mathcal{G}^k_{x,y} = \frac{k'}{4i\pi} \oint_{C'_{x,y}} \mathrm{Exp}_{x,y}(u|k) H(u|k) \mathrm{d}u, \tag{7.4}$$

where $C'_{x,y}$ is a trivial closed contour on $T(k)$ containing in its interior all the poles of $\mathrm{Exp}^k_{x,y}$ and the pole of H, located at $u = 2iK'$. One can then lift the contour $C'_{x,y}$ to a closed contour on the whole plane and compute explicitly the integral by the residue theorem. See Figure 7.1 for a representation of the contours $C_{x,y}$ and $C'_{x,y}$.

However, Formula (7.3) is well suited for asymptotic analysis via the saddle point method and allows one to write down very precise asymptotics, under some mild assumptions on the structure of the isoradial graph[2]:

Theorem 13 ([16], Theorem 14)**.** *Let x and y be two vertices of G. Let $\chi(u|k) = \frac{1}{|x-y|} \log \mathrm{Exp}_{(x,y)}(u + 2iK'|k)$, where $|x-y|$ is the graph distance between x and y in $G_\diamond$. When the distance $|x-y|$ goes to infinity,*

$$\mathcal{G}^k_{x,y} = \frac{k'}{2\sqrt{2\pi|x-y|\chi''(u_0|k)}} e^{|x-y|\chi(u_0|k)}(1 + o(1)),$$

where u_0 is the unique real u outside of $I_{x,y}$, such that $\chi'(u|k) = 0$.

The quantity, $\chi(u_0|k)$ is strictly negative, which implies exponential decay of the Green function. Moreover, it converges when the proportions of unit steps with a given angle on the path from x to y in $G_\diamond$ converge. The details are carried out in [16, Section 4.3].

[2] *e.g.*, that the total number of possible directions for the edges of $G_\diamond$ is finite.

7.6. Integrability

The fact that we have a zero curvature representation for a family of massive harmonic functions is an evidence of integrability of the massive Laplacian, understood as a nice behaviour of this operator under star-triangle transformations of the isoradial graphs. This is indeed the case, as we can see from the following statements Let G and G' be two infinite isoradial graphs differing by a star-triangle transformation, as in Figure 5.2. G has the star, and thus has an extra vertex x_0.

Lemma 4 ([16], Proposition 8)**.** *There is a bijection between harmonic functions on G and G' as follows:*

- *If f is massive harmonic on G, then its restriction to vertices of G' is massive harmonic on G'.*
- *If g is massive harmonic on G', then there exists a unique way to extend g to x_0 in a massive harmonic function f on G.*

This lemma implies in particular that there is a unique and well-defined way to transport a massive harmonic function along a flow of isoradial graphs differing by star-triangle transformations, or equivalently, of monotone hypersurface in $\mathbb{Z}^d$ differing by adding/removing a 3-cube. This property is called in [BS08] *3-dimensional consistency*. In fact this property does not require f or g to be massive harmonic at every vertices of the graph, but just that f is, at the vertex in the center x_0 of the star. The massive Laplacians of f and g will coincide on other vertices.

This lemma has a counterpart in statistical mechanics, in the context of rooted spanning forests:

Proposition 7 ([16], Theorem 41)**.** *The rooted spanning forest models with the (noncritical) conductances and masses is Z-invariant: the measure of a local event is unchanged if star-triangle transformations are performed outside of the locus of the event.*

A direct proof is given in [16, Section 6.4], in the same spirit as what we sketched for the Ising model in Section 5.5, by checking proportionality of local configurations in the graphs differing by a star-triangle transformation, given conditions on the boundary of the location of this transformation, which involves quite long and tedious computations. It is not the case that the identities the weights have to satisfy for Z-invariance reduce directly to the (elliptic version of) the triple tangent identity, as for spanning trees in the critical case.

A shorter but indirect proof is to say that the probability of a local event is given by a determinant of the transfer impedance matrix, which is a linear combination of entries of the Green function. Since the Green function is massive harmonic (expect on the diagonal), we can apply Lemma 4 and get that the entries of the Green function, and thus the probability of the event does not change.

7.7. Construction of Gibbs measures for Z-invariant spanning forests

Given the local property of the massive Green function, one can define, as what has been done for the critical Z-invariant model, a Gibbs measure on rooted spanning forest on any infinite isoradial graph, by mimicking writing a determinant formula involving the transfer impedance matrix (7.1), as in the finite case.

Theorem 14 ([16], Theorem 34)**.** *Let $k \in (0,1)$. There exists a unique measure $\mathbb{P}^k_{forest}$ on rooted spanning forests of G such that for any distinct edges $e_1, \dots, e_j$, and any distinct vertices $x_1, \dots, x_k$ of G, the probability of seeing these edges and roots in the random rooted spanning forest is:*

$$\mathbb{P}^k_{forest}(\{e_1, \dots, e_j, x_1, \dots, x_k\}) = \det \left(\begin{array}{c|c} \big(\mathsf{H}^k(e_i, e_\ell)\big) & \big(\mathsf{H}^k(e_i, x_\ell)\big) \\ \hline \big(\mathsf{H}^k(x_i, e_\ell)\big) & \big(\mathsf{H}^k(x_i, x_\ell)\big) \end{array} \right)$$

where H^k is the transfer impedance on G.

The measure $\mathbb{P}^k_{forest}$ is the weak limit of the sequence $(\mathbb{P}^{k,(n)}_{forest})$ on rooted spanning forests of any exhaustion $(G_n)_{n\geq 1}$ of G by finite graphs. Under $\mathbb{P}^k_{forest}$, the connected components of the random rooted spanning forests are finite almost surely.

The proof follows the same lines as the proof of the construction of the Gibbs measure for the critical Z-invariant Ising model from Theorem 10. It is even easier since we have the convergence of the massive Green functions for any exhaustion of G, and not only for toroidal exhaustions. See [16, Section D.4].

When the graph G is periodic, we compute explicitly the free energy $F(k)$ of rooted spanning forests, associated with the measure $\mathbb{P}^k_{\text{forest}}$, as a function of the half-angles of edges in a fundamental domain. It is obtained by a deformation argument using train-track tilting, as in [Ken02].

When $k = 0$, the probability measure is the measure on spanning trees from Burton and Pemantle [BP93]. We can study the phase transition from rooted spanning forests to spanning trees, and obtain the following phase transition of order 2 [16, Theorem 38]

$$F(k) = F_{\text{trees}} - k^2 \log k^{-1} |V_1| + O(k^2),$$

where $|V_1|$ is the number of vertices in a fundamental domain of G.

7.8. Spectral curves of massive Laplacians

We suppose in this section that G is periodic. One can define then as in Section 5.6 the characteristic polynomial P and the spectral curve C of the massive Laplacian on G for a given fixed $k \in (0,1)$.

In the same spirit as the work by Kenyon, Okounkov and Sheffield [KOS06, KO06, KS04] for bipartite periodic planar dimer models, we investigated algebraic properties of the spectral curve.

Theorem 15 ([16],Theorems 25 and 26)**.** *The following properties hold:*

- *The spectral curve is a Harnack curve of (geometric) genus 1 with a symmetry* $(z,w) \leftrightarrow (z^{-1}, w^{-1})$.
- *Every genus 1 Harnack curve with the* $(z,w) \leftrightarrow (z^{-1}, w^{-1})$ *is the spectral curve of a Z-invariant massive Laplacian on a periodic isoradial graph.*

Proof. The proof of the first statement is based on the fact that the exponential functions from a vertex to its translates by a basis of the lattice

$$z(u) = \mathrm{Exp}_{v,v+(1,0)}(u), \qquad w(u) = \mathrm{Exp}_{v,v+(0,1)}(u),$$

provide a complete parameterization $\psi : u \in T(k) \mapsto (z(u), w(u))$ of the spectral curve. This parameterization is birational, and $T(k)$ is a torus, thus the geometric genus of C is 1. The symmetry $(z,w) \leftrightarrow (z^{-1}, w^{-1})$ can be seen as a consequence of the fact that Δ^m is a Hermitian operator, or directly, from the fact that $z(u+2K) = z(u)^{-1}$ and $w(u+2K) = w(u)^{-1}$. We then notice that C has two real connected components (*i.e.*, invariant under complex conjugation), which are the image by ψ of two horizontal contours at height 0 and $2iK'$ on $T(k)$: C is thus a *maximal* curve. One of these components is bounded in $(\mathbb{C}^*)^2$ whereas the other one is unbounded and will intersect the coordinate axes. To prove that C is Harnack, it is then enough to show [Bru14] that this unbounded real component of C intersects the axes cyclically. But this property is a consequence of the compatibility between the cyclic order of the values of u corresponding to such an intersection with the axes (*i.e.*, when $z(u)$ or $w(u)$ become 0 or infinite), which are by definition of the exponential function, parameters associated to train-tracks, and the homology class in $H^1(\mathbb{T}, \mathbb{Z})$ of the train-tracks.

For the second statement, given a Harnack curve C of genus 1, one can construct a suitable periodic isoradial graph as follows. Since the curve is maximal (because Harnack) and has genus 1, and has the symmetry $(z,w) \leftrightarrow (z^{-1}, w^{-1})$, it has a parametrization of the form $\psi : u \mapsto (z(u), w(u))$, where u belongs to $T(k)$ for some $k \in (0,1)$, and

$$z(u) = \prod_{j=1}^{n} \left(i\sqrt{k'}\,\mathrm{sc}\big(\frac{u-\alpha_j}{2}\big)\right)^{-b_j}, \quad w(u) = \prod_{j=1}^{n} \left(i\sqrt{k'}\,\mathrm{sc}\big(\frac{u-\alpha_j}{2}\big)\right)^{-a_j},$$

where $\alpha_1, \dots, \alpha_n$ are ordered cyclically, $(a_j, b_j) \neq 0$ and both $\sum_j a_j$ and $\sum_j b_j$ are even. Several (consecutive) α_j can be equal, and a_j and b_j are coprime.

For any $j \in [1..n]$, draw on a torus $\mathbb{T}$ a simple loops L_j with homology class $H^1(\mathbb{T}, \mathbb{Z})$ given by $\{(a_j, b_j)\}$, and arrange these loops such there are only pairwise intersections and total number of intersections is minimal. This gives a graph with 4-valent vertices on the torus, which is the dual of a diamond graph on the torus. Now, since the curve C is Harnack, the cyclic order of the homology classes (a_j, b_j) in $\mathbb{Z}^2 \setminus \{(0,0)\}$ coincides with the cyclic order of the α_j's (see above). As a consequence one can put at an intersection between L_j and L_k a rhombus spanned by $e^{i\alpha_j}$ and $e^{i\alpha_k}$ to obtain the diamond graph of an isoradial graph on the torus, which can then be lifted to the plane. The spectral curve of the Laplacian on this isoradial graph will be exactly C. □

One can construct also the unique (up to a multiplicative constant) holomorphic form on C from Δ^m: define $Q(z,w)$ to be any principal minor of $\Delta^m(z,w)$ (they are all equal). Then

$$\eta = \frac{Q(z,w)}{zw\frac{\partial P}{\partial w}}\mathrm{d}z$$

is a holomorphic differential form on C. With the help of η, it is possible to show that in the periodic case, the Fourier expression for the Green function, as a double integral over the unit torus,

$$\mathcal{G}^k(x, y+(m,n)) = \iint_{|z|=|w|=1} \frac{Q_{x,y}(z,w)}{P(z,w)} z^{-m} w^{-n} \frac{\mathrm{d}z}{2i\pi z}\frac{\mathrm{d}w}{2i\pi w}$$

with $Q(z,w)$ the comatrix of $\Delta^m(z,w)$, reduces to the expression (7.3), by computing explicitly one integral, say that over z by the residue theorem, and performing a change of variable from the remaining variable w to u. Taking the limit when k goes to zero extends this connection between the Fourier formula and the local one to the massless case. This connection was not understood in the previous articles [Ken02, dT07a] and [9].

8. The XOR Ising model

We present another aspect of the connection between the Ising model and dimer models, studied in [14] in collaboration with Béatrice de Tilière, namely the correspondence between the XOR Ising model on a graph G and a bipartite dimer model on a decorated version of its medial graph, denoted by G_Q.

A configuration of the *XOR Ising model* is simply obtained by taking the pointwise product of two independent Ising configurations on the same graph[1]. In [14], we are interested in describing the contours separating the spins of different signs in a random XOR configuration as contours of the height function of a bipartite dimer model.

This work was motivated by a conjecture formulated by Wilson, supported by numeric simulations on the hexagonal lattice. At the critical temperature, the interfaces between XOR clusters seemed to behave like conformal invariant curves. More precisely,

Conjecture 1. *[Wil11] The scaling limit of the family of loops separating clusters in the critical XOR Ising model are the level lines of the Gaussian Free field, corresponding to levels that are odd multiples of* $\frac{\sqrt{\pi}}{2}$.

The result we proved can be seen as a discrete version of that conjecture, which is valid for any coupling constant of the Ising model, and not just at criticality:

Theorem 16 ([14], Theorem 1.3)**.** *The XOR contours have the same law as the level lines of the restriction of the height function of the bipartite dimer model on the graph* G_Q.

We explain at the end of this chapter the connection between these two statements.

Although most of this work is valid in the general context of the Ising model on a finite graph drawn on a surface, the extension to infinite planar graph can be carried out for isoradial graphs, since by locality properties, Gibbs measures for both XOR Ising configurations and dimer configurations can be constructed, by Theorem 10 and its analogue for dimers [dT07a], as limits of probability measures on finite graphs, which guarantees that this identity in law is still true in the limit.

8.1. Setting and definitions

To simplify the exposition, we will suppose here that G is a planar graph, although everything is valid for a graph G drawn on a compact surface Σ with no boundary, and genus g.

[1] The name XOR comes from the fact that if instead of ± 1, one uses 0 and 1 to represent the spins, then the product of two spins is mapped to the XOR logic operation, giving 1 if and only if the two spins are the same.

Let $\mathbb{P}_{\text{Ising}} = \mathbb{P}_{\text{Ising}}^{(G^*,J)}$ the probability measure on spin configurations on G^*, as in Section 5.5. Let (σ, σ') a pair of independent Ising configurations, with the same law $\mathbb{P}_{\text{Ising}}$. Consider the low-temperature expansion of these two configurations σ and σ', giving contours on G, represented in blue and red respectively. In the superposition of the two polygonal configurations, we see different kinds of dual edges:

- edges not covered at all by any of the polygonal configurations;
- *monochromatic edges*, which are present in exactly one of the polygonal configurations;
- *bichromatic edges*, appearing in both polygonal configurations.

The monochromatic edges have a simple interpretation in terms of the XOR configuration $\tau = \sigma \cdot \sigma'$.

Lemma 5. *The monochromatic edges are the low-temperature expansion of the XOR configuration τ: they separate clusters where $\tau = +1$ and $\tau = -1$.*

We are thus interested in the law of the random set of monochromatic edges. To understand this law, we rewrite the contribution of any monochromatic configuration to the partition function in a more convenient way, as explained below.

8.2. Mixed contour expansion for the double Ising model

We want to map the double Ising model to a *mixed contour model*, with polygonal contours on G and G^*. In this model, a contour on G and a contour on G^* are not allowed to cross one another, in such a way that monochromatic XOR contours are exactly the contours on G in this mixed contour model.

The idea is to reinterpret the contribution of a configuration of monochromatic edges is the following: the monochromatic polygonal contours cut the surface graph Σ into a certain number pieces $\Sigma_1, \Sigma_2, \dots$. On each of these pieces, the collection of bichromatic edges can be seen as the low temperature expansion of an Ising temperature, where the coupling constants are now doubled.

To compute the relative weight of this given configuration of monochromatic edges in the XOR Ising model, we need to resum all possible configurations of bichromatic edges in each piece Σ_i, and reinterpret it as the high temperature expansion of that Ising model, giving now contours on Σ_i^*.

There is a subtlety though: the number of bichromatic edges attached to a connected component of the boundary of a piece may not be even: the corresponding low temperature contours are thus not bounding real clusters, but have a topological defect (which can be realised as defect lines in the Ising model, along which signs of the interacting constants are changed). Thus the Kramers Wannier duality needs to be expanded to accommodate with these topological defects, as mentioned in Section 5.A.4. See [14, Section 2] for the details.

With some fine combinatorics and tools from relative homology, it is possible to write as follows the partition function for our model.

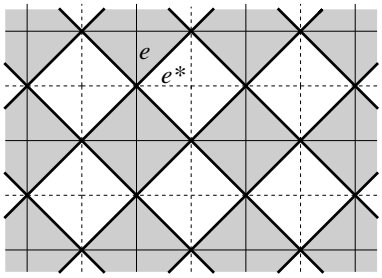

Figure 8.1.: A piece of the square lattice (horizontal and vertical plain lines), its dual (dotted lines) and its medial graph (diagonal bold lines).

Proposition 8 ([14], Proposition 1.2)**.** *The double Ising partition function can be rewritten as:*

$$\mathcal{Z}_{\substack{double\\Ising}}(G^*, J) = \mathcal{C} \sum_{(P,P^*)} \left(\prod_{e\in P} \frac{2e^{-2J_{e^*}}}{1+e^{-4J_{e^*}}} \right) \left(\prod_{e^*\in P^*} \frac{1-e^{-4J_{e^*}}}{1+e^{-4J_{e^*}}} \right),$$

where the sum is over pairs of polygonal contours P, P^* on G and G^* respectively, such that $P \cap P^* = \emptyset$, and $\mathcal{C} = 2^{\#faces\ of\ G+1} \prod_{e:edge\ of\ G} \cosh(2J_e^*)$.

The right hand side is the combinatorial sum for configurations of the mixed contour model. The weight of a configuration (P, P^*) in this model is a product of local contributions, for each primal or dual edge appearing in the mixed contour configuration.

8.3. From mixed contours to bipartite dimer models

We now map the mixed contour model to a dimer model on a bipartite graph G_Q, called *quadritilings* [dT07a]. This mapping is performed in two steps:

- first a mapping due to Nienhuis [Nie84] between the mixed contours and configurations of the 6-vertex model on the medial graph G_M.
- then Wu–Lin/Dubédat's mapping [WL75, Dub11b] between the 6-vertex model and the bipartite dimer model on the decorated graph G_Q

8.3.1. From mixed contours to the 6-vertex model

The *medial graph* G_M of the planar graph G is constructed as follows: its vertices are edges of G. Two vertices are connected if the corresponding edge in G share a vertex. It is the dual of the diamond graph $G_\diamond$ defined in Section 5.1, and all its vertices have degree four. Its faces can be colored in black and white in a checkerboard fashion: a face is white (resp. black) if it corresponds to a primal (resp. dual) vertex of G.

A *6-vertex configuration* or an *ice-type configuration* is usually defined in terms of orientations. We choose here the following equivalent representation in terms of even subgraph:

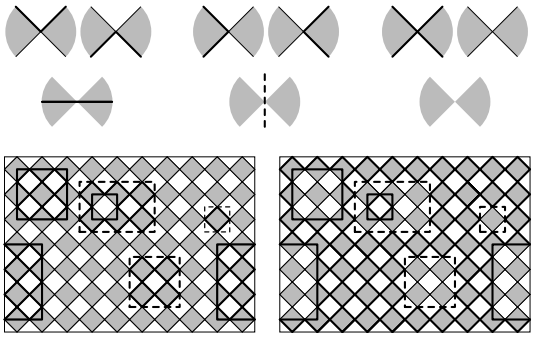

Figure 8.2.: Mapping from mixed contours to a 6-vertex configuration, on the local level (top), and on the global level (bottom).

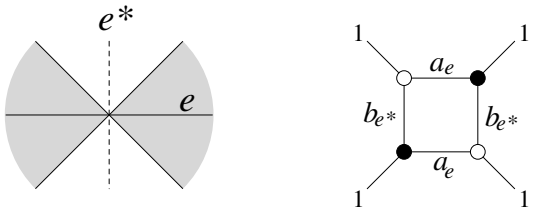

Figure 8.3.: Construction of the graph G_Q from the medial graph G_M by decorating vertices.

Definition 18. A 6-vertex configuration of G_M is a subgraph of G_M such that around each vertex, there is an even number of consecutive present edges.

The allowed configurations around a vertex v, grouped in 3 pairs (A, B, C) are represented on top of Figure 8.2.

The mapping [Nie84] between the 6-vertex model and the mixed contour expansion goes as follows: whenever a vertex of G_M has exactly two neighboring edges in the 6-vertex configuration, put the edge of G or G^* separating the present from the absent edges. See Figure 8.2. This mapping is two-to-one.

This mapping transfers weights on the edges and dual edges (e or e^*) of G to local configuration around a vertex of the medial graph corresponding to that edge: configurations of group A, B and C receive the following weights respectively:

$$a = \frac{2e^{-2J_{e^*}}}{1 + e^{-4J_{e^*}}}, \quad b = \frac{1 - e^{-4J_{e^*}}}{1 + e^{-4J_{e^*}}}, \quad c = 1.$$

8.3.2. From the 6-vertex model to a bipartite dimer model

The 6-vertex model can be mapped to dimer configurations of a new graph G_Q, constructed by replacing every vertex v of G_M by a small square, the vertices of which are connected to the four edges incident to v. See Figure 8.3.

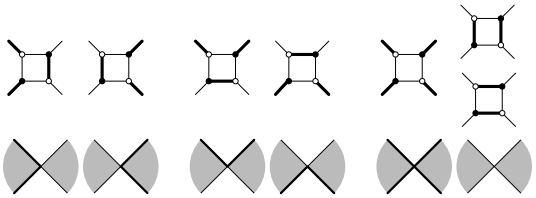

Figure 8.4.: Local configurations for dimer configurations of G_Q (*quadritilings* [dT07a]) and the corresponding 6-vertex local configurations.

The mapping by Wu and Lin [WL75], and rediscovered by Dubédat [Dub11b] is depicted on Figure 8.4, and consists in requiring exterior edges to match in the neighborhood of every vertex of G_M. This mapping between local configurations is one-to-one except in the empty edge case, where this mapping is two-to-one.

The weights for the mixed contour model are such that the 6-vertex model is *free fermionic*: this mapping can be made weight preserving by putting edge weights for dimers and requiring that the probability of a dimer configuration is proportional to the product of the weights of its edges. Our choice of weights for the mixed contour model arising from the double Ising model gives the following dimer weights:

$$a_e = \frac{2e^{-2J_{e^*}}}{1+e^{-4J_{e^*}}}, \quad b_{e^*} = \frac{1-e^{-4J_{e^*}}}{1+e^{-4J_{e^*}}},$$

for the interior edges, and 1 for the exterior edges.

8.4. The critical XOR Ising model on isoradial graphs

When the graph G is isoradial, then the graph G_Q turns out also to be isoradial (with circumradius 1/2). If we choose for the Ising model the coupling constants J_{e^*} to be the Z-invariant critical ones, given by (5.6), one get for all edges e and dual edges e^* of G:

$$a_e = \cos(\theta_e), \qquad b_{e^*} = \cos(\theta_e^*) = \sin(\theta_e).$$

these are the *critical weights* for dimer models on bipartite isoradial graphs introduced by Kenyon [Ken02]. Infinite Gibbs measures $\mathbb{P}^\infty_{\substack{\text{double}\\\text{Ising}}}$ and $\mathbb{P}^\infty_Q$ for both the double Ising model on G [9] and the dimer model on G_Q [dT07a] can be constructed in such a way that the mappings above are preserved.

Since G_Q is bipartite, the dimer model has a *height function* representation: a dimer configuration represents a unit flow on edges of G_Q from white to black vertices. The function which associates to each edge its probability to be covered by a dimer under $\mathbb{P}^\infty_Q$ is also a unit flow, since a vertex can be adjacent to exactly one dimer. Therefore, the difference is a divergence-free flow on edges of G_Q, thus its dual is the derivative of a function on faces of G_Q: *the height function*. Let us denote by $h_{V^*}(M)$ the restriction of this height function corresponding to a dimer configuration M on G_Q, restricted to the

faces of G_Q corresponding to a primal vertex of G. It is determined once we know its value at a given dual vertex v^*, which we take to be zero.

Lemma 6 ([14], Lemma 7.1)**.** *The restricted height function h_{V^*} has the following properties*

- *h_{V^*} takes only values in $\mathbb{Z}$.*
- *The increments of h_{V^*} are nonzero if and only if the two dual vertices are separated by a primal edge of G in the corresponding mixed contour model*

Since primal edges in the mixed contour model and monochromatic edges (or edges of contour separating clusters) in the XOR Ising model have the same law by Proposition 8, we get the following:

Theorem 17 ([14], Theorem 7.5)**.** *Monochromatic polygon configurations of the critical XOR-Ising model have the same distribution as level lines of the restriction to dual vertices of the height function of dimer configurations of G_Q.*

Theorem 17 can be interpreted as a proof of a version of Wilson's conjecture in a discrete setting, before passing to the scaling limit, and brings some elements for a complete proof of this conjecture. In particular, it explains the link with the Gaussian free field and the factor $\sqrt{2}$, as we will now show.

The contours on G separating distinct integer values of h_{V^*} can be understood as discrete level lines corresponding to half-integer values.

On infinite isoradial graphs, the dimer height function h_{V^*}, seen as a distribution on the graph G_Q with circumradius ϵ, is known to converge, as ϵ goes to zero (in a weak sense, unfortunately), to the Gaussian massless free field times $\frac{1}{\sqrt{\pi}}$, like the unrestricted height function [dT07b].

Therefore, it is natural to expect that these contour lines converge to the contour lines of the limiting object, *i.e.*, to level lines for the Gaussian free field with levels $(k+\frac{1}{2})\sqrt{\pi}$, $k \in \mathbb{Z}$. Unfortunately, the result for the convergence result of the height function to the Gaussian free field is too weak to ensure convergence of contour lines.

The Gaussian free field is a wild object: it is a random *generalized* function, and not a function, and as such, there is no direct way to define what its level lines are. The level lines of the Gaussian free field are understood here as the scaling limit when the mesh goes to zero of the level lines of the discrete Gaussian free field on a triangulation of the domain, which separate domains where the field is above or below a certain level [SS09].

The level lines of the Gaussian free field corresponding to levels that are odd multiples of $\lambda = \sqrt{\frac{\pi}{8}}$ form a CLE_4 [SS09, MS]. It is conjectured to be the full scaling limit for the critical double dimer loops, which can be seen as discrete half integer level lines of the difference of the two height functions. This difference, by independence, converges (in a weak sense) to $\sqrt{2/\pi}$ times the Gaussian free field, which would give a consistent spacing.

The contour lines of the XOR Ising models are conjectured by Wilson to have the same limiting behavior as the CLE_4, except that there are a factor of $\sqrt{2}$ times fewer loops in

the XOR Ising picture. This conjecture is in agreement with predictions of conformal field theory [IR11, PS11].

Therefore, the extra factor $\sqrt{2}$ compared to the CLE_4 spacing in Wilson's conjecture corresponds to the fact that contours in the XOR Ising model have to do with contour lines of only one dimer height function, as opposed to two for dimer loops.

Part III.

Other works and possible developments

9. Other works

In this chapter, we briefly describe the results of two other papers related to dimer models and random partitions. In Section 9.1, we present the results of a joint work [7] with Béatrice de Tilière, about the asymptotic distribution of the winding of dimer configurations on the honeycomb lattice wrapped on a large torus. In Section 9.2, we give the main results of [10] obtained with Dan Beltoft and Nathanaël Enriquez about the limit shape of a random Young diagram constrained in a large rectangular box, and the fluctuations around this limit shape.

9.1. Winding of the toroidal honeycomb dimer model

We consider the dimer model on a family of graphs $G_{m,n}$ obtained as the quotient of the biperiodic honeycomb graph by a two dimensional lattice.

A dimer configuration $\mathcal{C}$ can be interpreted as a function $\alpha_{\mathcal{C}}$ on edges with definite divergence at each vertex. The difference with a fixed function on edges α_0 with the same divergence (and which may or not come from a dimer configuration) is a divergence-free flow, whose dual is a closed form on dual edges.

If the graph is planar, then this closed form is exact, and is the differential of a function on faces: the *height function*. But as in classical differential topology, if the graph is drawn on a surface of higher surface, the height function is not well defined, and has *periods*.

In a joint work with Béatrice de Tilière [7], we determine the limit of the law of the periods of the height function of a uniform dimer configuration on $G_{m,n}$, as m and n go to infinity, with an aspect ratio $\rho = \frac{n}{m\sqrt{3}}$ kept fixed.

We prove the following theorem:

Theorem 18 ([7], Theorem 1)**.** *When n and m go to infinity, in such a way that $\lim \frac{n}{m\sqrt{3}} = \rho \in (0, \infty)$, the pair of horizontal and vertical periods converges in law to a two-dimensional random variable $wind_\rho$, with a discrete Gaussian distribution:*

$$\mathbb{P}(wind_\rho = (k, l)) \propto \exp\left(-\frac{\pi}{2}(\rho k^2 + \frac{l^2}{\rho})\right).$$

The proof of this result is based on a very precise asymptotic analysis of the partition function of the dimer model on the torus, with slightly perturbed weights on edges, depending on their orientation. We use then the combinatorial fact that the number of edges of each orientation is a linear function of the period to conclude. The partition function is a linear combination of four determinants, by Kasteleyn's theorem, each of

these being written as a double product over roots of unity, using periodicity of the underlying graph.

The asymptotic analysis is performed in this particular case for simplicity, but looking at the proof, one sees that the following ingredients are essential:

- the spectral curve of the corresponding dimer model is a Harnack curve, and the dimer model is in a liquid phase. As a consequence, the curve will intersect twice the unit torus.
- whereas the contributions of unit roots far from those points will contribute to the free energy (the global exponential growth of the partition function), the terms close to the intersection points with the spectral curve will give rise to terms looking like Jacobi's triple product formula, thus elliptic theta functions.
- The generating function for the discrete Gaussian distribution is also expressed in terms of theta functions, which are obtained as recombination of the various contributions of neighborhoods of the intersection points in the four determinants.

The program to extend this computation to all toroidal bipartite dimer models, and much more has been finalized in a work by Richard Kenyon, Nike Sun and David Wilson [KSW13]. This result is in agreement with predictions of the conformal field theory. On isoradial graphs on the torus, the height function converges to a compactified Gaussian massless free field [Dub11a]. The result above should thus be true for a more general class of graphs. Mathematical results in that direction can be found in a recent work by Julien Dubédat and Reza Gheissari [DG15], for the wide class of Temperleyan graphs, without assumption on periodicity, but with instead an assumption about the limiting behaviour of the simple random walk on the underlying graph. For other robust results about dimers using connection with the behaviour of the loop erased random walk, see [BLR16].

9.2. Limit shape and fluctuations of boxed partitions

In [10] in collaboration with Dan Beltoft and Nathanaël Enriquez, we considered a probability measure $\mathbb{P}^q_{a,b}$ on partitions contained in an $a \times b$ rectangle, *i.e.*, with at most a parts, each of length at most b. The probability of a partition λ fitting in this rectangle is

$$\mathbb{P}^q_{a,b}(\lambda) = \frac{1}{Z_{a,b}(q)} q^{|\lambda|},$$

where $Z_{a,b}(q)$, the *partition function*, is the sum of $q^{|\mu|}$ over all the partitions μ in the $a \times b$ rectangle.

We were interested in the large scale behavior of a typical partition when the dimensions of the box become very large. More precisely, we consider sequences of positive integers $(a_n)_{n\geq 1}$ and $(b_n)_{n\geq 1}$ satisfying

$$\forall\ n \geq 1, \quad a_n + b_n = 2n, \quad \text{and} \quad \lim_{n\to\infty} \frac{a_n}{b_n} = \frac{\rho}{1-\rho}$$

for some fixed parameter $\rho \in (0,1)$. In order to have a nontrivial limit, the parameter q needs to be scaled, and go to 1 when n goes to infinity. We set $q = e^{-\frac{c}{n}}$. Note that $c = 0$

corresponds to a uniform probability measure. We will assume that $c \neq 0$. The results for $c = 0$ can be obtained by taking limits. The physical meaning of the parameter c is that of a pressure, since it is the variable conjugated to the (two-dimensional) volume.

We obtain a law of large number and a central limit theorem for the shape of the random Young diagram in the limit as n goes to infinity.

In order to do so, it is convenient to use the so-called Russian coordinates and rotate by 45°, so that if the leftmost corner is at $(0, 0)$, the coordinate of the rightmost corner is at $(a_n + b_n, b_n - a_n)$. See Figure 9.1.

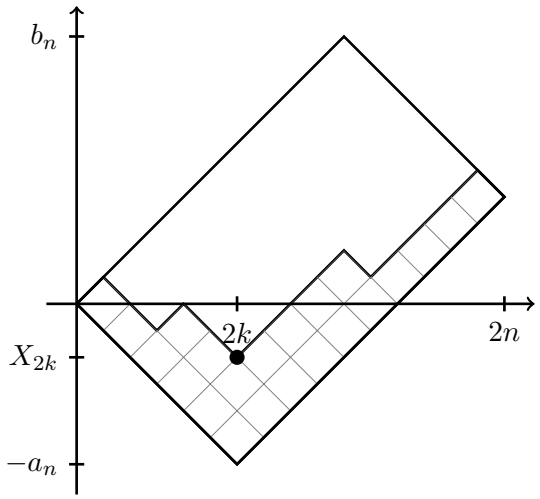

Figure 9.1.: A partition in a rectangular box.

For $\rho \in (0, 1)$ and $c \in \mathbb{R}^*$, let $L_{\rho,c}$ be the function defined by

$$\forall t \in [0,1], \quad L_{\rho,c}(t) = 1 - 2\rho + \frac{1}{c} \log \frac{\sinh(ct) + e^{c(2\rho-1)} \sinh(c(1-t))}{\sinh c}$$
$$= \frac{1}{c} \log \frac{e^{-ct} - e^{ct} + e^{-c(2-2\rho-t)} - e^{-c(t-2\rho)}}{e^{-c(2-2\rho)} - e^{2c\rho}}.$$

When we take the limit of this expression when c goes to 0, we get for $L_{\rho,c}$ a straight line joining $(0, 0)$ to $(1, 2\rho - 1)$.

Theorem 19 ([10], Theorem 1)**.** *The boundary of the rescaled random Young diagram converges in probability, for the uniform topology, to the curve of $t \mapsto L_{\rho,c}(t)$.*

$$\forall \varepsilon > 0, \ \lim_{n \to 0} \mathbb{P}^{e^{-c/n}}_{a_n, b_n} \big[\sup_{t \in [0,1]} \big| \tfrac{1}{2n} X_{2tn} - L_{\rho,c}(t) \big| > \varepsilon \big] = 0,$$

An important part of the proof is based on the fact that the partition function $Z_{a,b}(q)$ for partitions in an $a \times b$ box has a closed form: it is expressed as a q-deformed binomial coefficient, where integers j in factorials are replaced by their q-analogues $j_q = \frac{1-q^j}{1-q}$.

$$Z_{a,b}(q) = \binom{a+b}{a}_q = \prod_{j=0}^{b-1} \frac{1 - q^{a+b-j}}{1 - q^{b-j}}.$$

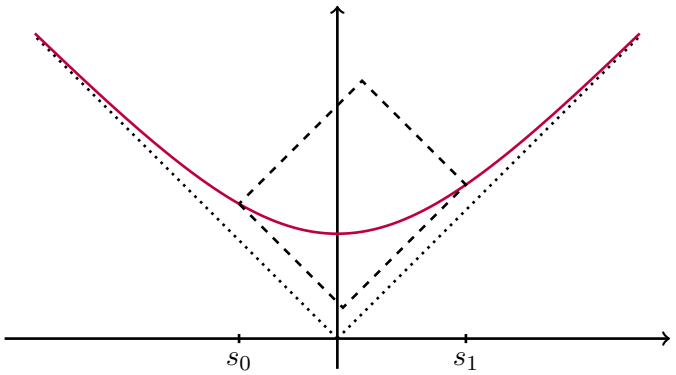

Figure 9.2.: Limit shapes $L_{\rho,c}$ are restrictions of the universal Temperley–Vershik curve.

for which we can derive asymptotics from a deformed version of Stirling formula [10, Proposition 3].

It should be noted that the curve $L_{\rho,c}$ is a restriction of the Temperley–Vershik curve, describing the limit shape of a uniform partition of a large integer [Ver96], to a rectangular box, as noticed by Petrov [Pet10]. See Figure 9.2.

In the case when the convergence of a_n/b_n to $\frac{\rho}{1-\rho}$ is fast enough (namely $\frac{a_n}{2n} = \rho + o(\frac{1}{\sqrt{n}})$), we have a result for the fluctuations around the limit shape. We define for $n \in \mathbb{N}^*$ a new rescaled process:

$$\forall t \in [0,1], \quad \tilde{X}_t = \tilde{X}_t^{(n)} = \sqrt{n}\left(\frac{1}{2n} X_{2nt} - L_{\rho,c}(t)\right). \tag{9.1}$$

and a normalisation function f:

$$f(s) = \frac{1}{\sqrt{2}} \frac{\sqrt{(e^{2c\rho}-1)(1-e^{-2c(1-\rho)})}}{\sinh cs + e^{c(2\rho-1)}\sinh(c(1-s))} = \frac{\sqrt{2\sinh(c\rho)\sinh(c(1-\rho))}}{e^{c(\frac{1}{2}-\rho)}\sinh(cs) + e^{c(\rho-\frac{1}{2})}\sinh(c(1-s))}.$$

Theorem 20 ([10], Theorem 2)**.** *The sequence $(\tilde{X}_s^{(n)}/f(s))_n$, converges weakly in the space D of càd-làg paths on $[0,1]$ (endowed with its usual topology) to the Ornstein–Uhlenbeck bridge $(Y_s)_{s\in[0,1]}$, which is the Gaussian process on $[0,1]$ with covariance*

$$\mathbb{E}[Y_s Y_t] = \frac{\sinh(cs)\sinh(c(1-t))}{c\sinh(c)},$$

for $0 \leq s < t \leq 1$.

This theorem is proved in two steps: first the convergence of finite dimensional marginals, and then a tightness argument. To prove convergence of all finite dimensional marginals, it is enough to prove that of the two point correlation function, because the process $(\tilde{X}_n)$ is Markov.

An analogue of Theorem 20 can also be written down for fluctuations around Temperley–Vershik's curve for the unconstrained case: it is described by a stationary Ornstein–Uhlenbeck process on $\mathbb{R}$, modulated by a cosh function. See [10, Theorem 4]. When we condition this process to have zero integral over $\mathbb{R}$, we obtain a new centered Gaussian process with covariance between time s and t is given by

$$\frac{e^{-|t-s|}}{2\cosh s \cosh t} - \frac{\pi^2}{6} h(s)h(t),$$

where $h(t) = \frac{6}{\pi^2} t \tanh t - \log(2\cosh t)$. Expressed in the original coordinates (by rotating by 45°), this covariance is the one obtained by Pittel [Pit97], who deals with the microcanonical ensemble of partitions (with a fixed area $|\lambda| = n \to \infty$). The fluctuations in that case are thus given by this Gaussian, but non-Markov process.

10. Some perspectives

We briefly list here some ongoing projects and some topics for future research related to the material presented in this manuscript.

Limit shape and fluctuations of the large pyramid partitions

We mentioned the Aztec diamond as an example of a steep domino tiling, which can be studied via vertex operators. An other example is the model of pyramid partitions in a strip of finite width. In a work in progress with Dan Betea and Mirjana Vuletić, we study the shape of large steep domino tilings, in particular pyramid partitions, using the vertex operator formalism. See Figure 10.1. Although of course many features in terms of limit shape and fluctuations for these objects are similar to skew plane partitions [OR07][11], some new phenomena appear, like the appearance of finite depth cups on the sides. See Figure 10.2. Due to their symmetry axis, fluctuations near these cups should not be governed by the Pearcy process [OR07], but described instead by the cusp Airy process [OR06, DJM15].

Vertex operators we use here are said to be of *type A*. There are also vertex operators of other types (similar to types in the classification of simple Lie algebras). Type B vertex operators have a boson-fermion correspondence [Ang13]. In a longer term, we would be interested in understanding and exploring connections between these vertex operators of other types and combinatorial models, and use them to derive, with this algebraic operators, information about corresponding large combinatorial objects.

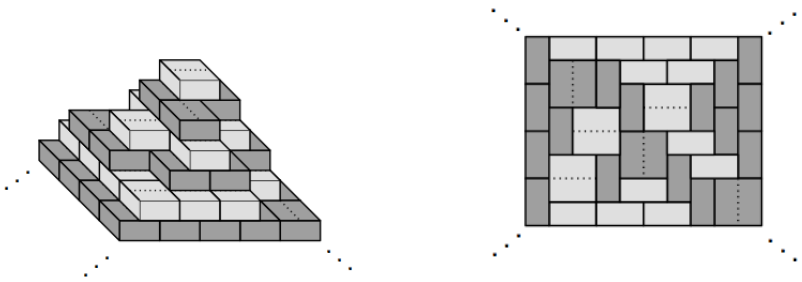

Figure 10.1.: A pyramid partition as a pile of $2 \times 2 \times 1$ blocks, and its projection, seen as a domino tiling.

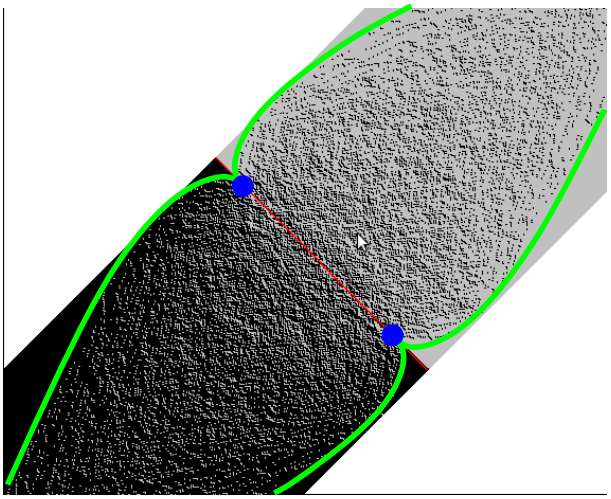

Figure 10.2.: A typical finite width pyramid partition, represented as a system of particles, the arctic curve separating the liquid region from the frozen zones where the color of a marble is asymptotically deterministic, and the finite depth cusp indicated by discs.

Non critical Z-invariant Ising and XOR Ising models on isoradial graphs

Now that the Z-invariant massive Laplacian is defined [16], the program to extend the results of [8, 9] to the non-critical Z-invariant Ising model on infinite isoradial is being implemented in a joint work with Béatrice de Tilière and Kilian Raschel. We show that the spectral curve of the Kasteleyn operator on the Fisher graph is the spectral curve of the Massive Laplacian on the original isoradial. We find an explicit formula for the inverse Kasteleyn operator on the associated Fisher graph, as a contour integral of discrete massive exponential functions against a measure, which allows us to construct the Gibbs measure on contours separating spin clusters. The parameter $k' = \sqrt{1-k^2}$ plays the role of the temperature. We can then study the phase transition of the model as k' goes to 1.

Some formulas we obtain show some duality, because of properties of elliptic functions, which seems to be more than the duality high/low temperature on a graph and its dual explained in Section 5.A.3, but it is not completely understood yet. In order to construct the measure on spins from the measure on contours, one needs to know the average sign of a spin (spontaneous magnetisation) when boundary conditions "at infinity" are all plus (or all minus). It is needed to determined the bias of the coin we should flip to fix a given spin. Then all the other spins are determined given the contours. For critical or high temperature, this average value of the spin is 0, because there is enough entropy to decouple the spin at a vertex and the boundary conditions. However, in the low temperature phase, boundary conditions at infinity still have an influence on spins. We don't know how to compute it yet.

The Ising model is coupled with the $q = 2$ FK-percolation (called also the random

cluster model) [FK72, Gri06]. In [Ken04], Kenyon recalls the weights for the self-dual (critical) FK percolation on isoradial graphs. It would be interesting to see what could be said in the case $q = 2$ about this model out of criticality. For example, is there a link, like for the decay of dimer correlations, between the exponential tail for quantities like the size of the finite clusters and the geometry of the isoradial embedding?

In this project on the non-critical Ising model, we also extend the correspondence between the XOR Ising model and a bipartite dimer model on G_Q. This is the first example of bipartite dimer model with elliptic weights and with a local formula for the inverse Kasteleyn operator.

Integrable dimer weights out of criticality

Kenyon introduced [Ken02] critical dimer weights on bipartite isoradial graphs, in relation with the conductances of the Laplacian from Section 5.4. Dimer models on periodic isoradial graphs with these weights are in correspondence with Harnack curves of genus zero [KO06].

With Béatrice de Tilière and David Cimasoni, we are investigating if such a correspondence exists for Harnack curves of genus one. More precisely, does there exist a parameterization for integrable dimer models with elliptic functions? Integrability for bipartite dimer models does not mean directly invariance under star-triangle transformation, simply because this transformation already breaks bipartiteness. It is replaced by the more elementary spider move [GK13], a variant of the urban renewal.

For isoradial graphs of the form G_Q, the study above for the non-critical Z-invariant Ising model provides a positive answer, but it is very specific to the structure of the graph where all vertices have degree 3, and it gives only Harnack curves with a $(z, w) \leftrightarrow (z^{-1}, w^{-1})$. Preliminary results seem to show that in general, such parameterizations of the spider move transformation can only be rational, and it may be that the only dimer weights on edges as a function of their half-angle are the critical ones on isoradial graphs, and their generalization, where we allow circumcenters to lie outside of the face (and thus some rhombi in $G_\diamond$ are upside-down). We plan to continue the investigations on this problem.

Massive Laplacians and fermionic observable for the non critical Ising model

In [CS12], strong discrete holomorphy of the fermionic observable [Smi10] is used in a fundamental way so that the scaling limit of a related quantity is almost harmonic for the Laplacian of Section 5.4. From the corresponding harmonic analysis toolbox [CS11] and convergence results from discrete harmonic functions to their continuous counterparts, conformal invariance of the critical Z-invariant Ising model on isoradial graphs is proved.

This fermionic observable can be defined out of criticality. On the square lattice, out of criticality, this observable is harmonic for a certain massive Laplacian [BDC12]. This study is however specific to the square lattice since it is used in a non trivial way the fact that the graph on which the fermionic observable is defined has the same structure as the graph where the spins live, and the Laplacian acts.

It would be interesting to see if this connection between massive Laplacian and non critical Ising model can be established for the Z-invariant models on isoradial graphs. This would yield a combinatorial link between the Ising model and the massive Laplacian, which would be more concrete than the equality of their spectral curves. More generally, is it possible to construct discrete massive Dirac operator, which would be a "square root" of the massive Laplacian, which would extend out of criticality the connection between the Laplacian and the Kasteleyn operator on the double graph with critical weights which gives a version of the discrete Cauchy–Riemann equations?

A natural but naïve candidate would be to just perturb the (full) Kasteleyn matrix by adding nonzero coefficients on the diagonal, as we did to add a mass for the Laplacian. Expanding the determinant would give a sum of configurations with dimers and monomers, but the signs are not compensated any more by the clockwise odd orientation.

The Green function on finite isoradial graphs and branched coverings

Explicit and local formulas for the Z-invariant Green [Ken02] and massive Green [16] functions are known, as integral of discrete exponential functions (or their massive analogues) against a singular measure along a contour.

There exists a representation theorem for discrete harmonic functions on finite isoradial graphs as a (generalized) linear combination of discrete exponential functions [BMS05, BS08]. Using the same arguments, we can formulate the analogue representation result for massive harmonic functions.

The problem is that the coefficients in this linear combination are not very explicit. We are wondering if an explicit formula for the Poisson kernel of a simply connected finite isoradial graph could be written down. It may be complicated due to all the flexibility these graphs can have on their boundary. Maybe a simpler problem would be already to give formulas for Green functions on isoradial graphs which are branch covers of the plane. In particular, can we understand the mechanism linking the branching structure, and the singular measure used to integrate the (massive) exponential functions? Can we do it also for the Green function associated to Laplacian with connexions along edges [Ken11]? These exotic Green functions can then be used for the purposes of statistical mechanics: for example, in [KW15], such a Green function is used to compute the probability that a loop erased random walk passes through a given edge.

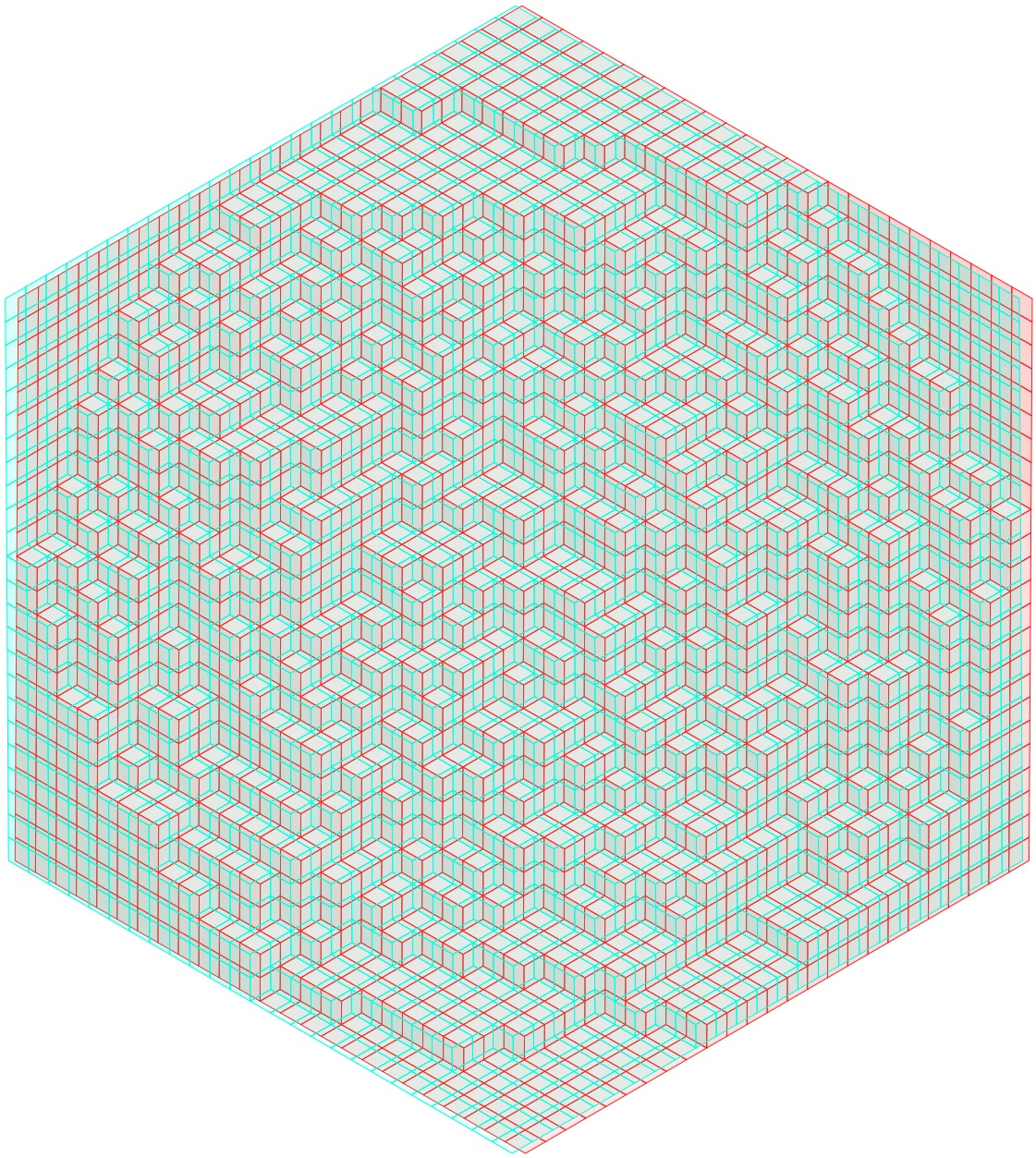

Figure 10.3.: A boxed plane partition, rendered to be seen with anaglyph glasses: red for the left eye, and cyan for the right eye.

Publications

[1] Cédric Boutillier, Paul François, Kirone Mallick, and Shamlal Mallick. A matrix ansatz for the diffusion of an impurity in the asymmetric exclusion process. *J. Phys. A*, 35(46):9703–9730, 2002.

[2] Cédric Boutillier. *Modèles de Dimères : comportements limites*. PhD thesis, Université Paris 11 – Orsay, 2005.

[3] Cédric Boutillier. Non-colliding paths in the honeycomb dimer model and the Dyson process. *J. Stat. Phys.*, 129(5-6):1117–1135, 2007.

[4] Cédric Boutillier. Pattern densities in non-frozen planar dimer models. *Comm. Math. Phys.*, 271(1):55–91, 2007.

[5] Cédric Boutillier. The critical Ising model on infinite isoradial graphs via dimers. *Oberwolfach Reports (Stochastic Analysis Workshop)*, (25/2008), 2008.

[6] Cédric Boutillier. The bead model and limit behaviors of dimer models. *Ann. Probab.*, 37(1):107–142, 2009.

[7] Cédric Boutillier and Béatrice de Tilière. Loops statistics in the toroidal honeycomb dimer model. *Ann. Probab.*, 37(5):1747–1777, 2009.

[8] Cédric Boutillier and Béatrice de Tilière. The critical Z-invariant Ising model via dimers: the periodic case. *Probab. Theory Related Fields*, 147(3-4):379–413, 2010.

[9] Cédric Boutillier and Béatrice de Tilière. The critical Z-invariant Ising model via dimers: locality property. *Comm. Math. Phys.*, 301(2):473–516, 2011.

[10] Dan Beltoft, Cédric Boutillier, and Nathanaël Enriquez. Random partitions in a rectangular box. *Moscow Mathematical Journal*, 12(4):719–745, 2012.

[11] Cedric Boutillier, Sevak Mkrtchyan, Nicolai Reshetikhin, and Peter Tingley. Random skew plane partitions with a piecewise periodic back wall. *Ann. Henri Poincaré*, 13(2):271–296, 2012.

[12] Cédric Boutillier and Béatrice Tilière. Statistical Mechanics on Isoradial Graphs. In Jean-Dominique Deuschel, Barbara Gentz, Wolfgang König, Max von Renesse, Michael Scheutzow, and Uwe Schmock, editors, *Probability in Complex Physical Systems*, volume 11 of *Springer Proceedings in Mathematics*, pages 491–512. Springer Berlin Heidelberg, 2012.

[13] Dan Betea, Cédric Boutillier, Jérémy Bouttier, Guillaume Chapuy, Sylvie Corteel, and Mirjana Vuletić. Perfect sampling algorithms for Schur processes. *arxiv:1407.3764, Markov Processes and Related Fields (accepted), proceedings of Inhomogenous Random Systems 2015*, 2014.

[14] Cédric Boutillier and Béatrice de Tilière. Height representation of XOR-Ising loops via bipartite dimers. *Electron. J. Probab.*, 19:no. 80, 33, 2014.

[15] Cédric Boutillier, Jérémy Bouttier, Guillaume Chapuy, Sylvie Corteel, and Sanjay Ramassamy. Dimers on rail yard graphs. *arXiv:1504.05176, Annals of IHP D (to appear)*, 2015.

[16] Cédric Boutillier, Béatrice de Tilière, and Kilian Raschel. The Z-invariant massive Laplacian on isoradial graphs. *Invent. Math.*, pages 1–81, 2016.

The publication listed here can be downloaded from:

`http://www.lpma-paris.fr/pageperso/boutil/publications/`.

Bibliography

[Ang13] Iana I. Anguelova. *Boson-Fermion Correspondence of Type B and Twisted Vertex Algebras*, pages 399–410. Springer Japan, Tokyo, 2013.

[AP04] H. Au-Yang and J. H. H. Perk. Q-dependent susceptibility in Z-invariant pentagrid ising model. *ArXiv Condensed Matter e-prints*, September 2004.

[AP07] H. Au-Yang and J. H. H. Perk. Q-dependent susceptibilities in ferromagnetic quasiperiodic Z-invariant ising models. *J. Stat. Phys.*, 127:265–286, April 2007.

[AYP87] Helen Au-Yang and Jacques H. H. Perk. Critical correlations in a Z-invariant inhomogeneous Ising model. *Phys. A*, 144(1):44–104, 1987.

[AZ13] Alexander Alexandrov and Anton Zabrodin. Free fermions and tau-functions. *Journal of Geometry and Physics*, 67(0):37–80, 2013.

[Bax86] Rodney J. Baxter. Free-fermion, checkerboard and Z-invariant lattice models in statistical mechanics. *Proc. Roy. Soc. London Ser. A*, 404(1826):1–33, 1986.

[Bax89] Rodney J. Baxter. *Exactly solved models in statistical mechanics*. Academic Press Inc. [Harcourt Brace Jovanovich Publishers], London, 1989. Reprint of the 1982 original.

[BC14] Alexei Borodin and Ivan Corwin. Macdonald processes. *Probab. Theory Related Fields*, 158(1-2):225–400, 2014.

[BCC14] Jérémie Bouttier, Guillaume Chapuy, and Sylvie Corteel. From Aztec diamonds to pyramids: steep tilings. 2014.

[BDC12] V. Beffara and H. Duminil-Copin. Smirnov's fermionic observable away from criticality. *Ann. Probab.*, 40(6):2667–2689, 2012.

[Bef08] Vincent Beffara. Is critical 2D percolation universal? In *In and out of equilibrium. 2*, volume 60 of *Progr. Probab.*, pages 31–58. Birkhäuser, Basel, 2008.

[BF14] A. Borodin and P. L. Ferrari. Anisotropic growth of random surfaces in $2 + 1$ dimensions. *Comm. Math. Phys.*, 325(2):603–684, 2014.

[BF15] A. Borodin and P. Ferrari. Random tilings and Markov chains for interlacing particles. *arXiv:1506.03910*, 2015.

[BG09] Alexei Borodin and Vadim Gorin. Shuffling algorithm for boxed plane partitions. *Adv. Math.*, 220(6):1739–1770, 2009.

[BG15] Alexey Bufetov and Vadim Gorin. Stochastic monotonicity in Young graph and Thoma theorem. *Int. Math. Res. Not. IMRN*, (23):12920–12940, 2015.

[BLR16] Nathanaël Berestycki, Benoit Laslier, and Gourab Ray. Universality of fluctutations in the dimer model. 2016.

[BMS05] A. I. Bobenko, C. Mercat, and Y. B. Suris. Linear and nonlinear theories of discrete analytic functions. Integrable structure and isomonodromic Green's function. *J. Reine Angew. Math.*, 583:117–161, 2005.

[Bor11] A. Borodin. Schur dynamics of the Schur processes. *Adv. Math.*, 228(4):2268–2291, 2011.

[BP93] R. Burton and R. Pemantle. Local characteristics, entropy and limit theorems for spanning trees and domino tilings via transfer-impedances. *Ann. Probab.*, 21(3):1329–1371, 1993.

[BP11] Yuliy Baryshnikov and Robin Pemantle. Asymptotics of multivariate sequences, part III: Quadratic points. *Adv. Math.*, 228(6):3127–3206, 2011.

[BP13] A. Borodin and L. Petrov. Nearest neighbor Markov dynamics on Macdonald processes. *arXiv:1305.5501*, 2013.

[BR05] Alexei Borodin and Eric M. Rains. Eynard-Mehta theorem, Schur process, and their Pfaffian analogs. *J. Stat. Phys.*, 121(3-4):291–317, 2005.

[Bru14] Erwan Brugallé. Pseudoholomorphic simple Harnack curves. *Enseign. Math.*, 2014. to appear.

[BS08] Alexander I. Bobenko and Yuri B. Suris. *Discrete differential geometry*, volume 98 of *Graduate Studies in Mathematics*. American Mathematical Society, Providence, RI, 2008. Integrable structure.

[CCK15] Dmitry Chelkak, David Cimasoni, and Adrien Kassel. Revisiting the combinatorics of the 2d Ising model. 2015.

[CDC13] David Cimasoni and Hugo Duminil-Copin. The critical temperature for the Ising model on planar doubly periodic graphs. *Electron. J. Probab.*, 18:no. 44, 18, 2013.

[CEP96] Henry Cohn, Noam Elkies, and James Propp. Local statistics for random domino tilings of the Aztec diamond. *Duke Math. J.*, 85(1):117–166, 1996.

[Cim14] David Cimasoni. The geometry of dimer models. 2014.

[CJ16] Sunil Chhita and Kurt Johansson. Domino statistics of the two-periodic Aztec diamond. *Adv. Math.*, 294:37–149, 2016.

[CJY15] Sunil Chhita, Kurt Johansson, and Benjamin Young. Asymptotic domino statistics in the Aztec diamond. *Ann. Appl. Probab.*, 25(3):1232–1278, 2015.

[CK01] Raphaël Cerf and Richard Kenyon. The low-temperature expansion of the Wulff crystal in the 3D Ising model. *Comm. Math. Phys.*, 222(1):147–179, 2001.

[CKP01] Henry Cohn, Richard Kenyon, and James Propp. A variational principle for domino tilings. *J. Amer. Math. Soc.*, 14(2):297–346 (electronic), 2001.

[CLP98] Henry Cohn, Michael Larsen, and James Propp. The shape of a typical boxed plane partition. *New York J. Math.*, 4:137–165 (electronic), 1998.

[CR07] David Cimasoni and Nicolai Reshetikhin. Dimers on surface graphs and spin structures. I. *Comm. Math. Phys.*, 275(1):187–208, 2007.

[CR08] David Cimasoni and Nicolai Reshetikhin. Dimers on surface graphs and spin structures. II. *Comm. Math. Phys.*, 281(2):445–468, 2008.

[CS06] Ruben Costa-Santos. Geometrical aspects of the Z-invariant ising model. *Eur. Phys. J. B*, 53(1):85–90, 2006.

[CS11] D. Chelkak and S. Smirnov. Discrete complex analysis on isoradial graphs. *Adv. in Math.*, 228(3):1590–1630, 2011.

[CS12] D. Chelkak and S. Smirnov. Universality in the 2D Ising model and conformal invariance of fermionic observables. *Inv. Math.*, 189:515–580, 2012.

[CY14] Sunil Chhita and Benjamin Young. Coupling functions for domino tilings of Aztec diamonds. *Adv. Math.*, 259:173–251, 2014.

[dB81a] Nicolaas G. de Bruijn. Algebraic theory of Penrose's non-periodic tilings of the plane. I. *Indagationes Mathematicae (Proceedings)*, 84(1):39–52, 1981.

[dB81b] Nicolaas G. de Bruijn. Algebraic theory of Penrose's non-periodic tilings of the plane. II. *Indagationes Mathematicae (Proceedings)*, 84(1):53 – 66, 1981.

[DG15] Julien Dubédat and Reza Gheissari. Asymptotics of height change on toroidal Temperleyan dimer models. *J. Stat. Phys.*, 159(1):75–100, 2015.

[DJM15] Erik Duse, Kurt Johansson, and Anthony Metcalfe. The Cusp-Airy Process. *arXiv:1510.02057*, 2015.

[DM15a] Erik Duse and Anthony Metcalfe. Asymptotic geometry of discrete interlaced patterns: Part I. *Internat. J. Math.*, 26(11):1550093, 66, 2015.

[DM15b] Erik Duse and Anthony Metcalfe. Asymptotic geometry of discrete interlaced patterns: Part II. *arXiv:1507.00467*, 2015.

[dT07a] Béatrice de Tilière. Quadri-tilings of the plane. *Probab. Theory Related Fields*, 137(3-4):487–518, 2007.

[dT07b] Béatrice de Tilière. Scaling limit of isoradial dimer models and the case of triangular quadri-tilings. *Ann.I. H. Poincaré B*, 43(6):729–750, 2007.

[dT15] Béatrice de Tilière. The dimer model in statistical mechanics. In *Dimer models and random tilings*, volume 45 of *Panor. Synthèses*, pages 1–45. Soc. Math. France, Paris, 2015.

[dT16] Béatrice de Tilière. Critical Ising model and spanning trees partition functions. *Ann. Inst. Henri Poincaré Probab. Stat.*, 52(3):1382–1405, 2016.

[Du11] Peng Du. The Aztec Diamond Edge-Probability Generating Function, 2011. Master Thesis, University of Pennsylvania.

[Dub11a] J. Dubédat. Dimers and analytic torsion I. *ArXiv e-prints*, October 2011.

[Dub11b] J. Dubédat. Exact bosonization of the Ising model. *ArXiv: 1112.4399*, 2011.

[Duf68] Richard J. Duffin. Potential theory on a rhombic lattice. *J. Combinatorial Theory*, 5:258–272, 1968.

[DZM+96] N. P. Dolbilin, Yu. M. Zinov′ev, A. S. Mishchenko, M. A. Shtan′ko, and M. I. Shtogrin. Homological properties of two-dimensional coverings of lattices on surfaces. *Funktsional. Anal. i Prilozhen.*, 30(3):19–33, 95, 1996.

[EKLP92a] N. Elkies, G. Kuperberg, M. Larsen, and J. Propp. Alternating-sign matrices and domino tilings. I. *J. Algebraic Combin.*, 1(2):111–132, 1992.

[EKLP92b] N. Elkies, G. Kuperberg, M. Larsen, and J. Propp. Alternating-sign matrices and domino tilings. II. *J. Algebraic Combin.*, 1(3):219–234, 1992.

[Fis66] M. E. Fisher. On the dimer solution of planar Ising models. *J. Math, Phys.*, 7:1776–1781, 1966.

[FK72] Cornelius Marius Fortuin and Piet W Kasteleyn. On the random-cluster model: I. Introduction and relation to other models. *Physica*, 57(4):536–564, 1972.

[FR37] R. H. Fowler and G. S. Rushbrooke. An attempt to extend the statistical theory of perfect solutions. *Transactions of the Faraday Society*, 33:1272–1294, 1937.

[Ges93] I. M. Gessel. Counting paths in Young's lattice. *J. Statist. Plann. Inference*, 34(1):125–134, 1993.

[GK13] Alexander B. Goncharov and Richard Kenyon. Dimers and cluster integrable systems. *Ann. Sci. Éc. Norm. Supér. (4)*, 46(5):747–813, 2013.

[GL99] A. Galluccio and M. Loebl. On the theory of Pfaffian orientations. I. Perfect matchings and permanents. *Electron. J. Combin.*, 6:Research Paper 6, 18 pp. (electronic), 1999.

[Gri06] Geoffrey Grimmett. *The random-cluster model*, volume 333 of *Grundlehren der Mathematischen Wissenschaften [Fundamental Principles of Mathematical Sciences]*. Springer-Verlag, Berlin, 2006.

[Hel00] H. Helfgott. Edge Effects on Local Statistics in Lattice Dimers: A Study of the Aztec Diamond (Finite Case). *ArXiv Mathematics e-prints*, July 2000.

[IR11] Y. Ikhlef and M. A. Rajabpour. Discrete holomorphic parafermions in the Ashkin–Teller model and SLE. *Journal of Physics A: Mathematical and Theoretical*, 44(4):042001, 2011.

[Joh02] Kurt Johansson. Non-intersecting paths, random tilings and random matrices. *Probab. Theory Related Fields*, 123(2):225–280, 2002.

[JPS98] William Jokusch, James Propp, and Peter Shor. Random Domino Tilings and the Arctic Circle Theorem. *arXiv:math/9801068 [math.CO]*, 1998.

[Kac90] Victor G. Kac. *Infinite-dimensional Lie algebras*. Cambridge University Press, Cambridge, third edition, 1990.

[Kas61] P. W. Kasteleyn. The statistics of dimers on a lattice : I. the number of dimer arrangements on a quadratic lattice. *Physica*, 27:1209–1225, December 1961.

[Kas67] P. W. Kasteleyn. Graph theory and crystal physics. In *Graph Theory and Theoretical Physics*, pages 43–110. Academic Press, London, 1967.

[Ken99] Arthur E. Kennelly. The equivalence of triangles and three-pointed stars in conducting networks. *Electrical World and Engineer*, 34:413–414, 1899.

[Ken93] Richard Kenyon. Tiling a polygon with parallelograms. *Algorithmica*, 9(4):382–397, 1993.

[Ken97] R. Kenyon. Local statistics of lattice dimers. *Ann. Inst. H. Poincaré Probab. Statist.*, 33(5):591–618, 1997.

[Ken00a] Richard Kenyon. The asymptotic determinant of the discrete Laplacian. *Acta Math.*, 185(2):239–286, 2000.

[Ken00b] Richard Kenyon. Long-range properties of spanning trees. *J. Math. Phys.*, 41(3):1338–1363, 2000. Probabilistic techniques in equilibrium and nonequilibrium statistical physics.

[Ken02] Richard Kenyon. The Laplacian and Dirac operators on critical planar graphs. *Invent. Math.*, 150(2):409–439, 2002.

[Ken04] R. Kenyon. An introduction to the dimer model. pages 267–304. ICTP Lect. Notes, XVII, Abdus Salam Int. Cent. Theoret. Phys., Trieste, 2004.

[Ken05] Richard Kenyon. Talk given at the workshop on Random partitions and Calabi–Yau crystals, Amsterdam, 2005. Slides available at `http://www.math.brown.edu/~rkenyon/talks/pyramids.pdf`.

[Ken08] Richard Kenyon. Height fluctuations in the honeycomb dimer model. *Comm. Math. Phys.*, 281(3):675–709, 2008.

[Ken09] Richard Kenyon. Lectures on dimers. In *Statistical mechanics*, volume 16 of *IAS/Park City Math. Ser.*, pages 191–230. Amer. Math. Soc., Providence, RI, 2009.

[Ken11] Richard Kenyon. Spanning forests and the vector bundle Laplacian. *Ann. Probab.*, 39(5):1983–2017, 2011.

[KO06] Richard Kenyon and Andrei Okounkov. Planar dimers and Harnack curves. *Duke Math. J.*, 131(3):499–524, 2006.

[KOO98] Sergei Kerov, Andrei Okounkov, and Grigori Olshanski. The boundary of the Young graph with Jack edge multiplicities. *Internat. Math. Res. Notices*, (4):173–199, 1998.

[KOS06] Richard Kenyon, Andrei Okounkov, and Scott Sheffield. Dimers and amoebae. *Ann. of Math. (2)*, 163(3):1019–1056, 2006.

[KPW00] Richard Kenyon, James Propp, and David Wilson. Trees and matchings. *Electron. J. Combin.*, 7:Research Paper 25, 34 pp. (electronic), 2000.

[Kra06] C. Krattenthaler. Growth diagrams, and increasing and decreasing chains in fillings of Ferrers shapes. *Adv. in Appl. Math.*, 37(3):404–431, 2006.

[KS04] Richard Kenyon and Scott Sheffield. Dimers, tilings and trees. *J. Combin. Theory Ser. B*, 92(2):295–317, 2004.

[KS05] Richard Kenyon and Jean-Marc Schlenker. Rhombic embeddings of planar quad-graphs. *Trans. Amer. Math. Soc.*, 357(9):3443–3458 (electronic), 2005.

[KSW13] Richard W. Kenyon, Nike Sun, and David B. Wilson. On the asymptotics of dimers on tori. *arXiv:1310.2603*, 2013.

[KW41a] H. A. Kramers and G. H. Wannier. Statistics of the two-dimensional ferromagnet. part I. *Phys. Rev.*, 60(3):252–262, Aug 1941.

[KW41b] H. A. Kramers and G. H. Wannier. Statistics of the two-dimensional ferromagnet. part II. *Phys. Rev.*, 60(3):263–276, Aug 1941.

[KW15] Richard W. Kenyon and David B. Wilson. Spanning trees of graphs on surfaces and the intensity of loop-erased random walk on planar graphs. *J. Amer. Math. Soc.*, 28(4):985–1030, 2015.

[Len20] W Lenz. Beitrag zum Verständnis der magnetischen Erscheinungen in festen Körpern. *Physikalische Zeitschrift*, 21:613–615, 1920.

[Li10] Z. Li. Spectral Curve of Periodic Fisher Graphs. *ArXiv e-prints*, August 2010.

[Li12] Z. Li. Critical temperature of periodic Ising models. *Comm. Math. Phys.*, 315:337–381, 2012.

[LJ11] Yves Le Jan. *Markov paths, loops and fields*, volume 2026 of *Lecture Notes in Mathematics*. Springer, Heidelberg, 2011. Lectures from the 38th Probability Summer School held in Saint-Flour, 2008, École d'Été de Probabilités de Saint-Flour. [Saint-Flour Probability Summer School].

[Mac15] I. G. Macdonald. *Symmetric functions and Hall polynomials*. Oxford Classic Texts in the Physical Sciences. The Clarendon Press, Oxford University Press, New York, second edition, 2015. With contribution by A. V. Zelevinsky and a foreword by Richard Stanley, Reprint of the 2008 paperback edition [MR1354144].

[McC10] Barry M. McCoy. *Advanced statistical mechanics*, volume 146 of *International Series of Monographs on Physics*. Oxford University Press, Oxford, 2010.

[Mer01] Christian Mercat. Discrete Riemann surfaces and the Ising model. *Comm. Math. Phys.*, 218(1):177–216, 2001.

[Mer04] Christian Mercat. Exponentials form a basis of discrete holomorphic functions on a compact. *Bull. Soc. Math. France*, 132(2):305–326, 2004.

[Mes06] RJ Messikh. The surface tension near criticality of the 2d-ising model. *Arxiv: 0610636*, 2006.

[MJD00] T. Miwa, M. Jimbo, and E. Date. *Solitons*, volume 135 of *Cambridge Tracts in Mathematics*. Cambridge University Press, Cambridge, 2000. Differential equations, symmetries and infinite-dimensional algebras, Translated from the 1993 Japanese original by Miles Reid.

[Mkr11] Sevak Mkrtchyan. Scaling limits of random skew plane partitions with arbitrarily sloped back walls. *Comm. Math. Phys.*, 305(3):711–739, 2011.

[MS] J. Miller and S. Sheffield. CLE(4) and the Gaussian Free Field. *(in preparation)*.

[MW73] B. McCoy and F. Wu. *The two-dimensional Ising model*. Harvard Univ. Press, 1973.

[Nie84] B. Nienhuis. Critical behavior of two-dimensional spin models and charge asymmetry in the Coulomb gas. *J. Statist. Phys.*, 34(5-6):731–761, 1984.

[Nor10] Eric Nordenstam. On the shuffling algorithm for domino tilings. *Electron. J. Probab.*, 15:no. 3, 75–95, 2010.

[Oko00] Andrei Okounkov. Random matrices and random permutations. *Internat. Math. Res. Notices*, (20):1043–1095, 2000.

[Oko01] Andrei Okounkov. Infinite wedge and random partitions. *Selecta Math. (N.S.)*, 7(1):57–81, 2001.

[OR03] Andrei Okounkov and Nikolai Reshetikhin. Correlation function of Schur process with application to local geometry of a random 3-dimensional Young diagram. *J. Amer. Math. Soc.*, 16(3):581–603 (electronic), 2003.

[OR06] Andrei Okounkov and Nicolai Reshetikhin. The birth of a random matrix. *Mosc. Math. J.*, 6(3):553–566, 588, 2006.

[OR07] Andrei Okounkov and Nicolai Reshetikhin. Random skew plane partitions and the Pearcey process. *Comm. Math. Phys.*, 269(3):571–609, 2007.

[ORV06] Andrei Okounkov, Nikolai Reshetikhin, and Cumrun Vafa. Quantum Calabi-Yau and classical crystals. In *The unity of mathematics*, volume 244 of *Progr. Math.*, pages 597–618. Birkhäuser Boston, Boston, MA, 2006.

[Per69] J. K. Percus. One more technique for the dimer problem. *J. Math. Phys.*, 10:1881, 1969.

[Pet10] F Petrov. Limit shapes of Young diagrams. Two elementary approaches. *Journal of Mathematical Sciences*, 166(1), 2010.

[Pet14] Leonid Petrov. Asymptotics of random lozenge tilings via Gelfand-Tsetlin schemes. *Probab. Theory Related Fields*, 160(3-4):429–487, 2014.

[Pet15] Leonid Petrov. Asymptotics of uniformly random lozenge tilings of polygons. Gaussian free field. *Ann. Probab.*, 43(1):1–43, 2015.

[Pit97] Boris Pittel. On a likely shape of the random Ferrers diagram. *Adv. in Appl. Math.*, 18(4):432–488, 1997.

[PP96] I. Pak and A. Postnikov. Oscillating tableaux, $(S_p \times S_p)$-modules, and Robinson-Schensted-Knuth correspondence. In *Proceedings of FPSAC '96, Minneapolis, MN*, 1996.

[PS11] M. Picco and R. Santachiara. Critical interfaces and duality in the Ashkin-Teller model. *Phys. Rev. E*, 83:061124, Jun 2011.

[RM97] J. R. Reyes Martìnez. Correlation functions for the Z-invariant Ising model. *Phys. Lett. A*, 227(3-4):203–208, 1997.

[RM98] J. R. Reyes Martìnez. Multi-spin correlation functions for the Z-invariant Ising model. *Phys. A*, 256(3-4):463–484, 1998.

[Smi10] Stanislav Smirnov. Conformal invariance in random cluster models. I. Holomorphic fermions in the Ising model. *Ann. of Math. (2)*, 172(2):1435–1467, 2010.

[SS09] O. Schramm and S. Sheffield. Contour lines of the two-dimensional discrete Gaussian free field. *Acta Math.*, 202(1):21–137, 2009.

[Sta99] R. P. Stanley. *Enumerative combinatorics. Vol. 2*, volume 62 of *Cambridge Studies in Advanced Mathematics*. Cambridge University Press, Cambridge, 1999. With a foreword by Gian-Carlo Rota and appendix 1 by Sergey Fomin.

[Sze08] Balázs Szendrői. Non-commutative Donaldson-Thomas invariants and the conifold. *Geom. Topol.*, 12(2):1171–1202, 2008.

[Tem74] H. N. V. Temperley. In Combinatorics: Proceedings of the British combinatorial conference 1973. page 202–204, 1974.

[Tes00] Glenn Tesler. Matchings in graphs on non-orientable surfaces. *J. Combin. Theory Ser. B*, 78(2):198–231, 2000.

[TF61] Harold N. V. Temperley and Michael E. Fisher. Dimer problem in statistical mechanics-an exact result. *Philos. Mag.*, 6(68):1061–1063, 1961.

[Tho64] Elmar Thoma. Die unzerlegbaren, positiv-definiten Klassenfunktionen der abzählbar unendlichen, symmetrischen Gruppe. *Math. Z.*, 85:40–61, 1964.

[Tin11] Peter Tingley. Notes on Fock space, 2011. `http://webpages.math.luc.edu/~ptingley/lecturenotes/Fock_space-2010.pdf`.

[Ver96] A. M. Vershik. Statistical mechanics of combinatorial partitions, and their limit configurations. *Funktsional. Anal. i Prilozhen.*, 30(2):19–39, 96, 1996.

[VK81] A. M. Vershik and S. V. Kerov. Asymptotic theory of the characters of a symmetric group. *Funktsional. Anal. i Prilozhen.*, 15(4):15–27, 96, 1981.

[Wer09] Wendelin Werner. *Percolation et modèle d'Ising*, volume 16 of *Cours Spécialisés [Specialized Courses]*. Société Mathématique de France, Paris, 2009.

[Wil96] David Bruce Wilson. Generating random spanning trees more quickly than the cover time. In *Proceedings of the Twenty-eighth Annual ACM Symposium on the Theory of Computing (Philadelphia, PA, 1996)*, pages 296–303. ACM, New York, 1996.

[Wil11] D. B. Wilson. XOR-Ising loops and the Gaussian free field. *ArXiv: 1102.3782*, 2011.

[WL75] F. Y. Wu and K. Y. Lin. Staggered ice-rule vertex model — the Pfaffian solution. *Phys. Rev. B*, 12:419–428, Jul 1975.

[You09] Ben Young. Computing a pyramid partition generating function with dimer shuffling. *J. Combin. Theory Ser. A*, 116(2):334–350, 2009.

[You10] Benjamin Young. Generating functions for colored 3D Young diagrams and the Donaldson-Thomas invariants of orbifolds. *Duke Math. J.*, 152(1):115–153, 2010. With an appendix by Jim Bryan.

Index